



SAPIENZA  
UNIVERSITA' DI ROMA

DOTTORATO DI RICERCA IN MEDICINA  
SPERIMENTALE  
XXIX CICLO

*“Autophagy in human keratinocytes:  
role of the fibroblast growth factor receptor 2b  
and its signaling”*

DOTTORANDO  
Monica Nanni

DOCENTE GUIDA  
Prof.ssa Francesca Belleudi

COORDINATORE DEL DOTTORATO  
Prof.ssa Maria Rosaria Torrisi

ANNO ACCADEMICO  
2015/2016

# INDEX

ABSTRACT .....	1
INTRODUCTION .....	4
Autophagy .....	5
The autophagic machinery .....	6
Sources of autophagosome membranes .....	8
Noncanonical autophagy .....	9
Intracellular signaling pathways involved in autophagy .....	11
Fibroblast growth factor receptors: receptor-mediated signaling pathways involved in the regulation of autophagy .....	12
The fibroblast growth factor receptor 2b and its signaling in the control of autophagy in human keratinocytes.....	17
MATERIALS AND METHODS .....	22
Cells and treatments .....	23
Immunofluorescence .....	24
Western blot analysis.....	25
Transmission electron microscopy .....	26
Primers.....	27
RNA extraction and cDNA synthesis .....	28
PCR amplification and real-time quantitation.....	28
RESULTS .....	29
FGFR2b-mediated phagocytosis and autophagy are convergent intracellular membrane pathways regulated by PLC $\gamma$ signaling. ....	30
FGFR2b-induced autophagy requires PLC $\gamma$ -mediated phosphorylation/ activation of JNK.....	33
FGFR2b enhances FGF7-mediated autophagy, phagocytosis and their convergence in light skin primary HKs.....	35
Impairment of FGFR2b-induced autophagy in HPV16E5 expressing keratinocytes .....	36
16E5 interferes with the transcriptional regulation of autophagy through the impairment of p53 function.....	43
DISCUSSION .....	46
REFERENCES.....	76

## **ABSTRACT**

Signaling of the epithelial splicing variant of the fibroblast growth factor receptor 2 (FGFR2b) induces both autophagy and phagocytosis in human keratinocytes. In this work I investigated, in our cell model of HaCaT keratinocytes, if the two processes might be related and the possible involvement of PLC $\gamma$  signaling in the autophagy triggered by FGFR2b activation. Using fluorescence and electron microscopy we demonstrated that the FGFR2b-induced phagocytosis and autophagy involve converging autophagosomal and phagosomal compartments. Moreover, the forced expression of FGFR2b signaling mutants and the use of specific inhibitors of FGFR2b substrates showed that the receptor-triggered autophagy requires PLC $\gamma$  signaling, which in turn activates JNK1 via PKC $\delta$ . Finally we found that, in primary human keratinocytes derived from light or dark pigmented skin and expressing different levels of FGFR2b, the rate of phagocytosis and autophagy and the convergence of the two intracellular pathways depend on the level of receptor expression. These results suggest that FGFR2b signaling would control *in vivo* the number of melanosomes in keratinocytes, determining skin pigmentation.

Since the early oncoprotein E5 of the human papillomavirus type 16 (16E5) is able to down-regulate FGFR2b expression and since it has been recently proposed a possible role of the entire “early protein pool” of HPV16 in inhibiting the autophagic process in epithelial cells, I also proposed to investigate the possible impairment of FGFR2b-induced autophagy in keratinocytes expressing 16E5. The results showed that the presence of 16E5 strongly inhibited the autophagic process, while forced expression and activation of FGFR2b counteracted this effect, demonstrating that the viral protein and the receptor exert opposite and interplaying roles not only on epithelial differentiation, but also in the control of autophagy. In W12 cells, silencing of the 16E5 gene in the context of the viral full length genome confirmed its role on autophagy inhibition. Finally, molecular approaches showed that the viral protein interferes with the transcriptional regulation of autophagy also through the impairment of p53 function, indicating that 16E5 uses parallel mechanisms for autophagy impairment. Overall our results further support the hypothesis that a transcriptional crosstalk among 16E5 and

FGFR2b might be the crucial molecular driver of epithelial deregulation during early steps of HPV infection and transformation.

# INTRODUCTION

## Autophagy

Autophagy is a lysosomal degradative pathway conserved from yeast to mammals, used by the cells to eliminate or recycle cytoplasmic components, such as damaged organelles, membranes and molecules, to maintain cellular homeostasis or to adapt the cells to stress conditions (Feng et al., 2014). There are three forms of autophagy: macroautophagy, microautophagy and chaperone-mediated autophagy. In macroautophagy substrates are sequestered in a double-membrane structure called autophagosome. This organelle then fuses with lysosome promoting the degradation of its inner membrane and the engulfed material by lysosomal enzymes (Mizushima et al., 2011). The second type of autophagy is chaperone-mediated autophagy (CMA). In this pathway cytosolic proteins, marked by a pentapeptide motif with a consensus sequence similar to KFERQ, are recognized and selectively translocated to the lysosomal membrane by the chaperon protein Hsc70, which promotes the translocation into the lysosomal lumen through the binding to LAMP-2A. Finally, the third type is microautophagy, in which part of the cytoplasm is engulfed by direct invagination of the lysosomal membrane (Ravikumar et al., 2010; Mizushima et al., 2011).

Macroautophagy, commonly called autophagy, is the most extensively studied membrane pathway, which is present at basal level and plays an important role in maintaining cellular homeostasis. However, this process can be up-regulated as a cytoprotective response by several stimuli such as nutrient starvation (glucose or amino-acid withdrawal), hypoxia, oxidative stress, pathogen infection, radiation and anticancer drug treatment (Yang and Klionsky, 2010). Macroautophagy can be also a selective process to target specific damaged organelles, such as mitochondria (mitophagy) and peroxisomes (pexophagy) (Deffieu et al., J Biol Chem 2009; Dunn et al., Autophagy 2005), or invasive pathogens (xenophagy) (Levine et al., Nature 2011) to the lysosomal compartment (Figure 1).

## The autophagic machinery

The autophagic machinery consists of about 40 autophagy-related genes (ATGs) first identified in yeast. Many of these genes have orthologs in mammals, although they present important differences in biology and architecture, and they have been defined as the core autophagy genes, mainly involved in autophagosome biogenesis (Lamb et al., 2013; Bento et al., 2016).

The process which leads to the formation of a mature autophagosome can be divided in three steps: the initiation, which consists in the transmission of the signal to the membrane source involved in the nucleation of the isolation membrane, with consequent recruitment of the initiating complexes; the nucleation, that leads to the formation of the isolation membrane from the membrane source; the expansion, where the isolation membrane expands until close completely, forming the autophagosome (Mizushima et al., 2011; Lamb et al., 2013; Feng et al., 2014).

The first complex involved in the stage of initiation is the ULK1/2. ULK1/2 is formed by UNC51 like Ser/Thr kinases ULK1/2, ATG13, FAK family kinase-interacting protein of 200 kDa (FIP200) and ATG101. ULK1/2 interact with ATG13, which directly binds FIP200 leading to its interaction with the ULKs (Hosokawa et al., 2009; Jung et al., 2009). The ULK1/2 complex can be activated/phosphorylated (Ser317 and Ser777) by an AMP-activated protein kinase (AMPK)-dependent (autophagy induced by glucose starvation) or AMPK-independent (autophagy induced by amino acid starvation) pathway (see below). Under fed conditions the ULK1/2 complex is inhibited by the binding with mTORC1, the key upstream negative regulator of autophagy, which phosphorylates/inactivates ULK1/2 (Ser757). On the contrary, upon nutrient starvation mTORC1 is released from the complex with consequent ULK1/2 activation (Kim et al., 2011).

Another important complex required for the initiation step of autophagosome formation is the class III phosphatidylinositol (PI) 3-kinase (PI3K) complex (also known as the Beclin 1 complex), which consists of vacuolar protein sorting 34 (Vps34, also known as the PI3K catalytic subunit 3), p150, Beclin 1 and ATG14 subunits and it is necessary for the generation of phosphatidylinositol 3-phosphate

(PI3P) (Mizushima et al., 2011). Beclin 1 is a key protein of the PI3K complex since it interacts with Vps34 and enhances its activity. Many other proteins can interact with Beclin 1 and positively regulate autophagy, such as AMBRA1, Bif-1 and vacuole membrane protein 1 (VMP1), while BCL-2 inhibits autophagy by sequestering Beclin 1 from the PI3K complex (Funderburk et al., 2010).

During the nucleation step the activated ULK1/2 and the PI3K complexes are recruited to the membrane site of autophagosome initiation. Here the ULK1/2 complex can phosphorylate different proteins at Ser and Thr residues, among which Beclin 1 and its interacting protein AMBRA1, which in turn enhance the activity of the PI3K complex (Di Bartolomeo et al., 2010; Russell et al., 2013). The PI3K complex generates a pool of PI3P in the membrane, necessary for the recruitment of other ATG proteins or autophagy-specific PtdIns(3)P effectors, such as double FYVE-containing protein 1 (DFCP1) and WD-repeat domain phosphoinositide-interacting (WIPI) proteins.

In the last stage of autophagosome formation, the elongation, two ubiquitin-like proteins are involved in the autophagosome membrane expansion and closure: ATG12 and LC3. ATG12 is conjugated to ATG5 through a mechanism that requires ATG7, an E1-like enzyme, and ATG10, an E2-like enzyme (Mizushima et al., 1998). The ATG12-ATG5 complex then interacts with ATG16L1, forming the ATG12-ATG5-ATG16L1 complex, which is recruited to the outer side of the isolation membrane. In parallel cytosolic LC3 is cleaved in the C-terminal by the cysteine protease ATG4, leaving a glycine residue, which is following activated by ATG7. Finally, the E2-like enzyme ATG3 and the ATG12-ATG5-ATG16L1 complex promote the conjugation of LC3 to the phosphatidylethanolamine (PE), generating lipidated LC3 (LC3-II), which associates to the autophagosomal membrane (Kabeya et al., 2004; Sakoh-Nakatogawa et al., 2013). ATG12-ATG5-ATG16L1 complex is released upon the autophagosome closure (Mizushima et al. 2001), while the LC3-II localized in the inner membrane of the autophagosome is retained (Kabeya et al., 2004). Recent evidences have shown also a role for actin filaments in autophagosome shaping. During the nucleation step, the actin-capping protein (CapZ) binds to PI3P and stimulates actin polymerization and branching, in the inner face of the isolation membrane (Aguilera et al., 2012; Mi et al., 2015). These evidences strongly suggest

a new important role for actin in the autophagosome biogenesis.

### **Sources of autophagosome membranes**

Even if a role for various organelles has been proposed as the membrane source of autophagosomes, such as the endoplasmic reticulum (ER), the Golgi complex, mitochondria, endosomes and plasma membrane (Figure 1), the origin of the autophagosomal membrane remains still unclear. Among the different possible membrane sources, the ER seems to be the best candidate, while the other organelles may contribute to the autophagosomal membrane expansion during the elongation step (Lamb et al., 2013; Ktistakis and Tooze, 2016; Bento et al., 2016).

The autophagosome originates from a preexisting membrane called isolation membrane, which appears to emerge from an omega-shaped subdomain of the ER (the omegasome) (Hayashi-Nishino et al., 2009). The ULK1/2 and the PI3K complexes are recruited in the omegasome, sustaining the expansion of the isolation membrane, until it reaches a sufficient size to allow ULK1/2 complex dissociation (Lamb et al., 2013). During the nucleation step the interaction between Beclin 1, a member of the PI3K complex, and the vacuole membrane protein 1 (VMP1), which is a multispinning transmembrane protein localized in the ER and in the Golgi, is required at the level of the omegasome (Molejon et al., 2013). In addition, during this stage the PtdIns(3)P-binding protein DFCP1 is mobilized from the Golgi to ER and partially co-localizes with the autophagic markers LC3 and ATG5 (Axe et al., 2008), while the PtdIns(3)P effector WIPI localizes in the omegasome and is required for the recruitment of the ATG12-ATG5-ATG16L1 complex binding ATG16L1 (Dooley et al., 2014), which then conjugates LC3-PE to the autophagosome membrane (see above).

Others membrane sources seem to be required for autophagosome formation like mitochondria and particularly the outer membrane of these organelles. In fact, during serum-starved induced autophagy ATG5 and LC3 colocalize with mitochondria, and their membranes seem to be in contact with the autophagosome membranes (Hailey et al., 2010).

Moreover, another theory about the autophagosome biogenesis proposes the ER-mitochondria contact site as a candidate in this process, since ATG14 and ATG5 were found localized in this site (Hamasaki et al., 2013).

The Golgi complex and endosomes also can participate to autophagosome expansion, possibly providing ATG9-positive vesicle. ATG9 is a transmembrane protein, which resides on the *trans*-Golgi network (TGN) and in the endosomal compartments but is mainly localized in endosomes during nutrient deprivation. The ULK complex regulates its distribution and the vesicles containing ATG9 participate to the expansion of the isolation membrane (Orsi et al., 2012; Puri et al., 2014). In addition, the recycling endosomes represent an alternative source for autophagosome formation, as suggested by the evidence of direct interaction between the PX-BAR protein SNX18 and ATG16L1 and LC3 at the level of the recycling endosome membranes (Knaevelsrud et al., 2013).

Moreover, the ER-Golgi intermediate compartment (ERGIC) is gaining an emerging role as a membrane source for autophagosome, indicated by the serum deprivation-induced budding of LC3-II positive vesicles from this compartment, which contribute to the expansion of the autophagosomal isolation membrane (Ge et al., 2013; Ge et al., 2014).

The plasma membrane can also contribute to autophagosome formation since some clathrin-coated vesicles (CCV) derived from this compartment are ATG16L1-positive and subsequently acquire LC3 and reach the omegasome (Ravikumar et al., 2010; Moreau et al., 2011).

### **Noncanonical autophagy**

Many studies have revealed the presence of a noncanonical autophagy. This definition includes an autophagosome formation in which some key ATG proteins and/or complexes are lost or alternative processes in which ATG proteins are recruited to single membrane structures involved in either lysosomal degradation or nondegradative functions (Juenemann and Reits, 2012; Ktistakis and Tooze, 2016). The ATG5/Atg7-independent pathway, possibly involved in the elimination of mitochondria in reticulocytes, was first discovered in mouse

embryonic fibroblasts (MEF) and consists in autophagic vesicle formation in response to autophagic stimuli, which requires ULK1/2 and Beclin 1 complexes recruitment, but not the LC3 lipidation/association (Nishida et al., 2009; Honda et al., 2014). Moreover, a noncanonical autophagy requiring ATG7 activity for LC3-I lipidation, but not Beclin 1 and Vps34 activation, has been described in mammalian neurons treated with the neurotoxic agent 1-metil-4-phenylpyridinium (Zhu et al., 2007).

Very recently, increased evidences have proposed that some ATG proteins could be recruited to the surface of different single membrane compartments to promote their convergence to lysosomes (Pimentel-Muñoz and Boada-Romero, 2014; Ktistakis and Tooze, 2016). This is the case of the LC3-associated phagocytosis (LAP), occurring in macrophages after toll-like receptor activation, in which Beclin 1 and LC3 are recruited on the phagosome membranes to facilitate their fusion with lysosomes (Sanjuan et al., 2007). In alternative, the recruitment of autophagic proteins on the membrane of compartments different from autophagosomes can be required to also promote nondegradative functions (Pimentel-Muñoz and Boada-Romero, 2014). This is the case of some stable LC3-II-positive phagosomes, compartments that promote the survival and replication of pathogens, such as bacteria, rather than induce their degradation (Figure 2). According to this more general role for the autophagic machinery in the regulation of nondegradative processes, it has been proposed for various ATG proteins also a role in the secretion pathways (Pimentel-Muñoz and Boada-Romero, 2014). For instance, in melanocytes the autophagosomal markers ATG5 and LC3 appear localized on the single membrane of melanosomes, possibly promoting their maturation and secretion (Ganesan et al., 2008). A similar mechanism appears to be also involved in the secretion of IL1B (Dupont et al., 2011), or in that of the secretory granules in PC12 cell line (Figure 2) (Ishibashi et al., 2012). These last recent findings sustain the importance of the autophagic machinery in nondegradative biological functions.

## **Intracellular signaling pathways involved in autophagy**

Various signaling pathways can control the autophagic process and the main activated upon several autophagic stimuli, like serum deprivation, hypoxia or stress conditions, is the mTOR pathway (Ravikumar et al., 2010; Russel et al., 2014). mTOR (mammalian target of rapamycin) is a serine/threonine kinase, which can form two different complexes, mTORC1 and mTORC2, among which only the mTORC1 complex is involved in autophagy regulation (Jewell et al., 2013). mTORC1 complex consists of five subunits: TOR, RAPTOR (regulatory-associated protein of mTOR), mLST8 (mammalian lethal with SEC13 protein), DEPTOR (DEP domain-containing mTOR-interacting protein) and PRAS40 (40 kDa Pro-rich AKT substrate) (Laplante et al., 2012). Under nutrient-rich conditions mTORC1 is active and associated to lysosomes. In these conditions, the Ragulator complex, which acts as a guanine nucleotide exchange factor (GEF), activates and recruits the RAG GTPases on the lysosomal surface (Sancak et al., 2010), which in turn binds the mTORC1 complex at the lysosomal membrane (Kim et al., 2008; Sancak et al., 2008). Here mTORC1 is activated by the small GTPase Rheb (Garami et al., 2003; Inoki et al., 2003; Tee et al., 2003). During growth factors stimulation, the main pathway involved in Rheb-mediated activation of mTORC1 is the PI3K/AKT pathway, (Inok et al., 2002; Potter et al., 2002). Thus, mTORC1 activation under fed conditions and growth factor stimulation acts as a powerful inhibitor of the autophagic process. In fact, active mTORC1 is able to inhibit the two autophagic complexes involved in autophagy initiation, ULK1/2 complex and PI3K complex (Russel et al., 2014). In fact, mTORC1 inhibits the PI3K complex inducing ATG14 phosphorylation (Yuan et al., 2013) and it can directly phosphorylate ATG13 and ULK1 in Ser757 inhibiting their kinase activity. Under nutrient starvation or treatment with the mTOR inhibitor, rapamycin, mTORC1 is released from ULK1/2 complex leading to its activation and autophagy initiation (Ganley et al., 2009; Hosokawa et al., 2009; Jung et al., 2009).

Another way to inhibit mTORC1 and induce the autophagic process is via AMPK. AMPK is a serine/threonine kinase, which is activated by AMP or ADP and therefore by low ATP levels. In these conditions AMPK inhibits mTORC1 by the activation of TSC, a complex involved in the release of mTORC1 from

lysosomes and consequently in its inhibition. AMPK can also directly inhibit mTORC1 via its phosphorylation (Gwinn et al., 2008). Alternatively, AMPK can directly activate ULK1, inducing its phosphorylation on Ser317 and Ser777 (Kim et al., 2011; Bach et al., 2011), or Vps34, through Beclin 1 phosphorylation on Ser91 and Ser94 (Kim et al., 2013).

Other kinases can regulate autophagy, such as the mitogen-activated protein kinase (MAPK)/extra-cellular signal-regulated kinase (ERK) pathway. In fact, this pathway is activated during starvation-induced autophagy and its inhibition, through the use of a MEK1/2 inhibitor, affects autophagy in the HT-29 cell line (Ogier-Denis et al., 2000). Upon serum deprivation AMPK induces a transient activation/phosphorylation of MAPK/ERK pathway, which promotes increased expression of Beclin 1, mTORC1 disassembly and consequently autophagy as cytoprotective mechanism. However, sustained MEK/ERK activation leads to a destructive autophagy, which results in cell death (Wang et al., 2009).

Serum deprivation also activates autophagy via c-Jun N-terminal protein kinase 1 (JNK1), which phosphorylates BCL-2 and allows the release of Beclin 1 from the autophagic inhibitor complex BCL-2/Beclin 1 (Wei et al., 2008).

### **Fibroblast growth factor receptors: receptor-mediated signaling pathways involved in the regulation of autophagy**

The fibroblast growth factor receptors (FGFRs) are receptor tyrosine kinases (RTKs) belonging to a family composed by four highly conserved transmembrane tyrosine kinase receptors (FGFR1, FGFR2, FGFR3 and FGFR4) encoded by four different genes. FGFRs are activated by fibroblast growth factor (FGF) family members, which is composed by 18 members clustered in five paracrine subfamilies and one endocrine subfamily. FGFRs are expressed on different tissues and regulate many key cellular physiological processes, such as proliferation, differentiation, migration and survival (Turner and Grose, 2010; Goetz and Mohammadi, 2013). FGFRs consist of an extracellular domain, a single-pass transmembrane domain and an intracellular tyrosine kinase domain (Figure

3). The extracellular domain is composed by three immunoglobulin (Ig) like domains (I-III), an “acid box” between domains I and II characterized by an acidic, serine-rich region and a conserved positively charged binding site for heparin (Schlessinger et al., 2000). The first Ig-like domain, together with the acid box, seem to be involved in receptor autoinhibition (Olsen et al., 2004), while the second and third Ig-like domains form the binding site for FGF ligands (Mohammadi et al., 2005). The ligand binding specificity by FGFR1, FGFR2 and FGFR3 is determined by the alternative splicing of the third Ig-like domain of these receptors, which generates FGFRb and FGFRc isoforms (Figure 3). In particular, for FGFR2 the N-terminal portion of the Ig-III domain is encoded by the exon 7 (exon IIIa), while the C-terminal portion is encoded alternatively by exon 8 (exon IIIb), and 9 (exon IIIc), which determines respectively FGFR2IIIb and FGFR2IIIc isoforms with different ligand-binding specificities; in fact, while FGFR2IIIb specifically binds FGF7/KGF (Rubin et al., 1989) and FGF10 (Igarashi et al., 1998), FGFR2IIIc binds FGF2 (Yayon et al., 1992) (Figure 4). The alternative splicing also determines the tissue specificity of the FGFRs; in fact the FGFR2IIIb isoform is exclusively expressed in epithelial cells, while the FGFR2IIIc isoform is expressed exclusively in mesenchymal cells (Miki et al., 1992; Orr-Urtreger et al., 1993). FGFs binding to FGFRs induces receptor dimerization and the juxtaposition of the two intracellular kinase domains of the two receptors inducing the phosphorylation of each other (Goetz and Mohammadi, 2013). However, FGF-FGFR binding requires the presence of a cofactor, heparan sulphate proteoglycan (HSPG), which is present in the cell plasma membrane and stabilizes the interaction between FGF and FGFR enhancing resistance to proteolysis and forming a dimeric 2:2:2 FGF-FGFR-HSPG ternary complex on the cell surface (Schlessinger et al., 2000).

FGF/FGFR interaction induces receptor dimerization, which leads to a conformational change in receptor structure inducing the activation of the intracellular kinase domain, which in turn triggers the intermolecular transphosphorylation of the tyrosine kinase domain and the carboxy-terminal tail (Turner and Grose, 2010; Brooks et al., 2012). Several tyrosine residues of the receptor can be autophosphorylated and for FGFR1 have been identified seven

residues (Y463, Y583, Y585, Y653, Y654, Y730, and Y766) (Lew et al., 2009). Once phosphorylated these residues act as docking sites for adaptor proteins, which are recruited and phosphorylated by FGFRs leading to activation of several signaling pathways (Figure 5) (Turner and Grose, 2010). The main downstream substrates of FGFRs are the FGFR substrate 2 (FRS2) and the phospholipase C $\gamma$  (PLC $\gamma$ ). FRS2 family is composed by two members, FRS2 $\alpha$  and FRS2 $\beta$  (Gotoh et al., 2008), which both contain a consensus myristylation sequence at the N-terminus for binding to lipids in the plasma membrane (Gotoh et al., 2008) and a phosphotyrosine binding (PTB) domain and multiple tyrosine phosphorylation sites at the C-terminus, which need to bind RTKs. FRS2 proteins can bind a limited specie of RTKs, such as neurotrophin receptors, RET and ALK, but in particular FGFRs and FRS2 $\alpha$  acts as the major mediator of intracellular signaling via FGFRs. The PTB domains of FRS2 proteins bind constitutively to unphosphorylated peptides at the juxtamembrane domain of the FGFR. The activation of FGFRs induces FRS2 phosphorylation on several sites creating docking sites for additional adaptor proteins. In fact, FRS2 $\alpha$  contains four tyrosine phosphorylation sites that bind the adaptor protein growth-factor-receptor-bound protein 2 (Grb2) and two binding sites for the SH2-containing tyrosine phosphatase protein (Shp2). Grb2 can bind many proteins via two SH3 domains, such as Gab1, SOS and Cbl. The recruitment of Gab1 by Grb2 forms a ternary complex with FRS2 $\alpha$ , which in turn induces the recruitment of PI-3 kinase and the activation of PI3K/AKT pathway (Figure 5) (Altomare et al., 2005). Sos is a guanine nucleotide exchange factor (GEF), which can activate Ras; therefore the recruitment of Grb2-Sos on FGFR induced by FRS2 $\alpha$  activation triggers Ras/mitogen-activated protein kinase (MAP kinase) pathway activation (Figure 5) (Eswarakumar et al., 2005). The binding of Shp2 to FRS2 $\alpha$  induces tyrosine phosphorylation of Shp2, which in turn induces a strong activation of ERK, a component of MAP kinases family, in response to FGF stimulation (Hadari et al., 1998). The activation of ERK induced by growth factors can be transient or sustained (Marshall 1995). In the transient phase, the growth factors-induced activation of ERK peaks within 5 minutes and returns to basal levels within 1 hour while in the sustained phase is maintained for several hours and reduces gradually. FRS2 $\alpha$  activation induced by FGF stimulation can triggers both transient and sustained activation of ERK by either its shp2-binding and

Grb2-binding sites even if they induce a strong and moderate activation of ERK respectively (Hadari et al., 2001). Another important signaling activated by FGF/FGFR binding, independent from FRS2, is the PLC $\gamma$  pathway (Figure 5). This phospholipase binds through its Src homology 2 (SH2) domain to a phosphotyrosine residue in the C-terminal receptor tail, inducing PLC $\gamma$  phosphorylation and activation. Particularly, it has been demonstrated that the tyrosine 766 residue in the C-terminal of FGFR1 is required for PLC $\gamma$  protein binding (Mohammadi et al., 1991), which corresponds to tyrosine 769 in FGFR2b (Ceridono et al., 2005; Cha et al., 2009). PLC $\gamma$  activation induces phosphatidylinositol-4,5-bisphosphate (PIP<sub>2</sub>) hydrolysis in phosphatidylinositol-3,4,5-trisphosphate (PIP<sub>3</sub>) and diacylglycerol (DAG), that in turn activates the members of the serine-threonine kinases family protein kinase C (PKC), which contribute to MAPK pathway activation by phosphorylating Raf (Brooks et al., 2012). In addition, several other pathways can be activated by FGFRs, such as signal transducer and activator of transcription (STAT) signaling, ribosomal protein S6 kinase 2 (RSK2), the p38 MAPK and Jun N-terminal kinase pathways (Touat et al., 2015), which can be activated downstream RAS by the MAPKKs, MKK4 and MKK7 (Katz et al., 2007) but also via PKC $\delta$  (Liu et al., 2006; Chen et al., 2008).

FGFR signaling is regulated by several factors that exert negative feedback control on many elements of the FGFR cascade. In fact, after receptor activation it is internalized and degraded or recycled through a Cbl-mediated monoubiquitylation. Cbl is an E3 ubiquitin ligase, which forms a ternary complex with FRS2 $\alpha$  and Grb2, inducing ubiquitination and degradation of FRS2 $\alpha$  and the sorting of the receptor to the endocytic lysosomal degradative pathway (Turner and Grose, 2010). The MAPK signaling, in particular ERK1 and ERK2, can phosphorylate FRS2 on many serine/threonine residues blocking Grb2 recruitment. In addition, the downstream signaling of FGFR can be attenuated by several negative regulators, such as the MAPK phosphatase 1 and 3 (MKP1 and MKP3), that dephosphorylate ERK1 and ERK2, Sprouty (SPRY) proteins, that compete for Grb2 binding with Sos preventing RAS activation or directly bind RAF blocking MAPK signaling, the Similar Expression to FGF (SEF) family members, which can interact with FGFRs and compete for substrate binding or cause

receptor dephosphorylation and FGFR1 that modulates ligand binding (Figure 5) (Turner and Grose, 2010).

Several growth factors/receptor tyrosine kinases (RTKs) signaling pathways, including those activated by FGF/FGFRs can exert a regulatory control on the autophagic process. In particular, insulin-like growth factor-1 (IGF1) (Sobolewska et al., 2009) as well as platelet-derived growth factor (PDGF) (Takeuchi et al., 2004), negatively regulate autophagy through the activation of the PI3K/AKT/mTOR pathway. More recently it has been described that PDGF is able to induce autophagy in vascular smooth muscle cells (VSMCs) via a PI3K/AKT/mTOR-independent pathway (Salabei et al., 2013). In addition, an inhibitor role on autophagy through a canonical mTOR-dependent mechanism has been demonstrated also for the epidermal growth factor (EGF) (Sobolewska et al., 2009). More recently an additional mTOR-independent inhibitory mechanism on autophagy, which directly involves Beclin 1 phosphorylation/inhibition, has been described for EGF/EGFR (Wei et al., 2013). More interestingly, a recent study demonstrated that the inactive form of EGFR is able to trigger autophagy, through a mTORC1-independent mechanism; this inactive receptor interacts with Rubicon, a Beclin 1 inhibitor, inducing Beclin 1 release from Beclin 1/Rubicon complex and its consequent activation (Tan et al., 2015).

Several evidences have proposed contrasting roles for FGFRs on autophagy regulation. In fact, previously studies have demonstrated that in mouse fibroblasts the fibroblast growth factor 2 (FGF2)-mediated activation of the fibroblast growth factor receptor 1/2 (FGFR1/2) inhibits autophagy, and in particular the autophagosome assembly, through the activation of the PI3K/AKT/mTOR pathway (Lin et al., 2011). This inhibitory role exerted by FGF2 is required to prevent premature differentiation of cardiac progenitor cells (Zhang et al., 2012), as well as to induce a protective effect in myocardial ischemia/reperfusion (Wang et al., 2015) or to maintain the proliferative potential of the mesenchymal stem cells (Eom et al., 2014). Recently it has been also demonstrated that FGF2-mediated activation of FGFR3 inhibits autophagy in chondrocytes inducing a decrease protein expression of the ATG12-ATG5 complex, which in turn induces a suppression of the cartilage development. This phenomenon plays a key role in

achondroplasia pathogenesis (Wang et al., 2015). Interestingly in the same context of chondrocytes it has been very recently shown that FGF18-induced activation of FGFR4 triggers autophagy via a JNK1-mediated, mTOR-independent pathway, which is required for bone growth (Cinque et al., 2015).

Finally, our previous studies have demonstrated that the activation of FGFR2b by FGF7 induces autophagy in human keratinocytes through a PI3K-AKT-mTOR-independent signaling, which is required to stimulate the autophagosome assembly (Belleudi et al., 2014). However, the molecular mechanism involved in FGFR2b-triggered autophagy is still to be elucidated (see below).

### **The fibroblast growth factor receptor 2b and its signaling in the control of autophagy in human keratinocytes**

The epithelial splicing transcript variant of the fibroblast growth factor receptor 2 (FGFR2b/KGFR) can be activated by the stimulation with the specific paracrine ligand FGF7 (see above), which is secreted by dermal fibroblasts. FGFR2b expression and signaling regulate different processes, including cell migration (Ceccarelli et al., 2007; Belleudi et al., 2011), differentiation (Belleudi et al., 2011; Purpura et al., 2013) and phagocytosis (Cardinali et al., 2005; Cardinali et al., 2008; Belleudi et al., 2011) in human keratinocytes.

The possible role of FGFR2b in the regulation of epidermal differentiation has been suggested in the past by several evidences. In fact, it has been observed that FGFR2b is mainly expressed in the spinous suprabasal layer of epidermis (La Rochelle et al., 1995; Marchese et al., 1995) and this receptor is up-regulated in the suprabasal keratinocytes compared to the basal cells (Marchese et al., 1997; Capone et al., 2000). More recently it has been demonstrated that FGFR2b induces early differentiation in keratinocytes during the switch from basal undifferentiated to suprabasal differentiating cells (Belleudi et al., 2011). The ligand-dependent activation and signaling of FGFR2b are required for the receptor ability to induce the early differentiation and using specific inhibitors of FGFR2b substrates, we demonstrated that the PI3K/AKT signaling pathway is the main involved in the

regulation of this process (Belleudi et al., 2011). The key role of FGFR2b in the regulation of early steps of keratinocyte differentiation has been also demonstrated by the evidence that the oncoprotein E5 of the human papillomavirus type 16 (HPV16) is able to impair this process (Purpura et al., 2013) also through a transcriptional and post-translational down-regulation of FGFR2b (Belleudi et al., 2011; Purpura et al., 2013).

Another important process regulated by FGFR2b is the phagocytosis, a key process used by the cells for the ingestion of particles larger than 0.5  $\mu\text{m}$  into single membrane compartments called phagosomes (Freeman and Grinstein, 2014). Phagocytosis particularly occurs in professional phagocytes, such as macrophages, dendritic cells and neutrophils (Freeman and Grinstein, 2014), but it can be triggered also in other cell types and, in particular, in epidermal keratinocytes this process is used for melanosome uptake. Melanosomes are large (0.5  $\mu\text{m}$ ) lysosomal-related organelles containing synthesized melanin, which are released by the neighboring melanocytes and are engulfed by keratinocytes to regulate photoprotection and pigmentation (Boissy et al., 2003; Van Den Bossche et al., 2006; Wasmeier et al., 2008). It has been previously demonstrated that FGF7-induced FGFR2b activation induces phagocytosis and consequently melanosome uptake in human keratinocytes (Cardinali et al., 2005; Cardinali et al., 2008; Belleudi et al., 2011). In addition, using a FGFR2b signaling mutant in which the tyrosine 769 required for PLC $\gamma$  binding and activation (Ceridono et al., 2005; Cha et al., 2009) has been substituted by phenylalanine (Y769F) (Ceridoni et al., 2005), we demonstrated that PLC $\gamma$ -mediated signaling is required for FGFR2b-triggered phagocytosis.

Even more recently a role of FGFR2b and its FGF7-induced signaling in the control of autophagy in human keratinocytes has been highlighted by us. Unlike other growth factors and similarly to FGF18 in chondrocytes, FGF7 and consequently its receptor activation triggers autophagy in human keratinocytes (Belleudi et al., 2014). In particular, using the inhibitor of endoplasmic reticulum (ER) Ca<sup>2+</sup>-ATPase pump family thapsigargin (Thastrup et al., 1990) to block the fusion between autophagosomes and lysosomes, we demonstrated that FGF7 triggers the early step of the autophagic process inducing the formation of new autophagosomes. In addition, we also found that FGF7 is also able to accelerate

the autophagosome fusion with lysosomes, protecting cells from their potentially dangerous accumulation and clustering in the cytosol (Belleudi et al., 2014). This last evidence is consistent with the well-known survival role of FGF7 in epithelial cells (Panos et al., 1995; Decraene et al., 2004; Lotti et al., 2007) and it is in agreement with recent evidences proposing a role for autophagy in contributing to skin pigmentation by regulating melanosome degradation in keratinocytes (Murase et al., 2013). The autophagic activity and consequently the melanosome degradation appeared to be higher in keratinocytes derived from light skin compared to those detected in keratinocytes from dark skin (Murase et al., 2013).

More interestingly we found an important link between autophagy and epidermal commitment to differentiation, demonstrating that FGF7-triggered autophagy is required for FGFR2b-induced early differentiation (Belleudi et al., 2014). The involvement of autophagy in cell differentiation may be explained by the fact that this degradative pathway could play a key role in mediating rapid proteins and organelles turnover which might be required for the rapid change of cell phenotype during differentiation (Cecconi et al., 2008; Di Bartolomeo et al., 2010). The differentiation program is essential to maintain tissue homeostasis and to promote keratinocyte regeneration through terminal differentiation, which involves cell organelle clearance, mediated in part by lysosomal degradation (Li et al., 2016). Starting from this hypothesis, a close interplay between differentiation and autophagy has been proposed in many cell types, including keratinocytes (Haruna et al., 2008; Aymard et al., 2011; Chatterjea et al., 2011; Moriyama et al., 2014 ; Belleudi et al., 2014, Chikh et al., 2014; Akinduro et al., 2016). In fact, autophagy seems to be required for epidermal terminal differentiation, as shown by the higher concentration of the autophagic marker LC3 in the granular layer (Haruna et al., 2008; Moriyama et al., 2014, Akinduro et al., 2016). However, other evidences indicated a role for this process even in the early stages of keratinocyte differentiation. In fact, the expression of LC3 is evident already in the suprabasal layer of the epidermis (Haruna et al., 2008) and it increases in parallel with the early differentiation markers keratin 1 (K1) and keratin 10 (K10) (Haruna et al., 2008; Belleudi et al., 2014; Chikh et al., 2014). In addition, K1 and K10 expression is repressed by the inhibition of autophagy in differentiating keratinocytes (Belleudi et al., 2014; Chikh et al., 2014). In addition, the autophagic markers, ATG5-ATG12

and Beclin 1, are expressed at high levels in the basal layer (Akinduro et al., 2016). Moreover, BCL2 and the adenovirus E1B 19-kDa-interacting protein 3 (BNIP3), a pro-apoptotic BH3-only protein, is able to promote keratinocyte differentiation inducing autophagy (Moriyama et al., 2014), while the expression of the protein iASPP, a p53 inhibitor, delays keratinocyte differentiation through the inhibition of autophagy (Chikh et al., 2014). iASPP is involved in a double positive loop with transcription factor  $\Delta Np63\alpha$ , which is expressed in the basal cells of stratified epithelia such as human epidermis (Candi et al., 2008) and it is required for keratinocytes differentiation (Truong et al., 2006; Candi et al., 2008). Therefore, the positive loop between iASPP and  $\Delta Np63\alpha$  plays a crucial role in epidermal homeostasis, and iASPP down-regulation is a key event determining autophagy induction,  $\Delta Np63\alpha$  repression and consequently induction of differentiation (Chikh et al., 2011; Chikh et al., 2014).

Autophagy is not only a degradative pathway correlated to cell differentiation, but it is also an interplaying process with phagocytosis at least in macrophages. In fact, it has been demonstrated that autophagy induction promotes the engulfment of phagosomes containing bacteria in autophagosomes to allow pathogen elimination (Gutierrez et al., 2004; Xu et al., 2007). Conversely, other studies have proposed that autophagy induction can lead to a down-modulation of the phagocytosis of yeast particles in murine macrophages (Lima et al., 2011) while its inhibition can enhance this process (Bonilla et al., 2013). Moreover, TLR signaling can induce the recruitment of some autophagic components, such as LC3 or Beclin 1, on the single membrane pathogen-containing phagosomes, without the formation of conventional autophagosome, in the process called LAP (LC3-associated phagocytosis) (Sanjuan et al., 2007). However, there are not evidences of a correlation between autophagy and phagocytosis in keratinocytes. Therefore, considering that these two processes are both regulated by FGF7-mediated activation of FGFR2b in keratinocytes, we proposed to investigate the existence of a possible interplay between FGF7-induced autophagy and phagocytosis. In addition, since it has been demonstrated that FGFR2b-induced phagocytosis required PLC $\gamma$  downstream signaling (Belleudi et al., 2011), while receptor-mediated autophagy is a PI3K-AKT-mTOR-independent process (Belleudi et al., 2014) whose specific signaling pathway

involved remains to be elucidated, we also proposed to investigate the role of PLC $\gamma$  signaling in FGF7-induced autophagy.

## **MATERIALS AND METHODS**

## Cells and treatments

The human keratinocyte cell line HaCaT was cultured in Dulbecco's modified Eagle's medium (DMEM) supplemented with 10% fetal bovine serum (FBS) plus antibiotics. HaCaT cells stably transfected with the construct pMSG 16E5 (HaCaT pMSG E5) or with the empty vector (HaCaT pMSG) were cultured as reported above and were treated with 1  $\mu$ M dexamethasone (Dex) for 12 h and 24 h to induce 16E5 expression. The human cervical keratinocyte cell line W12 initiated from a low-grade cervical lesion (Stanley et al., 1989), which retains ~100 to 200 copies of the HPV16 episomes per cell (Pett et al., 2004; Stanley et al., 2009; Gray et al., 2010), was cultured as previously described (Stanley et al., 1989) and used at the passage 6 (W12p6). Primary cultures of human keratinocytes derived from healthy skin (HKs) were obtained from patients attending the Dermatology Unit of the Sant'Andrea Hospital of Rome; all patients were extensively informed and their consent for the investigation was given and collected in written form in accordance with guidelines approved by the management of the Sant'Andrea Hospital. Primary keratinocytes were maintained in Medium 154-CF (Cascade Biologics, Portland, OR, USA) supplemented with Human Keratinocyte Growth Supplement (HKGS, Cascade Biologics) plus antibiotics and Ca<sup>2+</sup> 0,03 mM (CascadeBiologics Inc.).

Cells were transiently transfected or cotransfected with pCI-neo expression vector containing 16E5-HA (HaCaT E5, HKs E5), human FGFR2b WT (HaCaT FGFR2b WT), a kinase negative mutant FGFR2b Y656F/ Y657F (HaCaT FGFR2b kin-), a signaling mutant FGFR2b Y769F (HaCaT FGFR2b Y769F), the empty vector (HaCaT pCI-neo, HKs pCI-neo), with the pEGFP-C2 expression vector containing LC3 (engineered by Dr. Fimia, National Institute for Infectious Diseases IRCCS 'L. Spallanzani', Rome, Italy; and kindly provided by Prof. Francesco Cecconi, Tor Vergata University of Rome, Italy) (HaCaT EGFP-LC3, HKs EGFP-LC3, W12 EGFP-LC3) or with the pDest-mCherry-EGFP tandem expression vector containing LC3 (HaCaT mCherry-EGFP-LC3). For all transfections jetPEI™ DNA Transfection Reagent (Polyplus-transfection, New York, NY, USA) or Fugene HD (Promega, Madison, WI, USA) were used according to manufacturer's instructions.

For RNA interference and FGFR2b or 16E5 silencing, HaCaT cells were transfected with Bek small interfering RNA (Bek siRNA) (Santa Cruz Biotechnology Inc., Santa Cruz, CA, USA) or with unrelated siRNA as a control, while W12p6 cells were transfected with the E5 siRNA sequence (5'-TGGTATTACTATTGTGGATAA-3') (Oh et al., 2009) or the control sequence (5'-AATTCTCCGAACGTGTCACGT-3') (Oh et al., 2009) (Qiagen, Valencia, CA, USA), using Lipofectamine 2000 Transfection Reagent (Invitrogen, Carlsbad, CA, USA) according to the manufacturer's protocol.

For growth factor stimulation, cells were serum starved or incubated with FGF7 (Upstate Biotechnology, Lake Placid, NY, USA) 100 ng/ml for 24 h at 37°C. To inhibit AKT or ERK or JNK or PKC $\delta$ , cells were respectively incubated with the specific AKT inhibitor 1L-6-hydroxy-methyl-chiro- inositol 2-(R)-2-O-methyl-3-O-octadecylcarbonate (1  $\mu$ M; Calbiochem, San Diego, CA) or with the specific MEK1/2 inhibitor PD0325901 (1  $\mu$ M; Sigma-Aldrich Inc., Saint Louis, MO, USA) or with the specific JNK inhibitor SP600125 (50  $\mu$ M, Sigma) or with the specific PKC $\delta$  inhibitor rottlerin (0.5  $\mu$ M; Calbiochem) for 1 h at 37 °C before treatment with FGF7 in the presence of each inhibitor.

To irreversibly block the fusion between autophagosomes and lysosomes, HaCaT cells were incubated with bafilomycin A1 (20 nM; Sigma) for 3 h at 37 °C after treatment with FGF7 in the presence of the inhibitor.

To inhibit the autophagic degradation, cells were incubated with 20  $\mu$ M leupeptin (Sigma) for 24 h.

To analyze the uptake of beads in keratinocytes, HKs and HaCaT cells were incubated with fluorescent microspheres 0.5  $\mu$ m (red) in diameter (FluoSpheres Fluorescent Microspheres, Molecular Probes, Eugene, OR, USA) at the concentration of  $72 \times 10^7$  particles/ml for 4 hours. To evaluate the effects of FGFR2b activation on the phagocytic ability, the uptake was performed in the presence of FGF7 100 ng/ml (Upstate Biotechnology)

## **Immunofluorescence**

Cells, grown on coverslips and incubated as above, were fixed with 4% paraformaldehyde in PBS for 30 minutes at 25°C followed by treatment with 0.1 M

glycine for 20 minutes at 25°C and with 0.1% Triton X-100 for additional 5 minutes at 25°C to allow permeabilization. Cells were then incubated for 1h at 25°C with the following primary antibodies: rabbit polyclonal anti-Bek (1:50 in PBS; C-17, Santa Cruz Biotechnology), mouse monoclonal anti-HA (1:50 in PBS; Covance, Berkeley, CA, USA). The primary antibodies were visualized, after appropriate washing with PBS, using goat anti-rabbit IgG-Texas Red (1:200 in PBS; Jackson ImmunoResearch Laboratories, 111-075-144), goat anti-mouse IgG-Texas Red (1:200 in PBS; Jackson ImmunoResearch Laboratories) for 30 minutes at 25°C. Nuclei were stained with DAPI (1:1000 in PBS; Sigma). Coverslips were finally mounted with mowiol for observation.

Fluorescence signals were analyzed by scanning cells in a series of 0.5 mm sequential sections with an ApoTome System (Zeiss, Oberkochen, Germany); image analysis was then performed by the Axiovision software (Zeiss) and 3D reconstruction of a selection of three central optical sections was shown in each figure. Quantitative analysis of EGFP-LC3-positive dots per cell was performed analyzing 100 cells for each sample in 5 different microscopy fields from 3 different experiments. Quantitative analysis of the bead uptake was performed by counting the number of internalized beads in 100 cells for each condition, randomly taken from 10 microscopic fields in 3 different experiments. Quantitative analysis of the extent of colocalization of beads with EGFP-LC3 was performed by the analysis of 100 cells for each sample in 5 different fields randomly taken from 3 independent experiments and using the KS300 3.0 Image Processing System (Zeiss). Results have been expressed as mean values  $\pm$  standard errors (SE). p values were calculated using Student's t test and significance level has been defined as  $p < 0.05$ .

### **Western blot analysis**

Cells were lysed in a buffer containing 50 mM HEPES pH 7.5, 150 mM NaCl, 1% glycerol, 1% Triton X-100, 1.5 mM MgCl<sub>2</sub>, 5 mM EGTA, supplemented with protease inhibitors (10  $\mu$ g/ml aprotinin, 1mM PMSF, 10 $\mu$ g/ml leupeptin), and phosphatase inhibitors (1mM sodium orthovanadate, 20 mM sodium pyrophosphate, 0.5 M NaF). A range between 50 and 20  $\mu$ g of total protein were

resolved under reducing conditions by 8 or 12% SDS-PAGE and transferred to reinforced nitrocellulose (BA-S 83, Schleider and Schuell, Keene, NH, USA). The membranes were blocked with 5% nonfat dry milk in PBS 0.1% Tween 20 or with 3% BSA in PBS 0.1% Tween 20, and incubated with anti-Bek (C-17, Santa Cruz Biotechnology Inc.) polyclonal antibodies, anti-LC3 (MBL, Woburn, MA, USA) polyclonal antibodies, anti-SQSTM1 (BD Bioscience, San José, CA, USA) monoclonal antibody, anti-HA (Covance) monoclonal antibody, anti-P-p44/42 MAPK (P-ERK1/2) (Thr202/Tyr204, Cell Signaling Technology, Beverly, MA) polyclonal antibodies, anti-p-AKT (Ser 473, Cell Signaling) polyclonal antibodies, anti p-JNK (G9, Cell Signaling) monoclonal antibody, anti p-PKC $\delta$  (Tyr-155, Santa Cruz Biotechnology) polyclonal antibodies followed by enhanced chemiluminescence detection (ECL; Amersham, Alington Heights, IL). The membranes were rehydrated by being washed in PBS-Tween 20, stripped with 100 mM mercaptoethanol and 2% SDS for 30 min at 55°C, and probed again with anti-AKT (H-136, Santa Cruz Biotechnology Inc.) polyclonal antibodies, anti-p44/42 MAPK (ERK1/2) (137F5, Cell Signaling) polyclonal antibodies, anti-JNK (Cell Signaling) polyclonal antibodies, anti-PKC $\delta$  (C-20, Santa Cruz Biotechnology) polyclonal antibodies, anti- $\beta$ -actin (Sigma) monoclonal antibody or anti- $\alpha$ -Tubulin (Cell Signaling) polyclonal antibodies to estimate the protein equal loading.

Densitometric analysis was performed using Quantity One Program (Bio-Rad Laboratoires, Hercules, CA). Briefly, the signal intensity for each band was calculated and the background subtracted from experimental values. The resulting values from three different experiments were then normalized and expressed as fold increase respect to the control value.

### **Transmission electron microscopy**

HaCaT cells stimulated with FGF7 for 24 h and treated with red fluorescent beads for the last 4 h as above or HaCaT pMSG E5 and HaCaT pMSG cells treated with Dex and stimulated with FGF7 for 24 h as above were washed three times in PBS and fixed with 2% glutaraldehyde (Electron Microscopy Science, 16300) in PBS for 2 h at 4°C. Samples were postfixed with 1% osmium tetroxide in veronal

acetate buffer (pH 7.4) for 1 h at 25 °C, stained with uranyl acetate (5 mg/ml) for 1 h at 25°C, dehydrated in acetone and embedded in Epon 812 (EMbed 812, Electron Microscopy Science). Ultrathin sections were examined unstained or poststained with uranyl acetate and lead hydroxide, under a Morgagni 268D transmission electron microscope (FEI, Hillsboro) equipped with a Mega View II charge-coupled device camera (SIS, Soft Imaging System GmbH) and analyzed with AnalySIS software (SIS).

## Primers

Oligonucleotide primers for target genes and for the housekeeping gene were chosen with the assistance of the Oligo 5.0 computer program (National Biosciences, Plymouth, MN, USA) and purchased from Invitrogen. The following primers were used: for HPV 16E5 target gene 5'-CGCTGCTT TTGTCTGTGTCT-3'(sense), 5'-GCGTGCATGTGTATGTATTA AAAA-3'(antisense); for BECN1 target gene 5'-GGATGGTGTCTCTCGCAGAT-3'(sense), 5'-TTGGCACTTTCTIGTGG ACAT-3'(antisense); for ATG5 target gene 5'-CAACTTGTTTCACGCTATATCAGG-3'(sense), 5'-CACTTTGTTCAGTTACCAACGTCA-3'(antisense); for ATG7 target gene 5'-CCGTGGAATTGATGGTATCTG-3'(sense), 5'-TCATCCGATCGTCACTGCT-3'(antisense); for MAP1LC3B target gene 5'-CGCACCTTCGAACAAAGAG-3'(sense), 5'-CTCACCTTGTATCGTTCTATTATCA-3' (antisense); for ULK1 target gene 5'-CAGACGACTTCGTCATGGTC-3'(sense), 5'-AGCTCCCCTGCACATCAG-3'(antisense); for ULK2 target gene 5'-TTTAAATACAGAACGACCAATGGA-3'(sense), 5'-GGAGGTGCCAGAACACCA-3'(antisense); for ATG4a target gene 5'-CCGTCCGTAGTCAAGT TGC-3'(sense), 5'-TCTGATCTTCATACTTGGATAAAA CTG-3' (antisense); for p21 target gene: 5'-TCACTGTCTTGTACCCTTGTGC-3'(sense), 5'-GGC GTTTGGAGTGGTAGAAA-3'(antisense); for 14-3-3 sigma target gene: 5'-GACACAGAGTCCGGCATTG-3'(sense), 5'-ATGGCTCTGGGGACACAC- 3'(antisense); for the housekeeping 18S rRNA gene: 5'-AACCAACCCGGTCAGCCCCT-3'(sense), 5'-TTCGAATGGGTCGTCGCCGC-3'(antisense). For each primer pair, we performed no-template control and no-

reverse-transcriptase control (RT negative) assays, which produced negligible signals.

### **RNA extraction and cDNA synthesis**

RNA was extracted using the TRIzol method (Invitrogen, Carlsbad, CA) according to manufacturer's instructions and eluted with 0,1% diethylpyrocarbonate (DEPC)-treated water. Each sample was treated with DNAase I (Invitrogen). Total RNA concentration was quantitated by spectrophotometry. 1 µg of total RNA was used to reverse transcription using iScript<sup>TM</sup> cDNA synthesis kit (Bio-Rad Laboratories) according to manufacturer's instructions.

### **PCR amplification and real-time quantitation**

Real-time PCR was performed using the iCycler Real-Time Detection System (iQ5 Bio-Rad) with optimized PCR conditions. The reaction was carried out in 96-well plate using iQ SYBR Green Supermix (Bio-Rad) adding forward and reverse primers for each gene and 1µl of diluted template cDNA to a final reaction volume of 15 µl. All assays included a negative control and were replicated three times. The thermal cycling programme was performed as follows: an initial denaturation step at 95°C for 3 minutes, followed by 45 cycles at 95°C for 10 seconds and 60°C for 30 seconds. Real-time quantitation was performed with the help of the iCycler IQ optical system software version 3.0a (BioRad), according to the manufacturer's manual. The relative expression of the housekeeping gene was used for standardizing the reaction. The comparative threshold cycle ( $C_t$ ) method was applied to calculate the fold changes of expression compared to control cells. Results are reported as mean  $\pm$  standard deviation (SD) from three different experiments in triplicate.

## **RESULTS**

## **FGFR2b-mediated phagocytosis and autophagy are convergent intracellular membrane pathways regulated by PLC $\gamma$ signaling.**

It has been recently demonstrated that FGFR2b expression and signaling trigger both autophagy (Belleudi et al., 2014) and phagocytosis (Cardinali et al., 2005; Belleudi et al., 2011) in human keratinocytes. To assess the existence of a possible coordination between FGF7-induced autophagy and phagocytosis and to ascertain whether these processes could involve converging autophagosomal and phagosomal compartments, we took advantage of the use of an *in vitro* model of bead uptake widely used to study the phagocytic capacity of epidermal keratinocytes (Wolff et al., 1972; Virador et al., 1992; Desjardins et al., 2003). The ability of the human keratinocyte HaCaT cell line, spontaneously immortalized from a primary culture of keratinocytes (Boukamp et al., 1988), to either engulf and to sort the engulfed beads to the degradation also via autophagy was analyzed in response to FGF7. To this aim HaCaT cells were transiently transfected with pEGFP-C2-LC3 construct and stimulated with FGF7 for 24 h. For the last 4 h of the treatment cells were also incubated with inert latex red fluorescent beads 0.5  $\mu$ m in diameter. Concentrations of both FGF7 and bead, as well as the times of treatments, were selected based on our published results (Cardinali et al., 2005; Cardinali et al., 2008; Belleudi et al., 2011). Cells were fixed, permeabilized and nuclei were stained with DAPI. Quantitative fluorescence analysis performed as reported in Materials and Methods, showed that, as expected, the treatment with FGF7 increased bead uptake (Cardinali et al., 2005; Belleudi et al., 2011) (Figure 6A) as well as the amount of EGFP-LC3 positive dots per cell (Belleudi et al., 2014) (Figure 6A). In addition, only a part of internalized fluorescent beads (18%) appeared to colocalize with LC3 (Figure 6A). This not so tight colocalization and the presence of distal formation of autophagosomes (LC3-positive dots which did not colocalize with beads) strongly indicated that LC3 associates with canonical new-formed autophagic vesicles and not directly with the membrane of all the nascent phagosomes, as occurs during the LC3-associated phagocytosis (LAP). This is in agreement with previous findings demonstrating that inert beads fail to activate LAP in macrophages (Martinez et al., 2015). In order to unequivocally demonstrate that these LC3 positive dots containing beads

may correspond to autophagosomal structures, electron microscopy studies were performed in HaCaT cells stimulated with beads in presence of FGF7 as above. Ultrastructural examination revealed the presence of single (Figure 6B, asterisks, *i*, *ii*, *iii*) and clustered beads (Figure 6B, asterisks, *iv*) in either single-membrane (Figure 6B, arrows, *ii*) and double-membrane (Figure 6B, arrowheads, *ii*, *iii*, *iv*) vacuoles corresponding to phagosomes and autophagosomes, respectively. Several clustered beads are also visible in vacuoles ultrastructurally recognizable as lysosomes (data not shown), confirming that, independently from the chosen pathway, the final fate for the engulfed beads is the accumulation in the degradative compartment. These results clearly suggest that, in response to FGF7, part of the phagosomes containing the engulfed beads are isolated in new-forming autophagosomes, that possibly mediate their targeting to lysosomes.

Since PLC $\gamma$  activation/phosphorylation is required for FGFR2b-mediated phagocytosis (Belleudi et al., 2011), to investigate the role of this signaling in FGF7-induced autophagy we transiently transfected HaCaT cells with a FGFR2b signaling mutant in which the tyrosine 769, required for PLC $\gamma$  binding and activation (Ceridono et al., 2005; Cha et al., 2009) has been substituted by phenylalanine (Y769F) (Ceridono et al., 2005). The transfection with FGFR2b wild type (HaCaT FGFR2b WT), with a Y656F/Y657F FGFR2b kinase dead mutant (HaCaT FGFR2b kin<sup>-</sup>) (Belleudi et al., 2006) or with pCI-neo empty vector (HaCaT pCI-neo) was used as control. After transfection, cells were serum-starved and stimulated with FGF7 for 24 h and the amount of the widely accepted marker for autophagosomes (Kabeya et al., 2000; Wu et al., 2006), the 16-kDa membrane-associated microtubule associated protein 1 light chain 3-II (LC3-II) was analyzed by western blot. To focus the attention on the possible impact of PLC $\gamma$  signaling shut-down exclusively on the assembly step of the autophagosomes, their degradation was selectively blocked stimulating cells with FGF7 in the presence of bafilomycin A1, an inhibitor of the vacuolar type H<sup>+</sup>-ATPase (v-ATPase) able to block the fusion of autophagosomes with lysosomes (Juhász et al., 2012). We selected this drug for the interference of the autophagosome-to-lysosome fusion because, differently from other agents, including monensin or chloroquine, bafilomycin does not activate LC3 association with single intracellular membrane,

such as endosomes or lysosomes (Florey et al., 2015). The results surprisingly showed that, in a similar manner to what observed in cells overexpressing FGFR2b kin<sup>-</sup> (Figure 7A), in cells overexpressing FGFR2b Y769F the amount of LC3-II level was not affected by FGF7 stimulation (Figure 7A), suggesting that PLC $\gamma$  signaling downstream FGFR2b is indispensable for FGF7-induced autophagosome assembly. In agreement with our previous evidences (Belleudi et al., 2014) the increase of LC3-II levels after serum deficiency was further increased in response to FGF7 in pCI-neo cells (Figure 7A) and appeared more pronounced in FGFR2b WT cells (Figure 7A). The impact of PLC $\gamma$  signaling in the induction of autophagy was also investigated by fluorescence approaches. To quantify the autophagosome number in cells forced to overexpress the different forms of FGFR2b, HaCaT cells were alternatively co-transfected with pEGFP-C2-LC3 construct and pCI-neo empty vector, FGFR2b WT, FGFR2b kin<sup>-</sup> or the FGFR2b Y769F. Cells were then treated with FGF7 as above, fixed, permeabilized and nuclei were stained with DAPI. Quantitative immunofluorescence analysis performed using anti-FGFR2b polyclonal antibody, to visualize transfected FGFR2b WT or mutants, showed that, similarly to FGFR2b kin<sup>-</sup>, FGFR2b Y769F overexpression induced a drastic reduction of the number of LC3-positive dots compared to that observed in HaCaT EGFP-LC3/pCI-neo and in HaCaT EGFP-LC3/FGFR2b WT cells (Figure 7B) or in HaCaT EGFP-LC3/FGFR2b Y769F and in EGFP-LC3/FGFR2b kin<sup>-</sup> surrounding cells not showing detectable receptor mutant overexpression (Figure 7B, arrowheads). On the other hand, differently from the kinase dead mutant (Figure 7B), both FGFR2b WT and FGFR2b Y769F signals appeared concentrated in intracellular dots (Figure 7B) confirming that PLC $\gamma$  signaling is not required for ligand-dependent receptor internalization (Ceridono et al., 2005). Overall our evidences strongly suggest that the specific signaling downstream PLC $\gamma$  is indispensable for FGF7-induced autophagy and that its shut-down results in a significant inhibition of the process.

## **FGFR2b-induced autophagy requires PLC $\gamma$ -mediated phosphorylation/activation of JNK.**

Autophagy can be controlled by several mTOR-dependent or mTOR-independent signaling pathways (Yang et al., 2010; Russell et al., 2014). While it has been demonstrated that FGF2 negatively impacts on autophagy through the activation of AKT/mTOR signaling (Lin et al., 2011; Zhang et al., 2012), it has been recently demonstrated that FGF7 increases autophagy through a not yet identified PI3K/AKT/mTOR-independent pathway (Belleudi et al., 2014). Therefore, we focused our attention on the JNK1-mediated signaling pathway, which is mTOR-independent (Russell et al., 2014) and it has been recently identified as mainly involved in FGFR4-mediated autophagy in osteoclasts (Cinque et al., 2015). In order to assess the possible impact of the JNK1 pathway in FGF7-mediated autophagy, and to establish if and how PLC $\gamma$  is involved in the activation of the JNK1 pathway, we compared the levels of phosphorylation/activation of this kinase and of other important FGFR2b signaling substrates involved in the control of autophagy, such as ERK1/2, in HaCaT pCI-neo, HaCaT FGFR2b WT cells and HaCaT FGFR2b Y769F cells. AKT phosphorylation was checked to further confirm the independence of FGF7-mediated autophagy from the canonical PI3K/AKT/mTOR regulating pathway. Western blot analysis showed that upon FGF7 stimulation all the checked substrates appeared phosphorylated in HaCaT pCI-neo and HaCaT FGFR2b WT cultures, indicating that in these cells all the signaling pathways downstream FGFR2b are activated (Figure 8A). In contrast, in HaCaT FGFR2b Y769F cells ERK1/2 and AKT appeared normally phosphorylated, while JNK1 phosphorylation was significantly reduced (Figure 8A). These evidences indicated that PLC $\gamma$  recruitment to FGFR2b and its consequent phosphorylation are required for an efficient activation of the JNK1-mediated signaling pathway. JNK1 pathway is canonically activated by several MAP3 kinases, which in turn activate MKK4 and MKK7 that induce JNK phosphorylation (Katz et al., 2007). However, it has been recently demonstrated that PKC $\delta$  is the upstream substrate mainly responsible for the activation of the JNK1 pathway, during hypoxia-mediated autophagy (Chen et al., 2008; Chen et al., 2009). PKC $\delta$  is a direct substrate of PLC $\gamma$  (Steinberg, 2008) activated by FGFRs,

including FGFR2 (Kim et al., 2003). In order to establish the relevance of PKC $\delta$  activation in the triggering of FGF7-mediated autophagy, we compared its phosphorylation levels in cells alternatively overexpressing FGFR2b or FGFR2b Y769F or pCI-neo as control. Western blot analysis clearly demonstrated that, in agreement with the observed attenuation of JNK1 phosphorylation, a corresponding reduction of PKC $\delta$  phosphorylation was detectable in cells overexpressing FGFR2b Y769F (Figure 8B). These findings strongly suggest that in FGFR2b Y769F cells the observed block of FGF7-induced autophagy is due to the inhibition of PLC $\gamma$ -mediated signaling, which is accompanied by PKC $\delta$  inactivation and possibly consequent JNK1 pathway shut-down.

To ascertain the relevance of JNK1 repression for the block of FGF7-induced autophagy observed in cells expressing FGFR2b PLC $\gamma$  signaling mutant, we estimated the impact of specific kinase inhibitors on LC3-II levels in either HaCaT pCI-neo and in HaCaT FGFR2b WT. For JNK1, we used the same JNK inhibitor (SP600125) used to interfere with FGF18/FGFR4-triggered autophagy (Cinque et al., 2015), while the impairment of ERK1/2 signaling was obtained using the inhibitor of the upstream substrates MEK1/2, which efficiently blocks this pathway during ligand-mediated activation of FGFRs (Nakanishi et al., 2015). The effect of the AKT inhibitor previously used by us (Belleudi et al., 2011; Belleudi et al., 2014) was checked again to further confirm that the canonical PI3K/AKT/mTOR pathway could not affect the FGF7-mediated autophagy. Western blot analysis performed using antibodies directed against the phosphorylated forms of each substrate confirmed that all the inhibitors were highly specific (Figure 9). Results obtained in both HaCaT FGFR2b WT and HaCaT pCI-neo cells showed that only the JNK1 inhibitor was able to interfere with increase of LC3-II induced by FGF7 (Figure 10C), while both AKT and MEK1/2 inhibitors were ineffective (Figure 10A and B). The impairment induced by JNK1 inhibitor on FGF7-induced LC3 increase was comparable to that observed in cells expressing the PLC $\gamma$ -mediated signaling mutant FGFR2b Y769F (Figure 7A), strongly suggesting that in FGFR2b Y769F-expressing cells the observed attenuation of JNK1 signaling is responsible for the repression of FGF7-triggered autophagy. Since we have postulated that PKC $\delta$  could be possibly the substrate

downstream PLC $\gamma$  acting upstream JNK1, we also analyzed the effect of the direct inhibition of PKC $\delta$  on autophagy. We found that in cells stimulated with FGF7, the treatment with the PKC $\delta$  inhibitor resulted in reduction of phosphorylation/activation of PKC $\delta$  (Figure 9) and in a repressive effect on LC3-II levels (Figure 10D) that was comparable to that found upon JNK1 inhibition (Figure 10C) or PLC $\gamma$  signaling shut-down in FGFR2b Y769F expressing cells (Figure 7A). Overall our results suggest that the PLC $\gamma$  signaling pathway is the main responsible for the triggering of FGFR2b-induced autophagy. The use of specific inhibitors confirmed that the autophagic process controlled by FGFR2b is PI3K/AKT/mTOR independent and requires the activation of JNK1, which possibly occurs via PKC $\delta$  activation.

#### **FGFR2b enhances FGF7-mediated autophagy, phagocytosis and their convergence in light skin primary HKs.**

It has been previously demonstrated that FGFR2b-induced PLC $\gamma$  signaling is required for FGF7-stimulated phagocytosis and consequent melanosome uptake in keratinocytes (Belleudi et al., 2011); here we demonstrated that the same signaling pathway is involved in FGFR2b-mediated autophagy in these cells and that FGF7-mediated phagocytosis and autophagy are converging pathways to possibly ensure melanosome degradation. In agreement with this possibility, in HKs from light skin, where FGFR2b-mediated uptake of the melanosomes is higher than in HKs from dark skin as a consequence of an higher expression of FGFR2b (Cardinali et al., 2008), the reduced number of intracellular melanosomes was the consequence of an accelerated ability to degrade them by autophagy (Murase et al., 2013). In a recent work we also speculated that in light skin HKs FGFR2b, in virtues of its ability to accelerate the autophagosome turnover, could be responsible for melanosome removal via autophagy (Belleudi et al., 2014). On the base of this hypothesis we wondered if FGFR2b could be involved not only in the regulation of both phagocytosis and autophagy, but also in the fine control of their balance. To ascertain it, we used again the *in vitro* model of bead uptake and we compared the ability of HKs from light and dark skin to either engulf and to

sort the engulfed beads to the degradation via autophagy in response to FGF7. To this aim, light and dark keratinocytes were transiently transfected with pEGFP-C2-LC3 construct and treated with FGF7 and with inert latex red fluorescent beads as above. Quantitative fluorescence analysis performed as reported in Materials and Methods, confirmed that, as expected (Cardinali et al., 2008) and consistently with the increased expression of FGFR2b (Figure 11), the treatment with FGF7 increased the bead uptake more in light skin keratinocytes than dark skin ones (Figure 12). In addition, in light skin HKs, FGF7 stimulation significantly increased the amount of EGFP-LC3 positive dots per cell more than in dark ones and only a part of beads (26%) colocalized with them (Figure 12). In the complex the results indicate that, in light skin HKs, but not in the dark ones, the uptake of beads and their confluence in nascent autophagosomes for sorting to degradation are both enhanced by FGF7 stimulation.

### **Impairment of FGFR2b-induced autophagy in HPV16E5 expressing keratinocytes**

It has been demonstrated that FGFR2b expression can be down-regulated, both transcriptionally and post translationally, by the early protein E5 of the human papillomavirus type 16 (HPV16) (Belleudi et al., 2011; Purpura et al., 2013), which represents a major risk factor for cervical cancer development and progression (zur Hausen, 2002; Moody and Laimins, 2010). The E5 protein is a small, weakly oncogenic protein, which cooperates with the two oncogenes of HPV16, E6 and E7, promoting epithelial transformation and cervical carcinogenesis (Moody and Laimins, 2010; Venuti et al., 2011; DiMaio and Petti, 2013). The oncogenic activity of the E5 protein is also related to its ability to interfere with the expression signaling and trafficking of different receptor tyrosine kinases (RTKs) (Belleudi et al, 2011; reviewed in DiMaio and Petti, 2013). Consistently with the widely described correlation between autophagy and oncogenic virus infection (Mack and Munger, 2012; Silva and Jung, 2013), recent evidences have proposed the existence of an interplay between autophagy and HPV16 infection. In fact, autophagy seems to be induced after HPV16 infection in

host epithelial cells while the inhibition of this process enhances the viral infectivity (Griffin et al., 2013). Interestingly, another study has demonstrated that the depletion of all the HPV16 early proteins leads to a strong increase of autophagy in infected cervical keratinocytes (Hanning et al., 2013), suggesting for the entire “early protein group” of HPV16 an inhibitor role on autophagy. Nevertheless, the single contribution of each of the early proteins and the molecular mechanisms involved remain to be clarified. Starting from the observation that E5 protein of HPV16 (16E5) down-regulates the expression of FGFR2b (Belleudi et al., 2011; Purpura et al., 2013), which is able to induce autophagy in human keratinocytes (Belleudi et al., 2014), we investigated the effects of 16E5 ectopic expression on FGF7-induced autophagy in human keratinocytes.

To this aim, HaCaT cells were transiently transfected with pCI-neo E5-HA expression vector (Ashrafi et al., 2005) (HaCaT E5) or with the empty vector alone (HaCaT pCI-neo). The expected high expression of 16E5 mRNA transcript levels in HaCaT E5 (Purpura et al., 2013) was first confirmed by real-time relative RT-PCR and normalized with respect to the levels of the viral protein transcript in the HPV16-positive cervical epithelial cell line W12 (Stanley et al., 1989) at the passage 6 (W12p6) (Figure 13A). Then, to investigate the possible effects of 16E5 expression on FGF7-induced autophagy, HaCaT pCI-neo and HaCaT E5 cells were serum-starved in the presence or absence of FGF7 for 24 h. Both the growth factor concentration and the single time point of treatment have been previously selected as optimal experimental conditions for an efficient autophagic induction in HaCaT cells (Belleudi et al., 2014). The amount of LC3-II was monitored by western blot analysis. The results showed that, after FGF7 stimulation, the increase of the 16 kDa band corresponding to LC3-II marker, evident in HaCaT pCI-neo cells (Figure 13B), appeared significantly reduced in HaCaT E5 cells (Figure 13B), indicating that the FGF7-induced autophagosome formation was counteracted by the presence of 16E5.

To more carefully investigate the effect of 16E5 expression on the autophagic flux, the levels of the well-known autophagy substrate SQSTM1/p62 (sequestosome 1) were estimated by western blot analysis. The evident decrease of the 62 kDa band corresponding to SQSTM1, observed in HaCaT pCI-neo cells

upon FGF7 stimulation, appeared significantly recovered in HaCaT E5 cells (Figure 13C), indicating that the SQSTM1 degradation was prevented in 16E5-expressing cells. Moreover, the accumulation of this autophagic substrate seems to indicate that the viral protein acts by inhibiting the formation of new autophagosomes, rather than by accelerating their turnover.

The interference of 16E5 expression on the enhanced autophagy was also investigated by the widely accepted fluorescence approach. To directly quantify the autophagosome number in cells ectopically expressing 16E5 and to easily compare it with cells which did not express the viral protein, HaCaT cells were transiently cotransfected with pEGFP-C2-LC3 construct and pCI-neo E5-HA (HaCaT EGFP-LC3/E5) or pCI-neo empty vector (HaCaT EGFP-LC3) as a control. Cells were then treated with FGF7 as above, fixed, permeabilized and nuclei were stained with DAPI. Quantitative immunofluorescence analysis was performed using anti-HA monoclonal antibody to visualize the viral protein. Results clearly showed that, upon FGF7 treatment, a significant increase of the LC3-positive dots per cell, corresponding to the assembled autophagosomes, was evident in HaCaT EGFP-LC3 cells (Figure 13D, middle panels, arrows) or in HaCaT EGFP-LC3/E5 cells not showing 16E5 expression (Figure 13D, lower panels, arrows), while this increase appeared significantly abolished in HaCaT EGFP-LC3/E5 cells highly expressing 16E5 (Figure 13D, lower panels, arrowhead). Interestingly, in these latter cells, the number of LC3 positive dots was even lower than that observed in serum-starved control cells (Figure 13D, upper panels). Since serum starvation is per se an autophagic stimulus, these results suggest that 16E5 might play a more general role, independent on FGF7, in autophagy impairment.

To clarify whether the inhibition of FGF7-dependent autophagy induced by 16E5 is directly related to its previously reported ability to down-regulate FGFR2b expression and signaling (Belleudi et al., 2011; Purpura et al., 2013), we first compared the effects of 16E5 expression to those induced by FGFR2b depletion. HaCaT cells were singly transfected with 16E5 cDNA or with a small interfering RNA for FGFR2/Bek (HaCaT FGFR2b siRNA) or an unrelated siRNA (HaCaT control siRNA) as control and then stimulated with FGF7 as above. In addition, in order to assess whether the possible effects induced by FGFR2b depletion can be

counteracted by its simultaneous forced expression, cells were also doubly transfected with FGFR2b siRNA and pCI-neo vector containing human FGFR2b WT (HaCaT FGFR2b WT cDNA/FGFR2b siRNA). Western blot analysis showed that both 16E5-transfected and FGFR2b-depleted cells not only displayed receptor down-regulation as expected (Purpura et al., 2013), but also a significant decrease of LC3-II levels as well as a block of SQSTM1 degradation in response to FGF7 (Figure 14A). Moreover, the inhibitory effects on autophagy induced by FGFR2b depletion was reverted by the simultaneous overexpression of the receptor (Figure 14A). Thus, 16E5 expression and FGFR2b silencing appeared to affect the autophagic process in a similar manner. To further demonstrate the receptor involvement on the 16E5 effect on autophagy, we performed FGFR2b forced overexpression in the presence of the viral protein: to this aim, cells were transiently cotransfected with 16E5 (HaCaT E5) and FGFR2b WT (HaCaT E5/FGFR2b WT) or the kinase negative mutant FGFR2bY656F/Y657F (HaCaT E5/FGFR2b kin<sup>-</sup>). After transfection, cells were stimulated with FGF7 as above. Western blot analysis clearly showed that the 16E5-induced decrease of LC3-II levels as well as SQSTM1 accumulation was reverted by the expression of FGFR2b WT, but not by that of FGFR2b kin<sup>-</sup> (Figure 14B). Therefore, FGFR2b forced expression and receptor activation are sufficient to counteract the inhibitory effect of 16E5 on the autophagy upon growth factor treatment. These results demonstrate that, although the molecular mechanisms remain to be clarified, 16E5 appears to impact the pro-autophagic FGFR2b pathway through the down-regulation of the receptor.

To deeper investigate the possibility that 16E5 might play a more general role in autophagy impairment, the possible effects of its ectopic expression were analyzed in cells subjected to serum starvation, an autophagic stimulus in which the contribution of FGFR2b signaling is completely excluded. HaCaT pCI-neo and HaCaT E5 cells were kept in complete medium or serum-starved for the two time points (24 h and 48 h) previously selected as optimal conditions for an efficient induction of autophagy in HaCaT cells (Belleudi et al., 2014). Western blot analysis performed as above showed that in HaCaT E5 cells the progressive increase of LC3-II marker was significantly affected (Figure 15A), while the SQSTM1 degradation was totally abolished (Figure 15B). The interference of 16E5

expression was also investigated by immunofluorescence as above. The results showed that the significant increase of the LC3-positive dots induced by 24 h of serum starvation, evident in HaCaT EGFP-LC3 (Figure 15C, arrow), was completely blocked in HaCaT EGFP-LC3/E5 (Figure 15C, arrowheads), unequivocally demonstrating that the presence of the viral protein prevents the increase of autophagosomes in response to serum deprivation. Thus, independently from the stimulus that triggers the process, 16E5 appears to generally interfere with autophagy.

In order to confirm that 16E5 is able to impact the autophagy on-rate, rather than the autophagy off-rate, as already indicated above by SQSTM1 monitoring, immunofluorescence experiments were performed doubly transfecting HaCaT cells with 16E5 and a pDest-mCherry-EGFP-LC3 tandem construct (Pankiv et al., 2007). In fact, mCherry-EGFP-LC3 is an autophagic flux sensor, since EGFP fluorescence is quenched in acidic environments, whereas mCherry is an acidic-stable fluorescent tag: the nascent autophagosomes are both red and green (yellow) labeled, whereas the acidic autolysosomes appear red, as a consequence of the EGFP quenching. Quantitative immunofluorescence analysis performed upon either serum deprivation and FGF7 stimulation showed that 16E5 expression led to a significant decrease in the number of yellow dots per cells corresponding to newly assembled autophagosomes (Figure 16A), while the quantity of red dots corresponding to autophagosomes flowed in the lysosomes was not affected (Figure 16A). The inhibitory effect of 16E5 on autophagosome formation was further confirmed monitoring the LC3-II levels in presence or absence of the well known lysosomal protease inhibitor leupeptin (LEU, Figure 16B), which inhibits the vacuolar type H<sup>+</sup>-ATPase (v-ATPase) complex necessary for lysosomal acidification (Juhász et al., 2012). Western blot analysis performed upon serum deprivation or FGF7 stimulation showed that 16E5 expression significantly decreases LC3-II levels also in the presence of the inhibitor of the autophagic flux (Figure 16B), confirming that, independently from the stimulus that triggers autophagy, 16E5 exerts an inhibitory role in the autophagosome assembly.

In order to define whether the effect of 16E5 on autophagy could be dose-dependent, we took advantage of the use of HaCaT cells stably transfected with the construct pMSG 16E5 (HaCaT pMSG E5) (Oelze et al., 1995), in which the

expression of the viral protein can be progressively induced, in a time-dependent manner, by treatment with dexamethasone (Dex). The HaCaT pMSG cells were used as negative control. Cells were left untreated (0 h) or treated with Dex for 12 h or 24 h, and the increasing 16E5 mRNA transcript levels were quantitated by real-time relative RT-PCR. The mRNA amounts were normalized respect to the levels expressed in W12p6 cells. The results clearly indicated that in HaCaT pMSG E5 cells, which expressed very low levels of 16E5 mRNA also in absence of Dex treatment (Oelze et al., 2015; Muto et al., 2011; French et al., 2013), the increasing levels of 16E5 mRNA after Dex stimulation remain lower than those observed in the endogenous model of W12p6 cells (Figure 17A). To first analyse the impact of the progressive expression of 16E5 on basal autophagy, cells were kept in complete medium and treated with Dex as above. Western blot analysis showed that in HaCaT pMSG E5 cells the low expression of LC3-II protein was decreased already after 12 h of Dex treatment and no further decrease was observed after 24 h (Figure 17B, left panel). Interestingly, no changes on LC3-II amounts were induced by Dex in control cells (Figure 17B, left panel), demonstrating that the inhibitory effect observed in HaCaT pMSG E5 cells can be specifically ascribed to 16E5 expression. In addition, these results indicate that the observed inhibition of autophagy does not occur only when the viral protein is overexpressed.

Then, our attention was shifted from the basal to induced-autophagy. Western blot analysis showed that the evident increase of LC3-II levels induced by both serum starvation (Figure 17B, middle panel) and FGF7 stimulation (Figure 17B, right panel) appeared completely abolished upon Dex treatment in HaCaT pMSG E5 cells; again, no effects were found in control cells, confirming the exclusive role of 16E5. Interestingly, in absence of Dex treatment, the increase of LC3-II protein caused by FGF7 appeared significantly lower in HaCaT pMSG E5 than in control cells (Figure 17B, right panel), implying that the low levels of 16E5 expressed by these cells in Dex-untreated conditions (see Figure 17A) were sufficient to interfere with the enhancement of autophagy induced by FGF7 (Figure 17B, right panel). The ability of 16E5 to inhibit autophagy was also analyzed in detail by transmission electron microscopy (TEM). The ultrastructural observations revealed that the double-membrane autophagic vacuoles (Figure 17C, asterisks), varying in shapes and frequently tightly apposed to endoplasmic

reticulum cisternae, were numerous in HaCaT pMSG cells treated with FGF7 in the presence of Dex (Figure 17C, left and middle panels) and drastically reduced in HaCaT pMSG E5 subjected to the same treatment (Figure 17C, right panel). Thus, the ultrastructural analysis unequivocally demonstrated that the 16E5-induced impairment of autophagy shown by biochemical or immunofluorescence approaches corresponds to a real reduction in the number of double-membrane vacuolar structures morphologically identifiable as autophagosomes.

To verify whether the viral protein exerts the inhibitory effect on autophagy also in the presence of the HPV16 full-length genome, as it occurs in the context of cervical carcinogenesis, we used the well established *in vitro* model of cervical W12p6 cells, containing episomal HPV16. Western blot analysis clearly showed that no detectable changes in LC3-II marker levels could be found in these cells upon starvation or FGF7 treatment (Figure 18A). Fluorescence approaches were also performed using W12p6 cells transiently transfected with pEGFP-C2-LC3 (W12p6 EGFP-LC3). HaCaT cells or primary cultures of normal human keratinocytes (HKs) transiently transfected with EGFP-LC3 (HaCaT EGFP-LC3 and HKs EGFP-LC3) were used as controls. The results clearly demonstrated that, differently from control cells (Figure 18B), W12p6 EGFP-LC3 cells did not show any increase in the number of LC3-positive dots per cell after serum starvation and/or FGF7 stimulation (Figure 18B).

In order to investigate whether the lack of responsiveness to the autophagic stimuli detected in the endogenous context of W12p6 cells may be due to 16E5 expression, the effect of specific depletion of the viral protein was analyzed by siRNA transfection. We first confirmed the efficient depletion of the 16E5 protein in E5 siRNA-transfected cells performing experiments on HaCaT cells cotransfected with E5-HA cDNA and E5 siRNA in which the efficiency of 16E5 silencing was verified through western blot analysis using anti-HA monoclonal antibody (Figure 19). Then, W12p6 cells were transfected with the specific 16E5 siRNA or with an unrelated siRNA as control and the autophagic process was stimulated by serum starvation or FGF7 treatment as above. Western blot analysis clearly showed that both the autophagic stimuli significantly increased the LC3-II levels only in 16E5-depleted cells (Figure 18C). Consistent with the biochemical results, fluorescence approaches revealed that a significant increase of LC3-

positive dots was evident in 16E5-depleted W12 cells upon serum deprivation and FGF7 stimulation (Figure 18D), while no increase was found in control siRNA-transfected cells (Figure 18D). These results strongly indicated that in W12p6 cells, which are the most representative model of cervical cancerogenesis, the observed unresponsiveness to autophagic stimuli could be specifically ascribed to 16E5 expression.

### **16E5 interferes with the transcriptional regulation of autophagy through the impairment of p53 function**

Since it has been demonstrated that 16E5 is able to affect the expression of several host genes (Kivi et al., 2008; Greco et al., 2011) and growing evidences indicate that autophagy is not only post-translationally regulated, but also transcriptionally controlled (Kusama et al., 2009; Rouschop et al., 2010; Kenzelmann Broz et al., 2013), here we investigated whether 16E5 might interfere with autophagy by affecting the autophagic gene expression. To this aim, the mRNA transcript levels of different crucial autophagic genes acting at different steps of the process (BECN1, ATG5 and LC3) were estimated by real-time relative RT-PCR in HaCaT E5 cells and normalized respect to the levels detected in HaCaT pCI-neo cells. In cells kept in complete medium, BECN1 and ATG5, but not LC3 or ATG7, appeared down-regulated by 16E5 expression (Figure 20A, upper panels). Moreover, when autophagy is stimulated by serum starvation or FGF7 treatment, a drastic significant decreased expression of all genes examined, except BECN1 in serum-deprived cells, was evident (Figure 20A, lower panels). Thus, 16E5 down-regulates autophagy gene expression when the process is induced as well as under basal conditions. Interestingly, in agreement with our previous biochemical observations (Belleudi et al., 2014), FGF7 stimulation slightly but significantly increased the expression of BECN1 and LC3, while that of ATG5 seemed unaffected (Figure 20A, lower panels) indicating that FGF7/FGFR2b signaling plays a role in the transcriptional control of autophagy. The p53 protein has been recently identified as a possible transcriptional inductor of the autophagic program (Kenzelmann Broz et al., 2013) and several autophagy genes are found to

be positively regulated by p53 also in HaCaT cells (Martynova et al., 2012), although these cells are known to express mutant p53 alleles (Martynova et al., 2012). Therefore, in order to assess whether 16E5 might negatively affect the transcriptional program of autophagy also interfering with the expression of a set of p53-regulated autophagy core machinery genes (ULK1, ULK2, ATG4a, ATG7) (Kenzelmann Broz et al., 2013), we analyzed their transcript levels as above. Real-time relative RT-PCR showed that all the p53-regulated genes, with the only exclusion of ULK2, were significantly down-regulated by 16E5 expression upon either serum starvation or FGF7 stimulation (Figure 20B). Thus, during induced-autophagy, the viral protein is able to repress the expression of several autophagic genes, some of which are specific targets of p53. In addition, since no changes in the mRNA levels of the examined p53-target genes were observed upon FGF7 treatment (Figure 20B), these results show that the FGFR2b transcriptional regulation of autophagy is p53-independent. In order to verify if 16E5 could interfere with the transcriptional regulation of autophagy inducing impairment of p53 function, the expression of two well established p53 downstream target genes, such as p21 and 14-3-3 $\sigma$ , was analyzed in HaCaT E5 and HaCaT pCI-neo cells upon serum starvation or FGF7 stimulation. RT-PCR analysis showed in 16E5-expressing cells a significant decrease of p53 target gene expression (Figure 20B, lower panels), suggesting that 16E5 could be able to transcriptionally impair autophagy also interfering with p53 function. In contrast, consistent with the results described above, the stimulation with FGF7 was able to induce no significant changes of p21 or 14-3-3 $\sigma$  expression (Figure 20B, lower panels), further confirming that the induction of autophagy by FGF7 does not involve the p53 regulation. In order to verify if the ability of 16E5 to transcriptionally regulate autophagy is a general phenomenon, we examined the expression of the autophagic genes in primary human keratinocytes transiently transfected with 16E5 (HKs E5) or with the pCI-neo empty vector (HKs pCI-neo) as control. The results showed that, also in primary cultures, the expression of 16E5 appeared to down-regulate most of the p53-independent (Figure 21A) and p53-regulated (Figure 21B) autophagy genes, as well as that of the main p53-target gene p21 (Figure 8b). Consistently with the results obtained in HaCaT cells, also in HKs pCI-neo the stimulation with FGF7 significantly increased the expression of

BECN1, ATG5 and LC3, while p53-target genes appeared unaffected (Figure 21A and B), confirming that FGF7 appears to exert a transcriptional control only on the p53-independent autophagy genes. To assess whether the repression of the autophagic gene transcription induced by 16E5 could be observed in the presence of HPV16 full-length genome and to analyze whether this effect could be directly due to the E5 viral protein expression, all the previously examined genes were re-analyzed in W12p6 cells transfected with a specific E5 siRNA or with an unrelated siRNA. The mRNA levels of the different genes in HKs were used as normalizers. Real-time relative RT-PCR showed that the very low levels of most of the genes in W12p6 control siRNA cells (Figure 21C and D) were recovered upon 16E5 depletion (Figure 21C and D). These results strongly suggested that the decreased expression of both p53-regulated and p53-independent autophagic genes observed in W12 cells compared to HKs can be directly ascribed to 16E5 expression.

## DISCUSSION

In the first part of this work I investigate the crosstalk between autophagy and phagocytosis in human keratinocytes and the possible involvement of FGFR2b-induced PLC $\gamma$  signaling in the induction of the FGF7-mediated autophagic process. The interplay between autophagy and phagocytosis is widely accepted to occur in the context of macrophages (Gutierrez et al., 2004; Sanjuan et al., 2007; Xu et al., 2007; Lima et al., 2011; Bonilla et al., 2013); however, a similar crosstalk has not been already described in other cell types. In this work, not only we confirmed our previous results showing that FGF7 stimulation is able to trigger either phagocytosis (Belleudi et al., 2011) and autophagy (Belleudi et al., 2014) in both HaCaT keratinocyte cell line and in primary HKs, but interestingly we found that the activation and signaling of FGFR2b are able to drive phagosomes and autophagosomes to converge. This phenomenon might be explained as an additional strategy of this type of cells to more efficiently redirect the engulfed material toward a lysosomal degradative fate.

It has been reported that, in addition to the conventional autophagy, several non-canonical autophagic mechanisms can be activated and, in particular, a direct recruitment of Beclin 1 and LC3 to the phagosomal membranes has been described as LAP (LC3-associated phagocytosis) in murine macrophages during phagocytosis (Sanjuan et al., 2007). However, our findings strongly indicate that, in our cell model, the autophagic process involves a canonical pathway to isolate the newly formed phagosomes. In fact, our fluorescence results, showing a not complete colocalization between the internalized beads and the LC3-positive dots upon FGF7 stimulation, appears to exclude the involvement of a non-canonical autophagy, such as LAP. In addition, our ultrastructural analysis showed that part of the engulfed beads were included in double membrane organelles morphologically corresponding to canonical autophagosomes, suggesting that some of the autophagosomal structures might close around the phagosomes containing the beads. Although this canonical intracellular membrane pathway may represent the main mechanism involved in such convergence of the two processes, several single membrane organelles containing beads were also visible: therefore, we may speculate that, as previously described in macrophages during bacterial clearance (Levine et al., 2011), also in keratinocytes other mechanisms, including the fusion between the phagosomal membrane and the outer membrane

of autophagosomes, can not be excluded.

The ability of FGFR2b to regulate the phagocytic process appears to be functionally linked to the control of the melanosome uptake by recipient keratinocytes for skin pigmentation (Cardinali et al., 2005; Belleudi et al., 2011). In fact, this ability is more efficient in HKs from light skin, that are known to express more FGFR2b compared to those from dark skin (Cardinali et al., 2008). In the other hands, a recent study highlighted the crucial role of the autophagic process in melanosome degradation in the context of human keratinocytes (Murase et al., 2013). Our present results, indicating a key role of FGFR2b not only in the induction of both autophagy and phagocytosis, but also in the regulation of their convergence, encouraged us to envisage a new scenario in which FGFR2b would differently control autophagy, and possibly melanosome turnover, in light and dark skin. This hypothesis appears to be confirmed by our fluorescence results showing that autophagy and phagocytosis may converge only in HKs from light skin. Taken together our results indicate that, particularly in light skin, FGFR2b signaling could be crucial in determining melanosome intracellular amount and consequently skin pigmentation through a fine modulation of the interplay between phagocytosis and autophagy. Our speculations are consistent with those of Li and coworkers (Li et al., 2016), which hypothesized that the UVB-induced persistence of melanosomes, especially in HKs from light skin, can be due to the inhibition of autophagy consequent to UVB-mediated internalization and degradation of FGFR2b (Marchese et al., 2003; Belleudi et al., 2006). These authors also proposed that the modulation of FGF7-induced autophagy might be a useful strategy for treating skin pigmentation disorders (Li et al., 2016).

While in our previous work (Belleudi et al., 2011) it has been demonstrated that, in human keratinocytes, the FGFR2b-induced phagocytosis occurs via PLC $\gamma$  signaling, suggesting that diacylglycerol formation and consequent cortical actin reorganization could be required, the molecular pathways responsible for FGF7-induced autophagy remain to be clarified. It is well-known that the autophagic process can be regulated by either mTOR-dependent and mTOR-independent molecular mechanisms (Yang et al., 2010; Russell et al., 2014) and it has been previously demonstrated that FGF7-mediated autophagy is a PI3K/AKT/mTOR-independent process (Belleudi et al., 2014). Therefore, in this work we further

progress on the identification of the molecular mechanisms underlying FGF7-mediated autophagy, identifying PLC $\gamma$  as a crucial player acting downstream FGFR2b. Using biochemical and immunofluorescence approaches we assessed the key role of the tyrosine 769 residue in FGFR2b, responsible for the activation/recruitment of PLC $\gamma$ , not only in the receptor-mediated phagocytosis as previously shown (Belleudi et al., 2011), but also in the induction of autophagy. In fact, the point mutation of this receptor site (Y769F), which generates a PLC $\gamma$  signaling dead mutant (FGFR2b Y769F), resulted in the impairment of the autophagosome formation following FGF7 stimulation. Thus, PLC $\gamma$  signaling appears to be the main pathway involved in the regulation of both FGFR2b-mediated phagocytosis and autophagy (Figure 22).

Then, in order to identify the molecular machinery acting downstream PLC $\gamma$ , we focused our attention on JNK1, a RTK substrate able to activate an mTOR-independent autophagic pathway (Russell et al., 2014) and recently identified as the main player involved in FGFR4-mediated autophagy (Cinque et al., 2015). We found that, upon FGF7 stimulation, the phosphorylation/activation of JNK1 is strongly attenuated in cells overexpressing the FGFR2b Y769F mutant. Moreover, only the inhibition of JNK1, but not that of other FGFR2b substrates, such as MEK1/2 or AKT, was able to affect FGF7-mediated autophagy. These findings demonstrated that, consistently with what has been reported for FGFR4 in osteoclasts (Cinque et al., 2015), FGFR2b-mediated autophagy in keratinocytes is induced via the activation of JNK1 signaling. Taking advantage of the use of a specific inhibitor, we finally identified the PLC $\gamma$  substrate PKC $\delta$  (Steinberg, *Physiol Rev*, 2008) as the molecular player directly involved in JNK1 activation and consequently in FGF7-induced autophagy. These results are consistent with previous findings indicating PKC $\delta$  as crucial activator of JNK1 during autophagy induced by hypoxia (Chen et al., 2008; Chen et al., 2009).

Overall the data collected in the first part of this work strongly suggest that PLC $\gamma$  is the FGFR2b substrate, which acts as an upstream regulator of both phagocytosis and autophagy in HKs. While the PLC $\gamma$ -mediated formation of diacylglycerol and consequent cortical actin reorganization might be responsible for the triggering of phagocytosis, PKC $\delta$ /JNK1 signaling would be the main

PLC $\gamma$  downstream pathway required for the induction of FGF7-mediated autophagy (Figure 22).

In the second part of this work, I focused my attention on the possible impairment of the autophagic response in keratinocytes expressing the oncoprotein 16E5.

The interference of the host cell autophagic response is a general strategy used by viruses during the early steps of infection in order to ensure their intracellular survival and subsequent replication (Silva et al., 2013). In the case of human papillomavirus 16 (HPV16), a role in inhibiting the host cell autophagy has been proposed for the entire “early protein group” (Hanning et al., 2013), but neither the single contribution of the viral oncogenic proteins, nor the molecular mechanisms involved in such inhibition, have been investigated. Starting from our recent results dealing with the ability of FGF7/FGFR2b signaling in promoting autophagy (Belleudi et al., 2014) and with the capacity of HPV16 E5 to down-regulate the receptor expression for perturbation of epithelial homeostasis and differentiation (Belleudi et al., 2011; Purpura et al., 2013), we speculated that 16E5 might be the HPV16 early product major candidate for the role of interference with the autophagic process, possibly occurring through FGFR2b down-modulation. Consistent with this hypothesis we demonstrated, using biochemical and immunofluorescence approaches, that the ectopic expression of 16E5 efficiently counteracts FGF7-mediated autophagy. In fact, the inhibitory effects induced by the viral protein were comparable to those observed under receptor depletion and the forced receptor overexpression and the triggering of its signaling was able to contrast the repressive function of 16E5 on the autophagic process. These results suggest that 16E5 and FGFR2b would exert opposite and interplaying roles not only on epithelial differentiation, as recently proposed (Purpura et al., 2013), but also on the control of autophagy

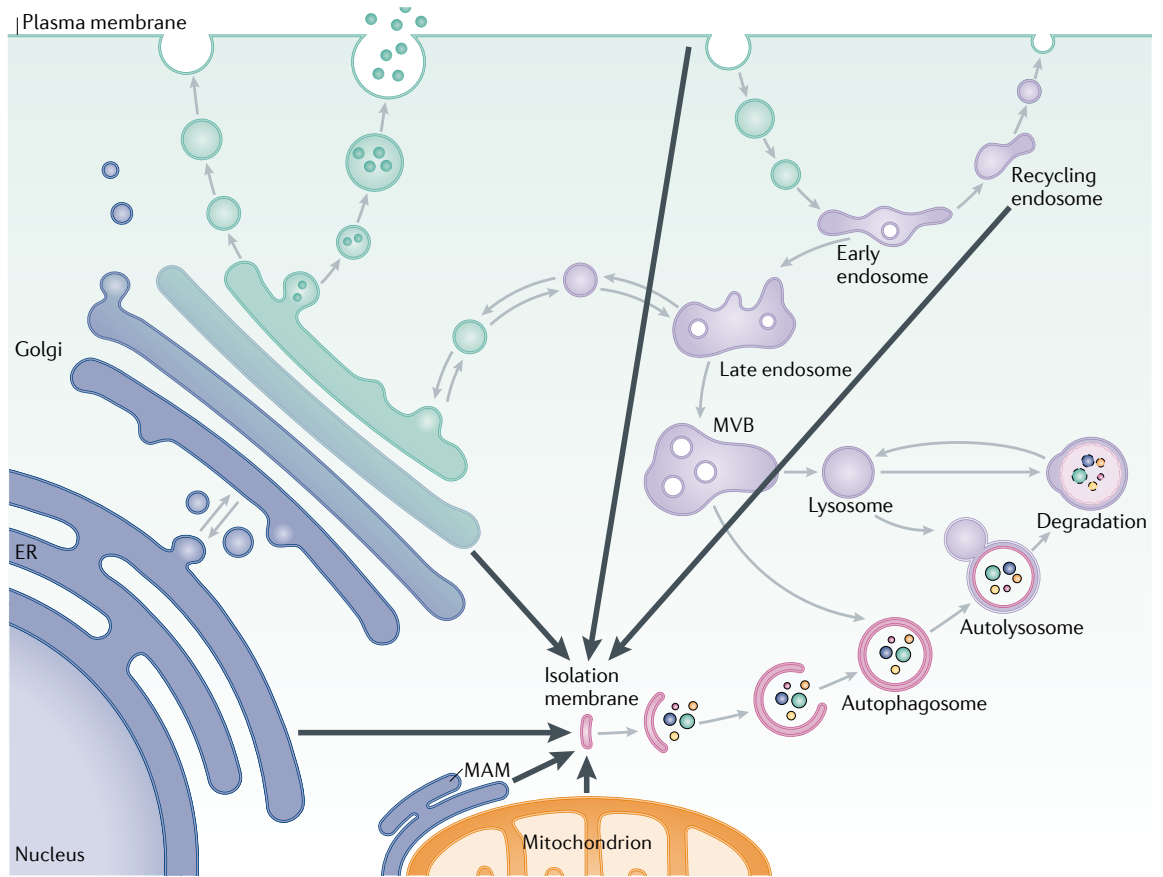
Interestingly, taking advantage of the use of serum starvation as autophagic stimulus in which the contribution of FGFR2b signaling was excluded, we provided the first evidence that 16E5 affects autophagy also through transcriptional regulation. In fact, our molecular analysis showed that 16E5 is able to repress most of the autophagy core machinery genes, some of which are direct

targets of p53, one of the main transcriptional inductor of the autophagic program (Kenzelmann Broz et al., 2013). However, differently from the 16E6 oncoprotein, whose crucial role as p53 down-regulator has been proposed (Scheffner et al., 1990), only a modest ability to repress p53 expression has been ascribed to 16E5 (Greco et al., 2011). Therefore, it is possible that, in the case of 16E5 expression, p53 would be mainly functionally-regulated, rather than transcriptionally-regulated. To investigate such possibility we decided to analyze also the expression of the general p53-target genes p21 and 14-3-3 $\sigma$ , in order to monitor p53 function in our cell model (Martynova et al., 2012). In agreement with the hypothesis of a functional regulation of p53, we found that, when 16E5 is expressed and autophagy is induced by serum starvation or FGF7 stimulation a significant decrease in p53-target gene transcription was observed, indicating functional repression of p53. These results provide new elements to assume that the negative impact of 16E5 on autophagy might be also due to the ability of the viral protein to induce a functional inhibition of p53 activity, which in turn results in down-regulation of autophagy genes. Moreover, the observed repressing effect on autophagy genes, which are not directly regulated by p53, suggests that 16E5 may in parallel interfere with other autophagy transcriptional regulators still unknown.

It has been reported that autophagy is linked to epithelial cell differentiation (Haruna et al., 2008; Aymard et al., 2011; Chatterjea et al., 2011; Moriyama et al., 2014 ; Belleudi et al., 2014, Chikh et al., 2014; Akinduro et al., 2016) and it has been recently proposed the existence of a direct interplay between the two processes in human keratinocytes demonstrating that the induction of autophagy in response to FGFR2b activation is necessary for the triggering of early differentiation (Belleudi et al., 2014). Accordingly with the knowledge that 16E5 acts during HPV infection perturbing keratinocyte differentiation (Fehrmann et al., 2003; Barbaresi et al., 2010) and that this occurs through FGFR2b down-modulation (Purpura et al., 2013), our present study shows that a finely controlled impairment of the autophagic process, also through FGFR2b down-regulation, could be one of the molecular mechanisms used by 16E5 to inhibit and delay epithelial cell differentiation for maintenance of an undifferentiated status indispensable for virus replication.

On the other hand, a close interplay between p53 activity and epidermal cell differentiation has been also proposed: in fact, in suprabasal differentiating keratinocytes, p53 is activated by the dramatic decrease of its functional repressor  $\Delta Np63\alpha$  (Westfall et al., 2003) and several keratinocyte differentiation-specific markers, including Notch1, Hsp70 and keratin 14, are finely regulated by the  $\Delta Np63\alpha$ /p53 inverse functional cooperation (Agoff et al., 1993; Wu et al., 2005; Nguyen et al., 2006; Yugawa et al., 2007; Cai et al., 2012). Moreover, it has been observed that p53 activity promotes differentiation in HaCaT cells (Paramio et al., 2000). Based on these evidences, our results may indicate that 16E5 is able to utilize parallel and not interconnected mechanisms, involving both FGFR2b down-regulation and functional repression of p53, for the impairment of both autophagy and differentiation. Since we demonstrated here that also the autophagy induced by FGF7 signaling appears to be transcriptionally controlled, although in a p53-independent manner, the data obtained in the second part of this work allow us to conclude that a transcriptional crosstalk among 16E5 and FGFR2b is the crucial molecular driver of epithelial deregulation during early steps of HPV infection and transformation.

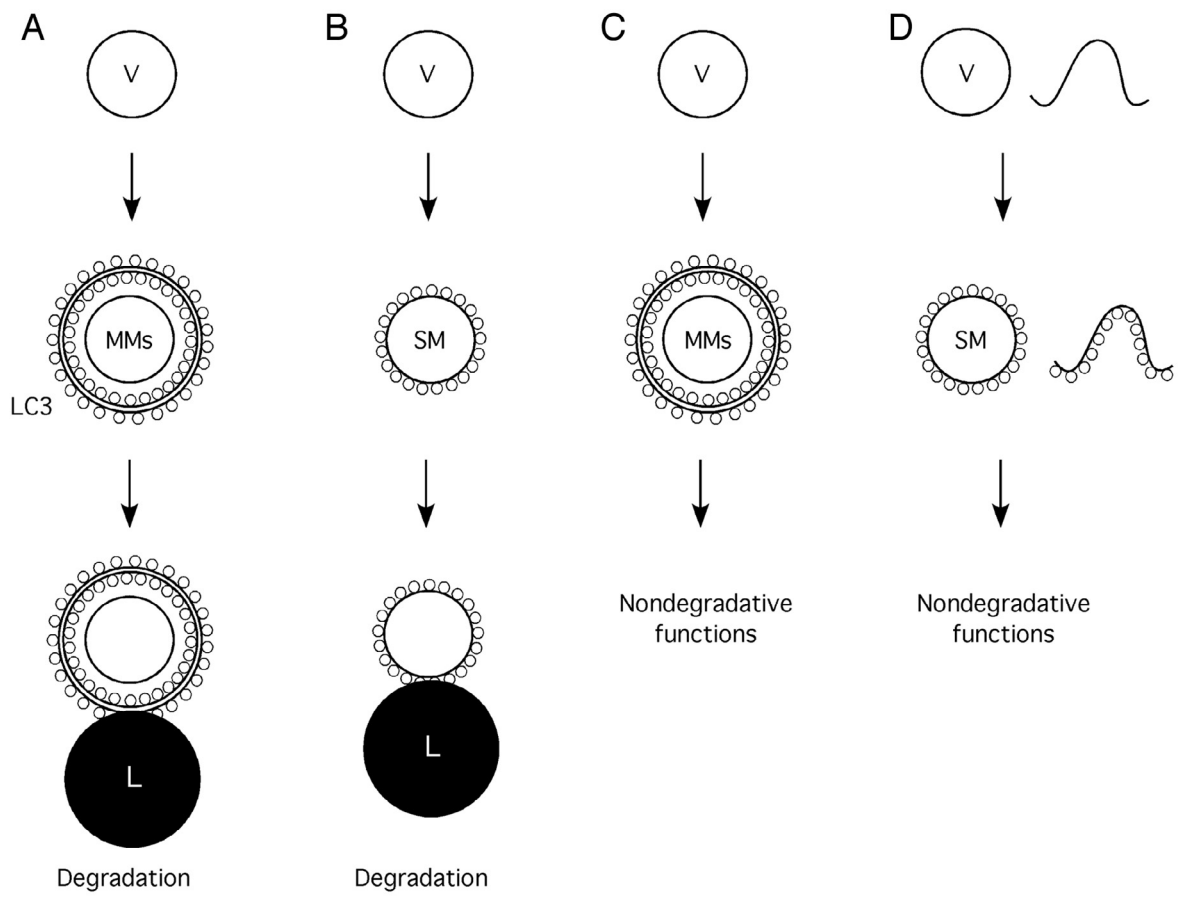
## FIGURES



Lamb et al., 2013

Figure 1

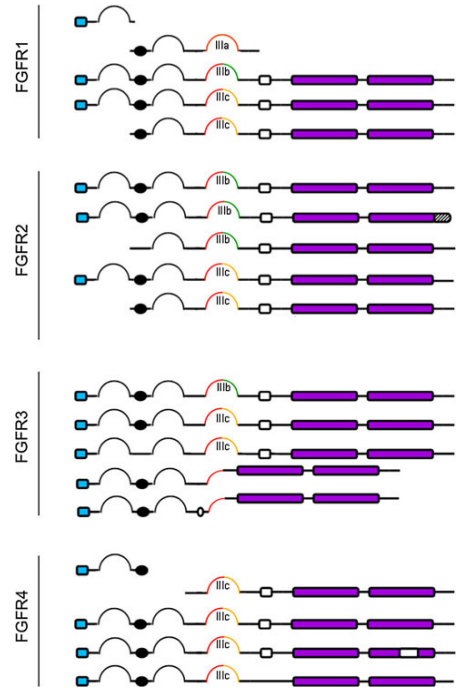
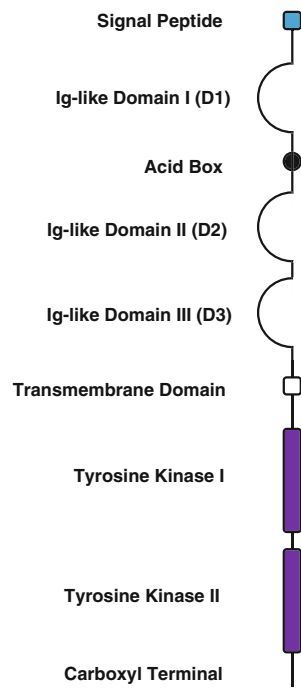
**Figure 1.** Overview of the autophagic pathway and organelles that might contribute to autophagosome. Macroautophagy is mediated by a double-membrane organelle called autophagosome, by which a portion of the cytoplasm is enclosed. The outer membrane of the autophagosome then fuses with the lysosome, which allows lysosomal enzymes to degrade the sequestered cytoplasmic materials in autolysosomes and release the degradation products into the cytoplasm for use in cellular processes, including protein biosynthesis and energy production. Whereas organelles in the biosynthetic and secretory pathways are always present in the cell, the autophagosome forms quickly and disappears, and its formation can be increased by signals that activate autophagy. Thus, the origin and source of the autophagosomal membrane is a major question in the field. Various organelles, including the endoplasmic reticulum (ER), mitochondria, mitochondria-associated membranes (MAMs), the Golgi, the plasma membrane and recycling endosomes have been implicated in autophagosome formation (that is, in the nucleation of the isolation membrane) and in the subsequent growth of the membrane. Autophagy is a cell survival pathway that is required to keep cells healthy by degrading damaged organelles and eliminating invading pathogens, but it has also been shown to be dysregulated in a number of human disease, (for example, Crohn's disease, cancer and neurodegeneration), which makes it a potential target for future therapeutic intervention. MVB, multivesicular body.



(modified from Pimentel-Muiños and Boada-Romero, 2014)

Figure 2

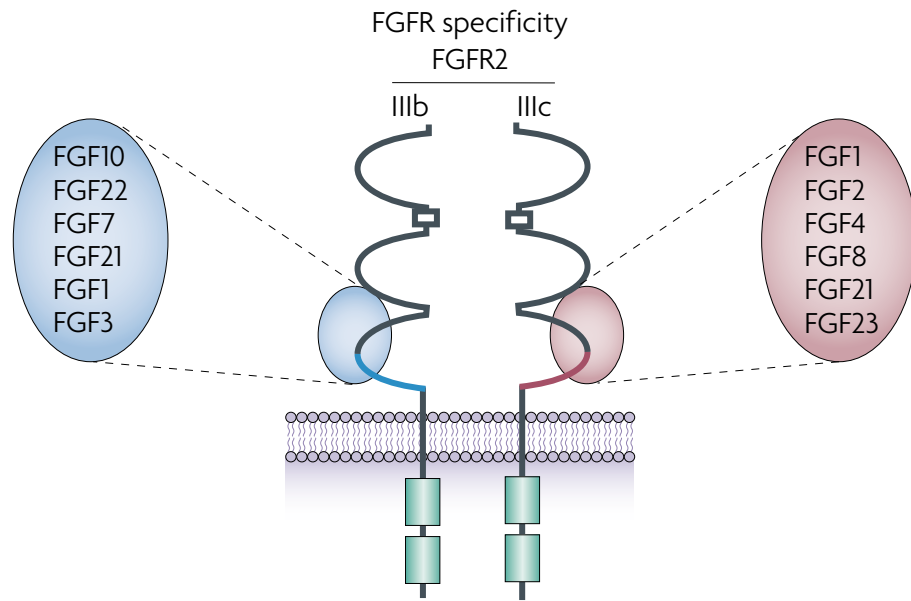
**Figure 2.** Scheme of the different modalities of autophagy involving membrane compartments. (A) Regular, single-membrane vesicles are targeted by conventional autophagy to produce multimembrane vacuoles that fuse with lysosomes for degradation of their contents. (B) Regular, single-membrane vesicles become directly labeled with LC3-II and eventually fuse with lysosomes for degradation. (C) Regular, single-membrane vesicles are targeted by conventional autophagy producing multimembrane vacuoles with nondegradative functions. (D) Regular, single-membrane vesicles or other membranous structures become directly labeled with LC3-II for a variety of nondegradative functions. (V, vesicle; MMs, multiple membranes; SM, single membrane; L, lysosome).



(Modified from Tiong et al., 2013)

Figure 3

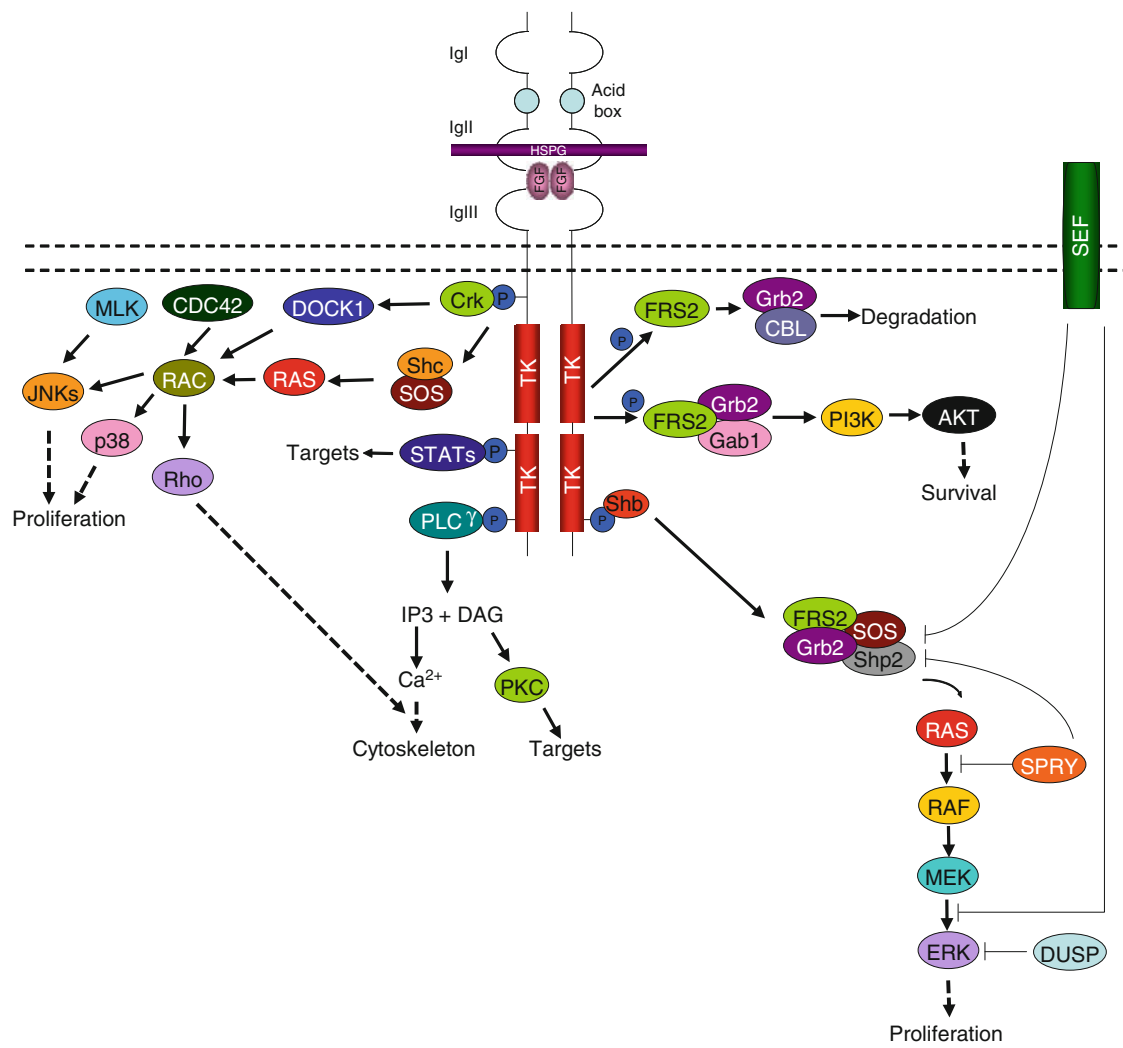
**Figure 3.** The basic structure of FGFR and splice variants. The FGFRs are phylogenetically closely related to the VEGFRs and PDGFRs, consist of three extracellular immunoglobulin (Ig) domains (D1-D3), a single transmembrane helix, an intracellular split tyrosine kinase domain (TK1 and TK2) and an acidic box. D2 and D3 form the ligand-binding pocket and have distinct domains that bind both FGFs and heparan sulfate proteoglycans (HSPGs). Acidic box is required for binding of bivalent cations for optimal interaction between FGFRs and HSPGs. The FGFRs isoforms are generated mainly by alternative splicing of the Ig III domain (D3). The D3 could be encoded by an invariant exon 7 (red) to produce FGFR-IIIa isoform or spliced to either exon 8 (green) or 9 (yellow) to generate the FGFR-IIIb or FGFR-IIIc isoforms, respectively. Epithelial tissues predominantly express the IIIb isoform and mesenchymal tissues express IIIc. FGFR4 is expressed as a single isoform that is paralogous to FGFR-IIIc. Hatched box represents a truncated carboxyl terminal. Clear box indicates a deletion of an exon.



Turner and Grose, 2010

Figure 4

**Figure 4.** FGFR2IIIb and FGFR2IIIc isoforms structure. Examples of the extent to which ligand specificity can differ between FGFR2IIIb and FGFR2IIIc isoforms, illustrated with the differing ligand specificity of FGFR2 isoforms. The FGFR2IIIb ligands are shown in blue and the FGFR2-IIIc ligands are shown in brown. For example, FGF7 and FGF10 bind specifically to FGFR2-IIIb and have essentially no binding to FGFR2IIIc.

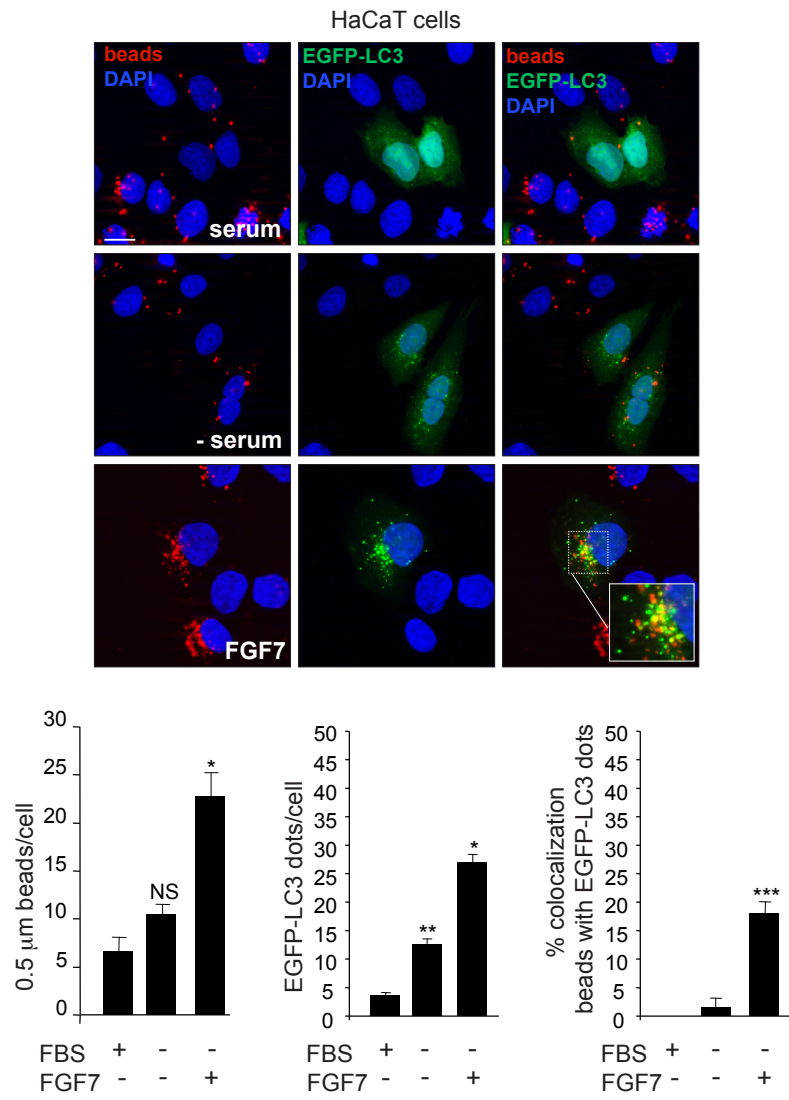


(Tiong et al., 2013)

Figure 5

**Figure 5.** FGFR signaling pathway. FGFs induce FGFR-mediated signaling pathway by interacting with specific FGFRs and HSPGs. The macromolecular interactions mediate FGFRs dimerization or oligomerization and activate multiple signal transduction pathways, including those involving FRS2, RAS, p38 MAPKs, ERKs, JNKs, Src, PLC $\gamma$ , Crk, PKC and PI3K. These pathways are negatively regulated in part by the activities of DUSPs, SPRY, SEF and CBL.

A



B

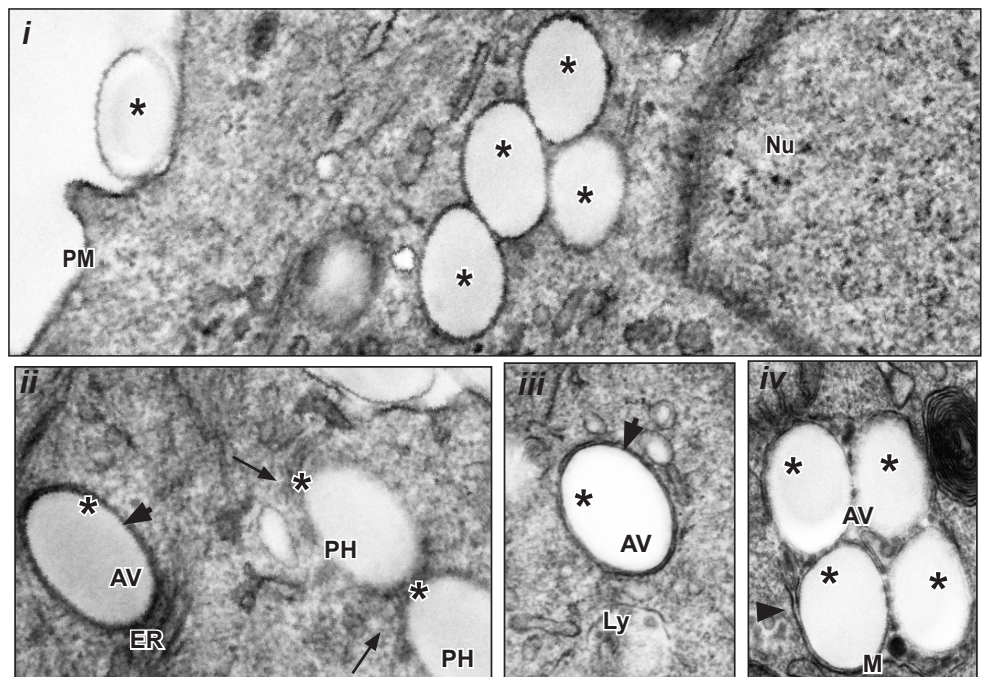


Figure 6

**Figure 6.** Presence of internalized beads in autophagosomes after FGF7 stimulation. (A) HaCaT cells transiently transfected with pEGFP-C2-LC3 construct were serum starved or stimulated with FGF7 for 24 h and with inert latex red fluorescent beads 0.5  $\mu\text{m}$  in diameter for the last 4 h. Cell nuclei were stained with DAPI. Quantitative fluorescence analysis shows that an increase of either the number of EGFP-LC3 positive dots per cell and fluorescent bead uptake, as well as a partial colocalization between LC3 and fluorescent beads are detectable only upon FGF7 stimulation. The quantitative analysis was performed as described in Materials and Methods and results are expressed as mean values  $\pm$  standard errors (SE). Student *t* test was performed and significance levels have been defined as  $p < 0.05$ : \* $p < 0.001$  vs the corresponding FGF7-unstimulated cells, \*\* $p < 0.001$  vs the corresponding serum-cultured cells, \*\*\* $p < 0.01$  vs the corresponding FGF7-unstimulated cells, NS vs the corresponding serum-cultured cells. Bar: 10  $\mu\text{m}$ . (B) Ultrastructural analysis of HaCaT cells stimulated with FGF7 in presence of beads as described above. Single (asterisks, *i*, *ii*, *iii*) and clustered beads (asterisks, *iv*) were visible in either single-membrane (arrows, *ii*) or double-membrane vacuoles (arrowheads, *ii*, *iii*, *iv*) corresponding to phagosomes and autophagosomes respectively. AV, autophagic vacuole; ER, endoplasmic reticulum; Ly, lysosome; M, mitochondrion; Nu, nucleus; PH, phagosome; PM, plasma membrane. Bar: 0.25  $\mu\text{m}$ .

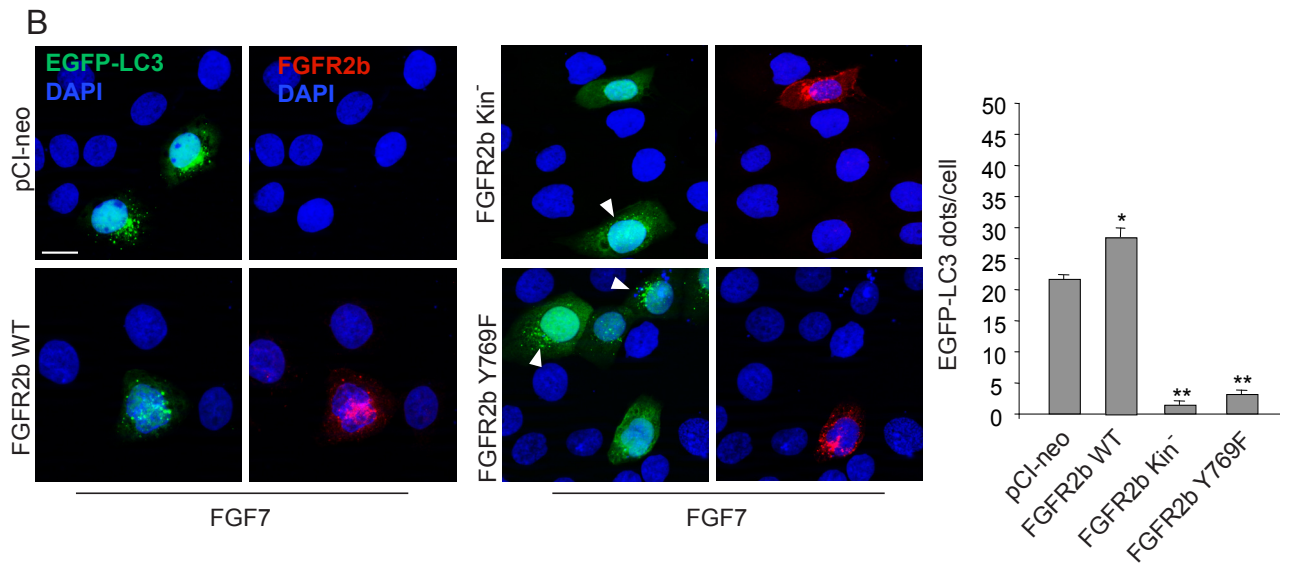
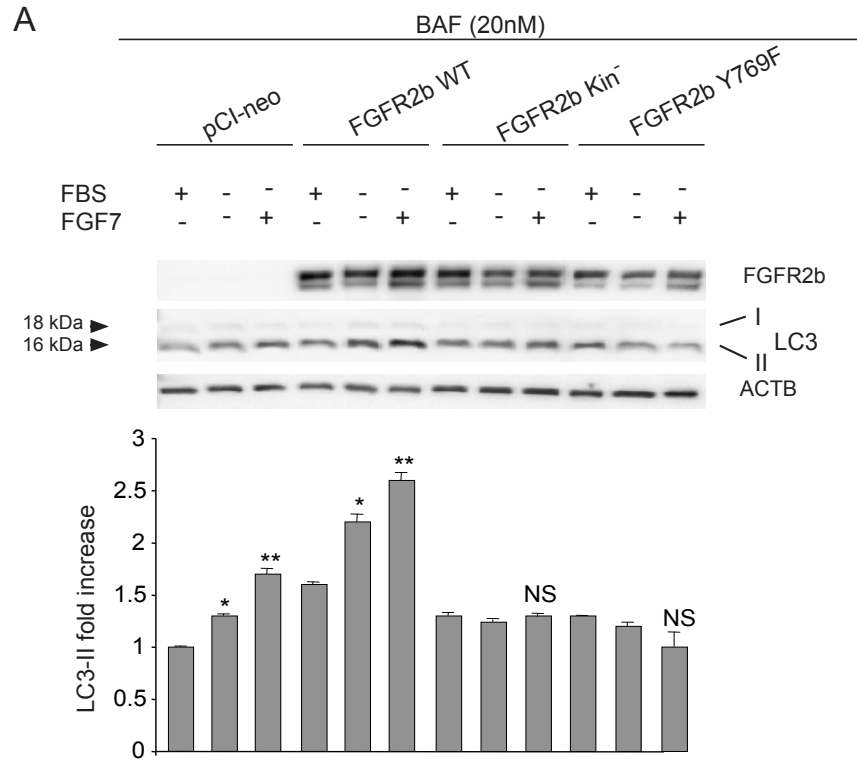
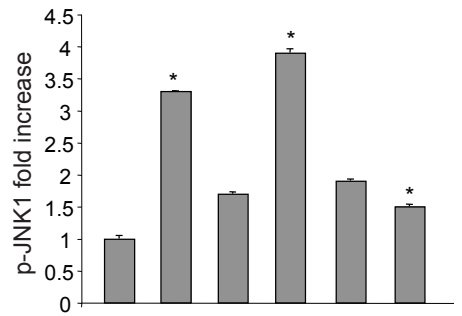
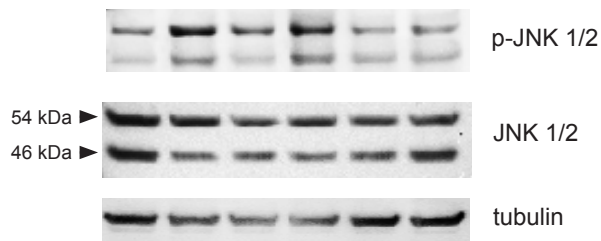
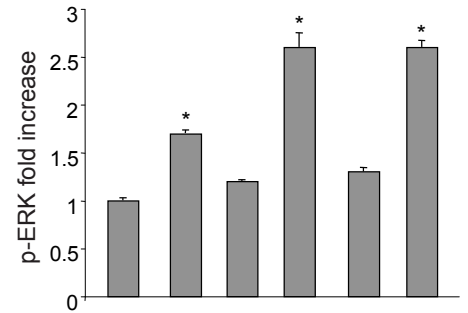
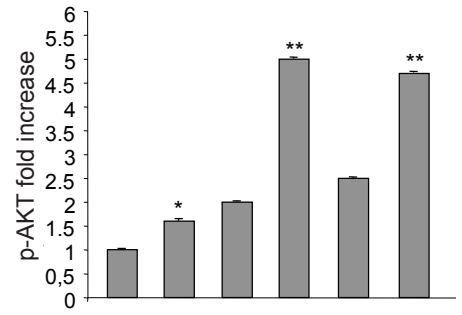
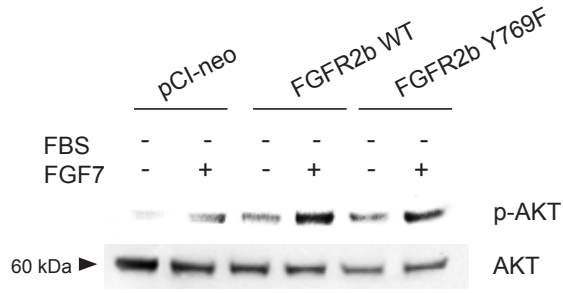


Figure 7

**Figure 7.** PLC $\gamma$  signaling is required for FGF7-induced autophagy. (A) HaCaT cells were transiently transfected with the FGFR2b WT or with the Y769F FGFR2b mutant. The transfection with the kinase negative Y656F/Y657F FGFR2b or with pCI-neo empty vector was performed as control. Upon transfection, cells were serum-starved and stimulated with FGF7 in the presence of bafilomycin A1 for the last 3 h. Western blot analysis shows that FGFR2b Y769F expression, as well as FGFR2b kin<sup>-</sup> expression, inhibits the increase of LC3-II levels induced by FGF7 in pCI-neo cells and even more in FGFR2b WT cells. The equal loading was assessed using anti-ACTB antibody. For the densitometric analysis, the values from 3 independent experiments were normalized, expressed as fold increase and reported in graph as mean values  $\pm$  standard deviation (SD). Student *t* test was performed and significance levels have been defined as  $p < 0.05$ : \* $p < 0.05$  vs the corresponding serum-cultured cells, \*\* $p < 0.05$  vs the corresponding FGF7-unstimulated cells, NS vs the corresponding FGF7-unstimulated cells. (B) HaCaT cells were transiently cotransfected with pEGFP-C2-LC3 construct and with the FGFR2b WT, with the Y769F FGFR2b mutant, with the kinase negative Y656F/Y657F FGFR2b or with pCI-neo empty vector and stimulated with FGF7 as above. Immunofluorescence was performed using anti-FGFR2b polyclonal antibodies to visualize transfected FGFR2b WT or mutants. Upon FGF7 treatment the number of LC3-positive dots per cell is reduced in HaCaT EGFP-LC3/FGFR2b Y769F cells, as well as in HaCaT EGFP-LC3/FGFR2b kin<sup>-</sup> cells, compared to the surrounding cells not showing detectable receptor mutant overexpression (arrowheads), or to HaCaT EGFP-LC3/pCI-neo and HaCaT EGFP-LC3/FGFR2b WT cells. Differently from the kinase negative dead mutant, both FGFR2b WT and FGFR2b Y769F signals appear internalized upon FGF7 stimulation. The quantitative analysis and Student *t* test were performed as above: \* $p < 0.05$  vs HaCaT pCI-neo, \*\* $p < 0.001$  vs HaCaT FGFR2b WT cells. Bar: 10  $\mu$ m.

A



B

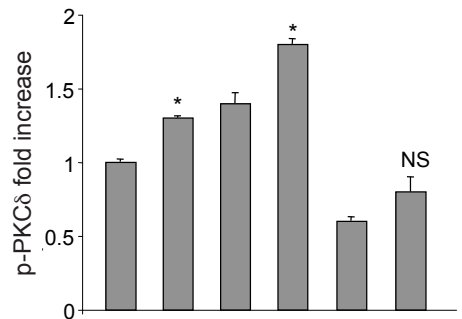
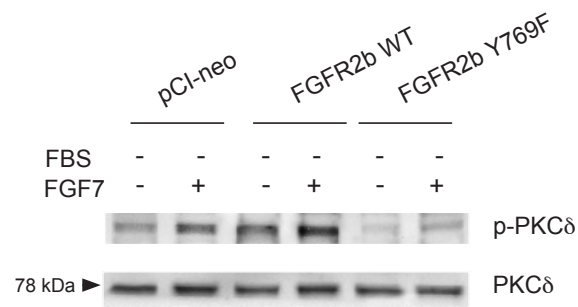


Figure 8

**Figure 8.** The inhibition of PLC $\gamma$  signaling is accompanied by JNK pathway shut-down and PKC $\delta$  inactivation. (A, B) HaCaT pCI-neo, HaCaT FGFR2b WT and HaCaT FGFR2b Y769F cells were serum starved or stimulated with FGF7 as above. Western blot analysis shows that the phosphorylation of both JNK1 (A) and PKC $\delta$  (B) in response to FGF7 stimulation appears attenuated only in HaCaT FGFR2b Y769F cells, while AKT and ERK1/2 substrates (A) are highly phosphorylated in all cells. The equal loading was assessed using anti-AKT, anti-ERK1/2, anti-JNK1/2 and anti-PKC $\delta$  antibodies. The densitometric analysis and Student t test were performed as reported above: (A) \*p < 0.05 vs the corresponding FGF7-unstimulated cells; \*\*p < 0.01 vs the corresponding FGF7-unstimulated cells. (B) \*p < 0.05 vs the corresponding FGF7-unstimulated cells; NS vs the corresponding FGF7-unstimulated cells.

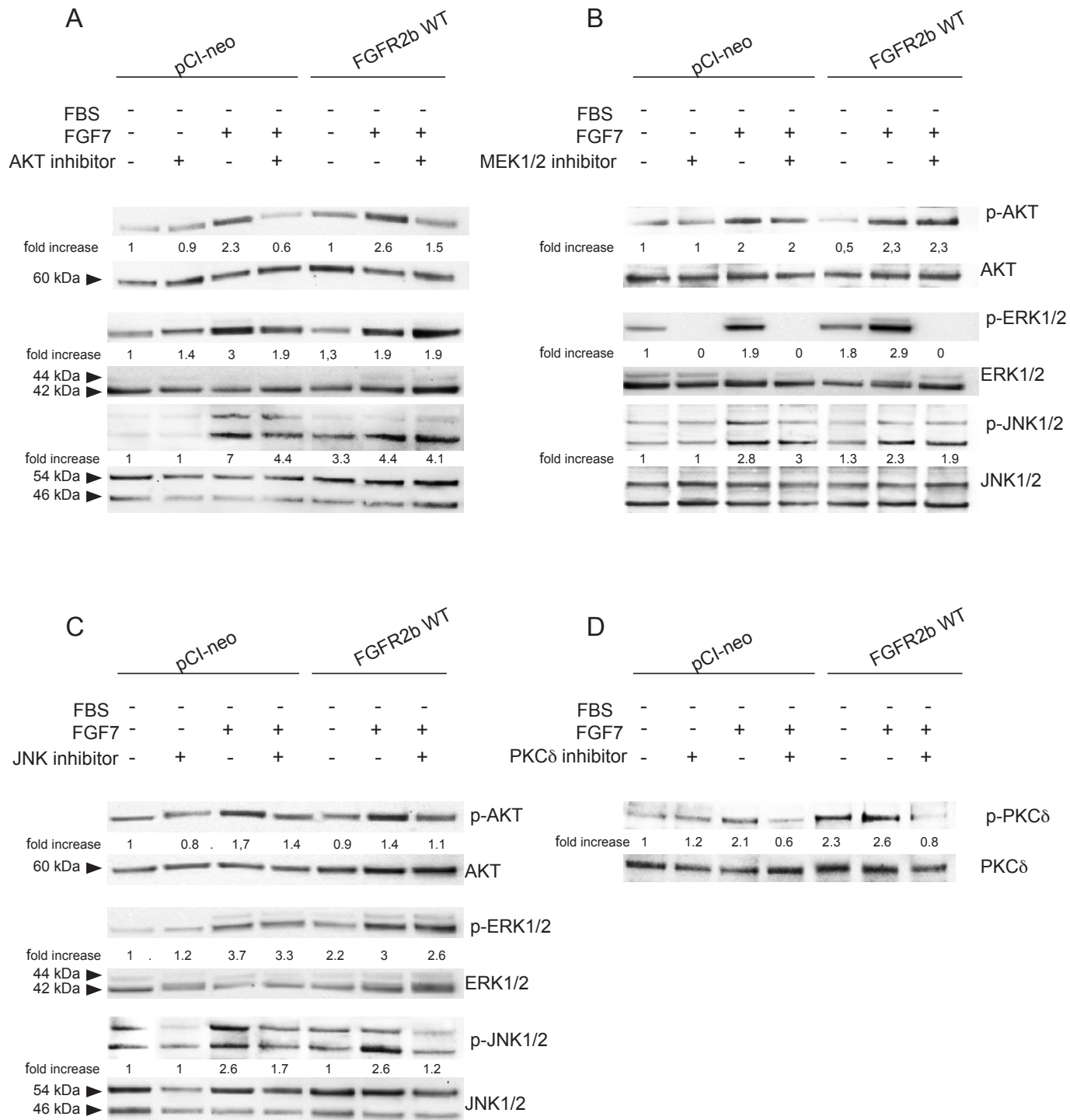


Figure 9

**Figure 9.** HaCaT pCI-neo and HaCaT FGFR2b WT cells were serum starved or stimulated with FGF7 in presence or not of the indicated substrate inhibitors as reported in Materials and Methods. Western blot analysis performed using antibodies directed against the phosphorylated forms of each substrate confirms that all the inhibitors were highly specific.

The equal loading was assessed with anti-AKT, anti-ERK1/2, anti-JNK1/2 and anti-PKC $\delta$  antibodies. The densitometric analysis was performed as reported above

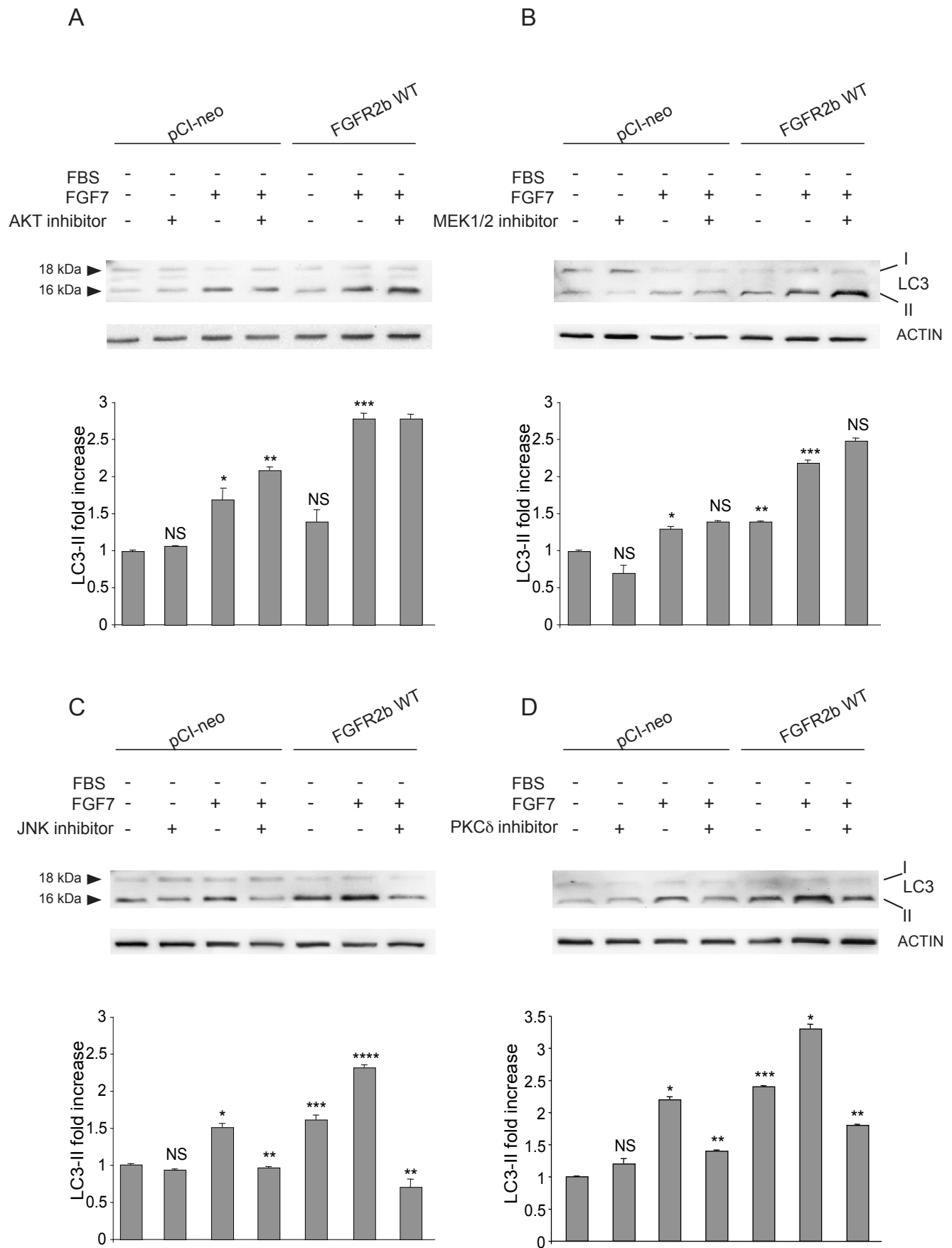


Figure 10

**Figure 10.** The inhibition of either JNK1 or PKC $\delta$  substrates blocks FGFR2b-induced autophagy. (A, B, C, D) HaCaT pCI-neo and HaCaT FGFR2b WT were serum starved or stimulated with FGF7 in presence or not of the indicated substrate inhibitors as reported in Materials and Methods. Western blot analysis shows that either AKT inhibitor (A) or MEK1/2 inhibitor (B) do not affect the increase of LC3-II levels induced by FGF7, while JNK inhibitor (C) and PKC $\delta$  inhibitor (D) attenuate it. The equal loading was assessed with anti-ACTB antibody. The densitometric analysis and Student t test were performed as reported above: (A) \* $p < 0.05$  vs the corresponding FGF7-unstimulated cells; \*\* $p < 0.05$  vs the corresponding FGF7-stimulated cells; \*\*\* $p < 0.01$  vs the corresponding FGF7-unstimulated cells; NS vs HaCaT pCI-neo cells. (B) \* $p < 0.05$  vs the corresponding FGF7-unstimulated cells; \*\* $p < 0,01$  vs HaCaT pCI-neo cells; \*\*\* $p < 0.01$  vs the corresponding FGF7-unstimulated cells; NS vs the corresponding MEK1/2 inhibitor-untreated cells. (C) \* $p < 0.05$  vs the corresponding FGF7-unstimulated cells; \*\* $p < 0.01$  vs the corresponding FGF7-stimulated cells; \*\*\* $p < 0.01$  vs HaCaT pCI-neo cells; \*\*\*\*  $p < 0.01$  vs the corresponding FGF7-unstimulated cells; NS vs the corresponding JNK inhibitor-untreated cells. (D) \* $p < 0.05$  vs the corresponding FGF7-unstimulated cells; \*\* $p < 0.05$  vs the corresponding FGF7-stimulated cells; \*\*\* $p < 0.01$  vs HaCaT pCI-neo cells; NS vs the corresponding PKC $\delta$  inhibitor-untreated cells.

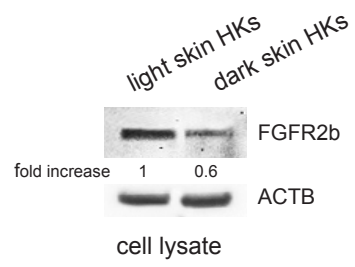


Figure 11

**Figure 11.** HKs from light skin and from dark skin were grown in complete medium. Western blot analysis performed using anti FGFR2 polyclonal antibodies shows that light skin HKs have higher expression of FGFR2b than dark skin HKs. The equal loading was assessed with anti-ACTB antibody. The densitometric analysis was performed as reported above.

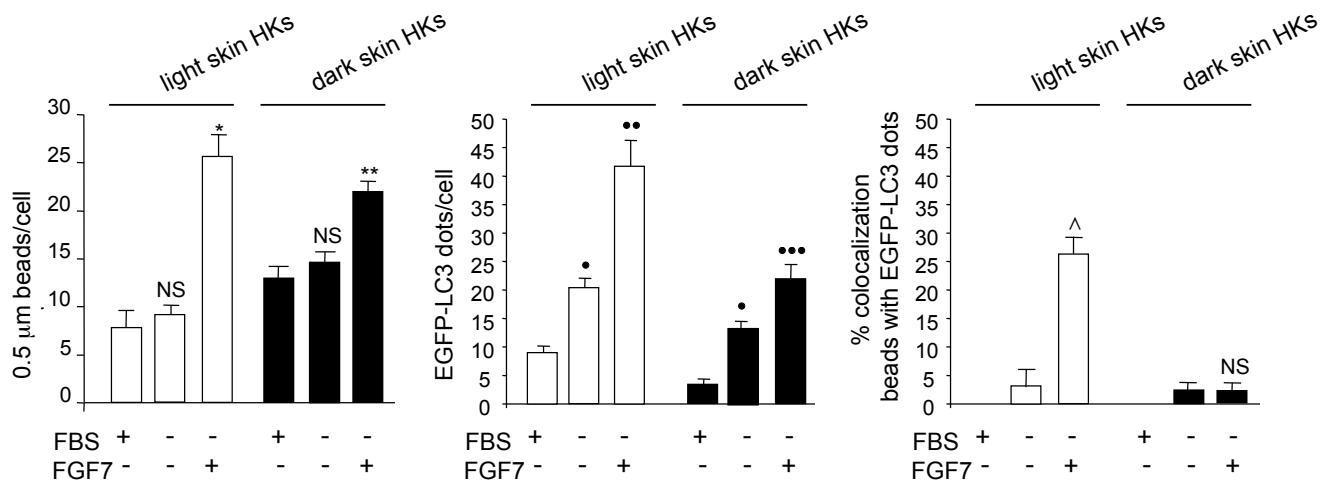
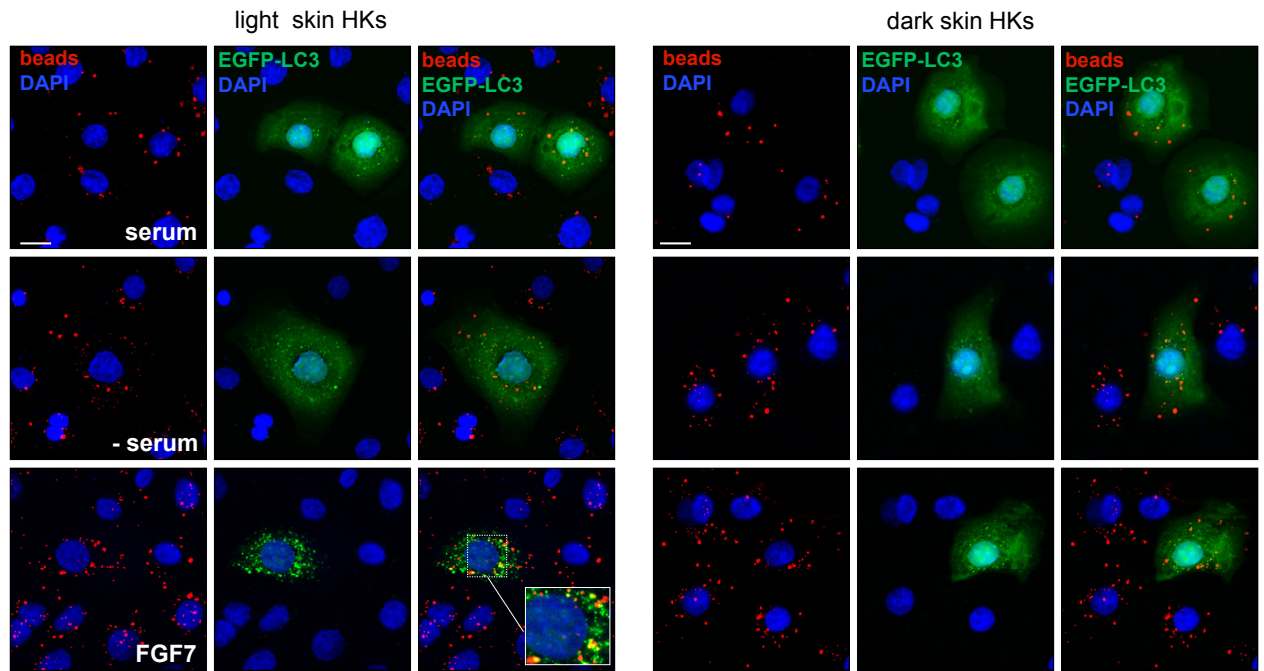


Figure 12

**Figure 12.** FGF7-induced phagocytosis and autophagy are convergent pathways only in light skin HKs. HKs from light skin and from dark skin were transiently transfected with pEGFP-C2-LC3 construct and serum starved or stimulated with FGF7 in the presence of fluorescent beads as reported in figure 6. Quantitative fluorescence analysis shows that the increase of the bead uptake and the number of LC3-positive dots per cell upon FGF7 stimulation is more evident in light skin HKs than in dark ones. A partial colocalization between fluorescent beads and LC3 signal (26%) is detected only in light skin HKs. The quantitative analysis and Student *t* test were performed as above: \**p* < 0.01 vs the corresponding FGF7-unstimulated cells; \*\**p* < 0.05 vs the corresponding FGF7-unstimulated cells; NS vs the corresponding serum-cultured cells; •*p* < 0.01 vs the corresponding serum-cultured cells; ••*p* < 0.01 vs the corresponding FGF7-unstimulated cells; •••*p* < 0.05 vs the corresponding FGF7-unstimulated cells; ^ *p* < 0.05 vs the corresponding FGF7-unstimulated cells; NS vs the corresponding FGF7-unstimulated cells. Bar: 10 μm.

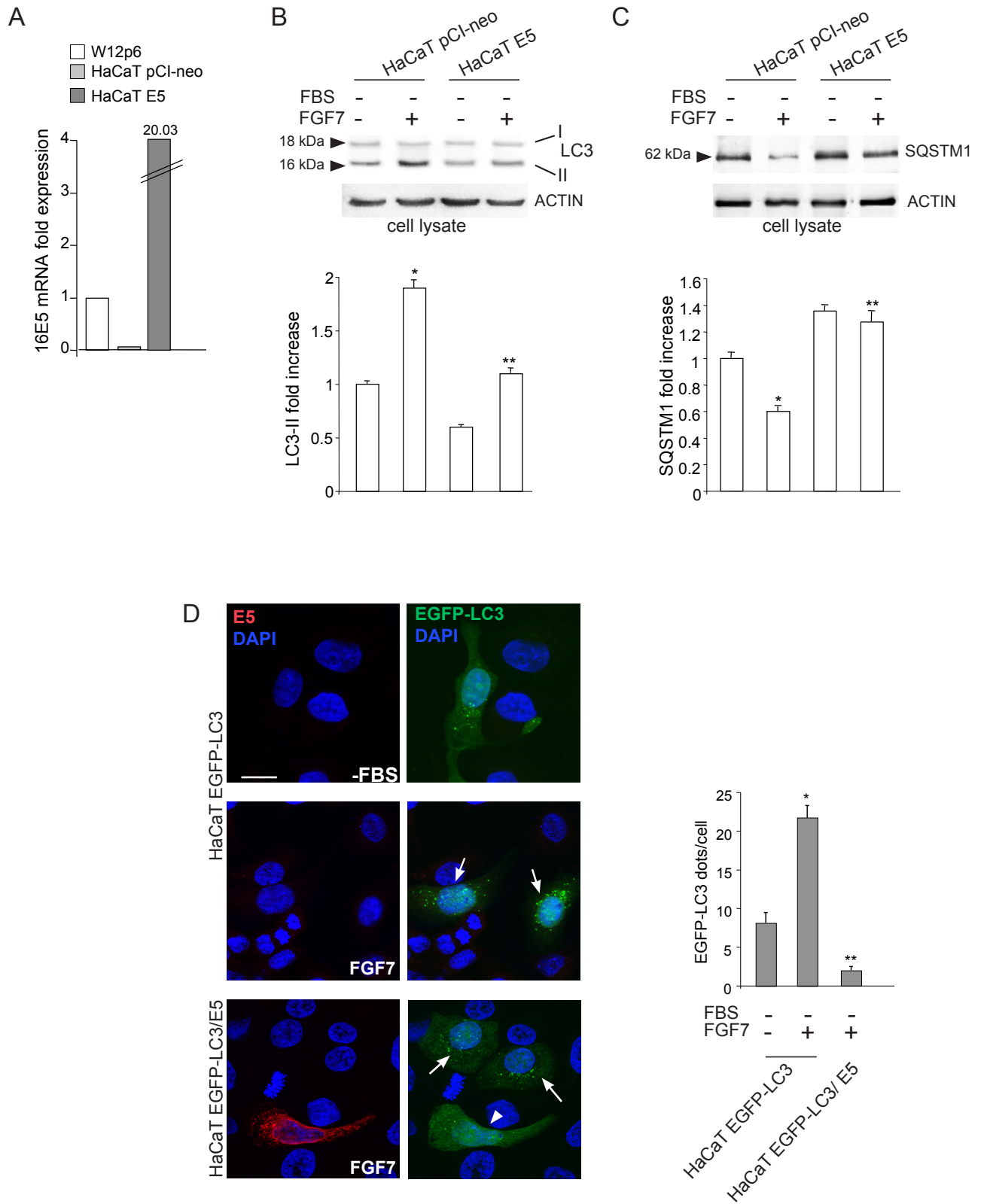


Figure 13

**Figure 13.** 16E5 inhibits FGF7-induced autophagy. (A) HaCaT cells were transiently transfected with pCI-neo E5-HA expression vector (HaCaT E5) or with the empty vector alone (HaCaT pCI-neo). The 16E5 mRNA transcripts, quantitated by real-time relative RT-PCR and normalized with respect to those detected in the HPV16-positive cervical epithelial cell line W12 at the passage 6 (W12p6), are highly expressed only in HaCaT E5 cells. (B, C) HaCaT E5 and HaCaT pCI-neo cells were serum-starved in the presence or absence of FGF7 100 ng/ml for 24 h. Western blot analysis shows that, upon FGF7 stimulation, the LC3-II band is reduced (B), while the SQSTM1 band is enhanced (C), in HaCaT E5 cells compared to HaCaT pCI-neo cells. The equal loading was assessed using anti- $\beta$  actin antibody. The densitometric analysis and Student *t* test were performed as reported above: (B, C)  $*p < 0.05$  vs the corresponding unstimulated cells,  $**p < 0.05$  vs the corresponding HaCaT pCI-neo cells. (D) HaCaT cells were transiently cotransfected with pEGFP-C2-LC3 construct and pCI-neo E5-HA (HaCaT EGFP-LC3/E5) or pCI-neo empty vector (HaCaT EGFP-LC3) before stimulation with FGF7 as above. Immunofluorescence was performed using anti-HA monoclonal antibody (red), to visualize 16E5, and cell nuclei were stained with DAPI. Upon FGF7 treatment, the number of LC3-positive dots per cell is increased in HaCaT EGFP-LC3 cells and in HaCaT EGFP-LC3/E5 cells not showing 16E5 staining (arrows), but is reduced in HaCaT EGFP-LC3/E5 cells strongly labeled for 16E5 (arrowhead) if compared to serum-starved HaCaT EGFP-LC3 cells. The quantitative analysis and Student *t* test were performed as above:  $*p < 0.001$  vs the corresponding serum starved-cells,  $**p < 0.001$  vs the corresponding HaCaT EGFP-LC3 cells. Bar: 10  $\mu$ m.

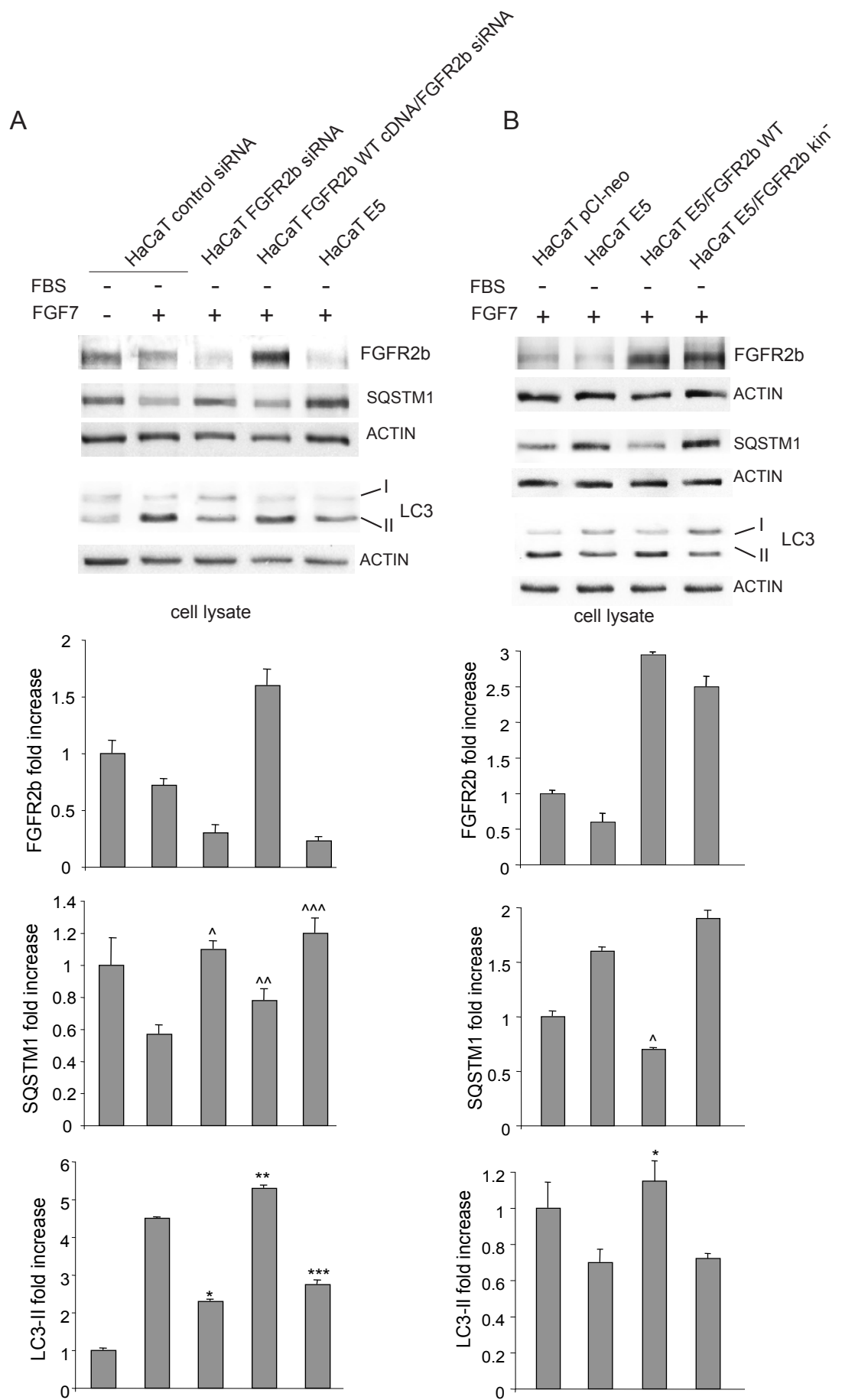


Figure 14

**Figure 14.** The inhibitory effect of 16E5 on FGF7-triggered autophagy depends on FGFR2b expression and signaling. (A) HaCaT cells were transfected with 16E5 cDNA (HaCaT E5), with a small interfering RNA for FGFR2/Bek (HaCaT FGFR2b siRNA) or with an unrelated siRNA (HaCaT control siRNA) as control. Alternatively cells were cotransfected with FGFR2b WT cDNA and with FGFR2b siRNA. Cells were then stimulated with FGF7 as above. Western blot analysis shows that, upon FGF7 stimulation, both FGFR2b and LC3-II bands are reduced, while the SQSTM1 band is increased either in 16E5-transfected and FGFR2b-depleted cells. (B) Cells were transiently transfected with 16E5 (HaCaT E5) or cotransfected with 16E5 and pCI-neo vector containing human FGFR2b WT (HaCaT E5/FGFR2b WT) or the kinase negative mutant FGFR2b Y656F/Y657F (HaCaT E5/FGFR2b kin-) and stimulated with FGF7 as above. Western blot analysis shows that the decrease of LC3-II as well as the increase of SQSTM1 induced by 16E5 expression is counteracted only by FGFR2b WT overexpression. The densitometric analysis and Student *t* test were performed as reported above: (A) <sup>^</sup>, <sup>^^^</sup>, <sup>\*\*\*</sup>*p* < 0.05 and <sup>\*</sup>*p* < 0.01 vs the corresponding HaCaT control siRNA cells, <sup>^^</sup>*p* < 0.05 and <sup>\*\*</sup>*p* < 0.01 vs the corresponding HaCaT FGFR2b siRNA cells; (B) <sup>\*</sup>, <sup>^</sup>*p* < 0.05 vs HaCaT E5 cells.

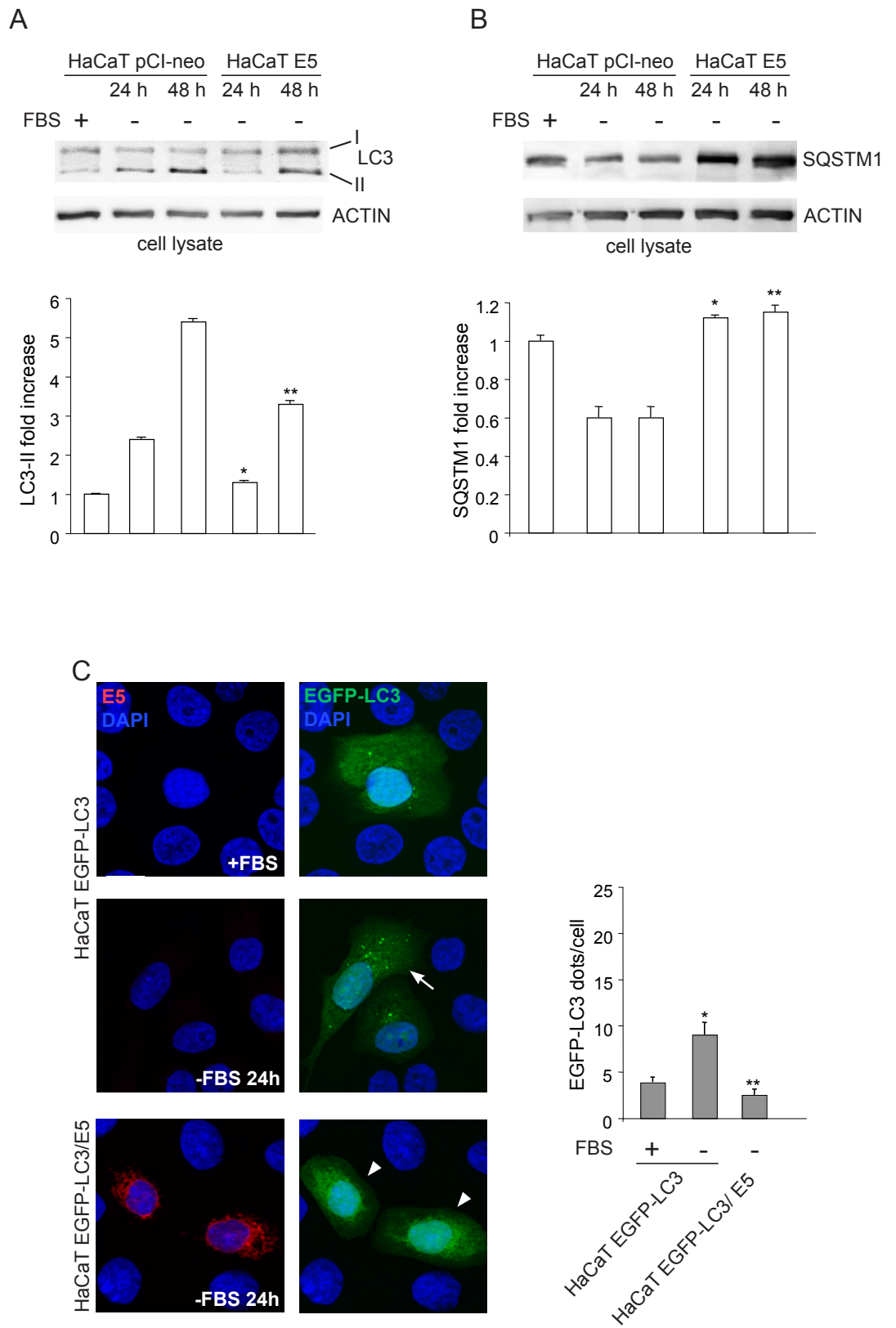


Figure 15

**Figure 15.** 16E5 inhibits also the serum starvation-induced autophagy. (A, B) HaCaT pCI-neo and HaCaT E5 cells were kept in complete medium or serum-starved for 24 h or 48 h. Western blot analysis shows that in HaCaT E5 cells the serum deprivation-induced progressive increase of LC3-II band is reduced, while the decrease of SQSTM1 is blocked. The densitometric analysis and Student *t* test were performed as above: (A)  $*p < 0.01$  vs the corresponding HaCaT pCI-neo cells,  $**p < 0.05$  vs the corresponding HaCaT pCI-neo cells; (B)  $*$ ,  $**p < 0.05$  vs the corresponding HaCaT pCI-neo cells. (C) Immunofluorescence analysis performed in HaCaT EGFP-LC3 and HaCaT EGFP-LC3/E5 cells serum-starved as above shows no increase in LC3-positive dots in cells expressing 16E5 (arrowheads) compared to HaCaT EGFP-LC3 (arrow). The quantitative analysis and Student *t* test were performed as above:  $*p < 0.005$  vs the corresponding serum cultured-cells,  $**p < 0.005$  vs the corresponding HaCaT EGFP-LC3 cells. Bar: 10  $\mu\text{m}$ .

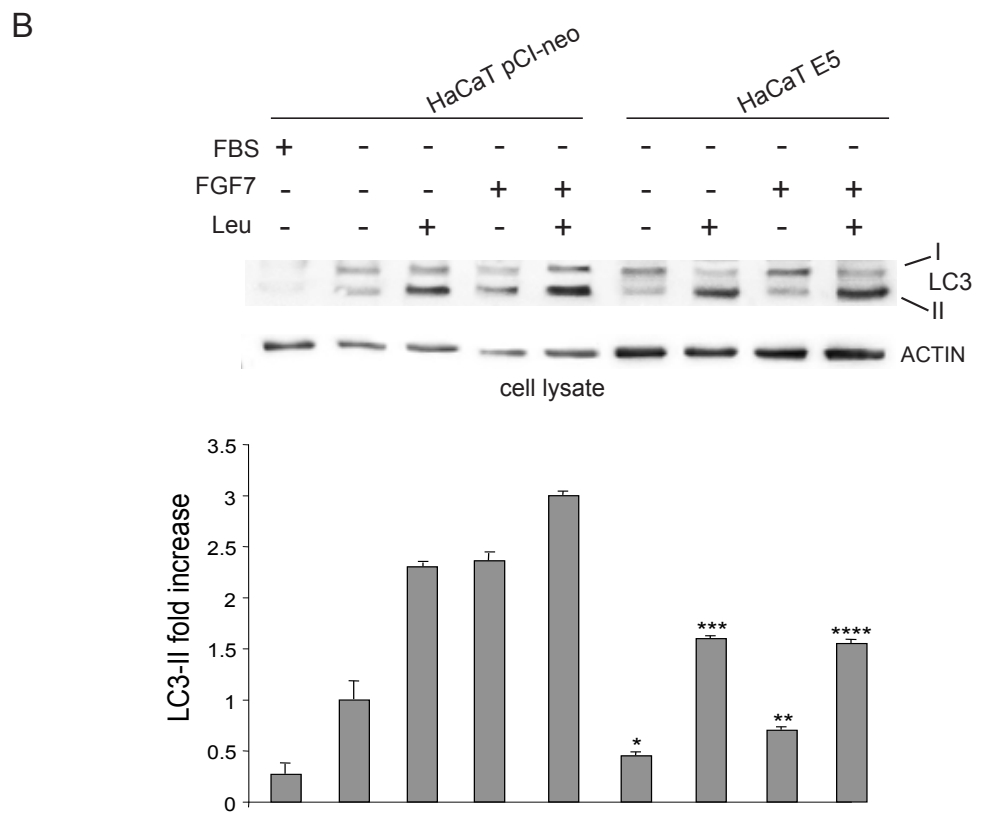
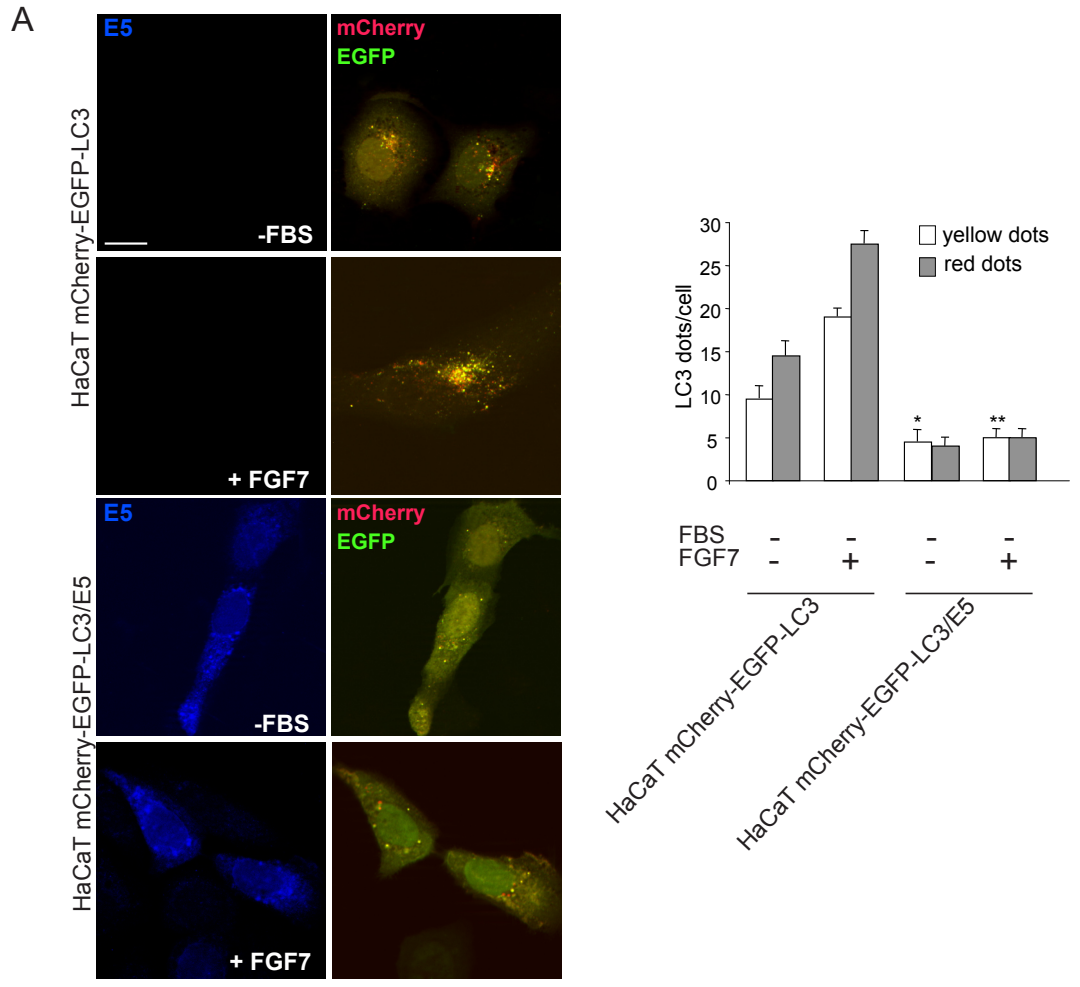


Figure 16

**Figure 16.** 16E5 inhibits autophagosome assembly. (A) HaCaT mCherry-EGFP-LC3 and HaCaT mCherry-EGFP-LC3/E5 cells were serum-starved or treated with FGF7 as above. Immunofluorescence analysis shows that in E5 expressing cells the number of yellow dots corresponding to newly assembled autophagosomes is decreased, while the red dots corresponding to autolysosomes are not increased compared to control cells. The quantitative analysis and Student *t* test were performed as above: \**p* < 0.05, \*\**p* < 0.01 vs the corresponding HaCaT mCherry-EGFP-LC3 cells. Bar: 10 μm (B) HaCaT pCIneo and HaCaT pCI-neo/E5 cells were serum-starved or treated with FGF7 in the presence or absence of leupeptin (LEU) as reported in Materials and Methods. Western blot shows that in 16E5 expressing cells the LC3-II levels are significantly reduced also in the presence of the inhibitor of the lysosomal degradation. The densitometric analysis and Student *t* test were performed as reported above: \* and \*\**p* < 0.05 vs the corresponding HaCaT pCI-neo cells, \*\*\* and \*\*\*\**p* < 0.01 vs the corresponding HaCaT pCI-neo cells.

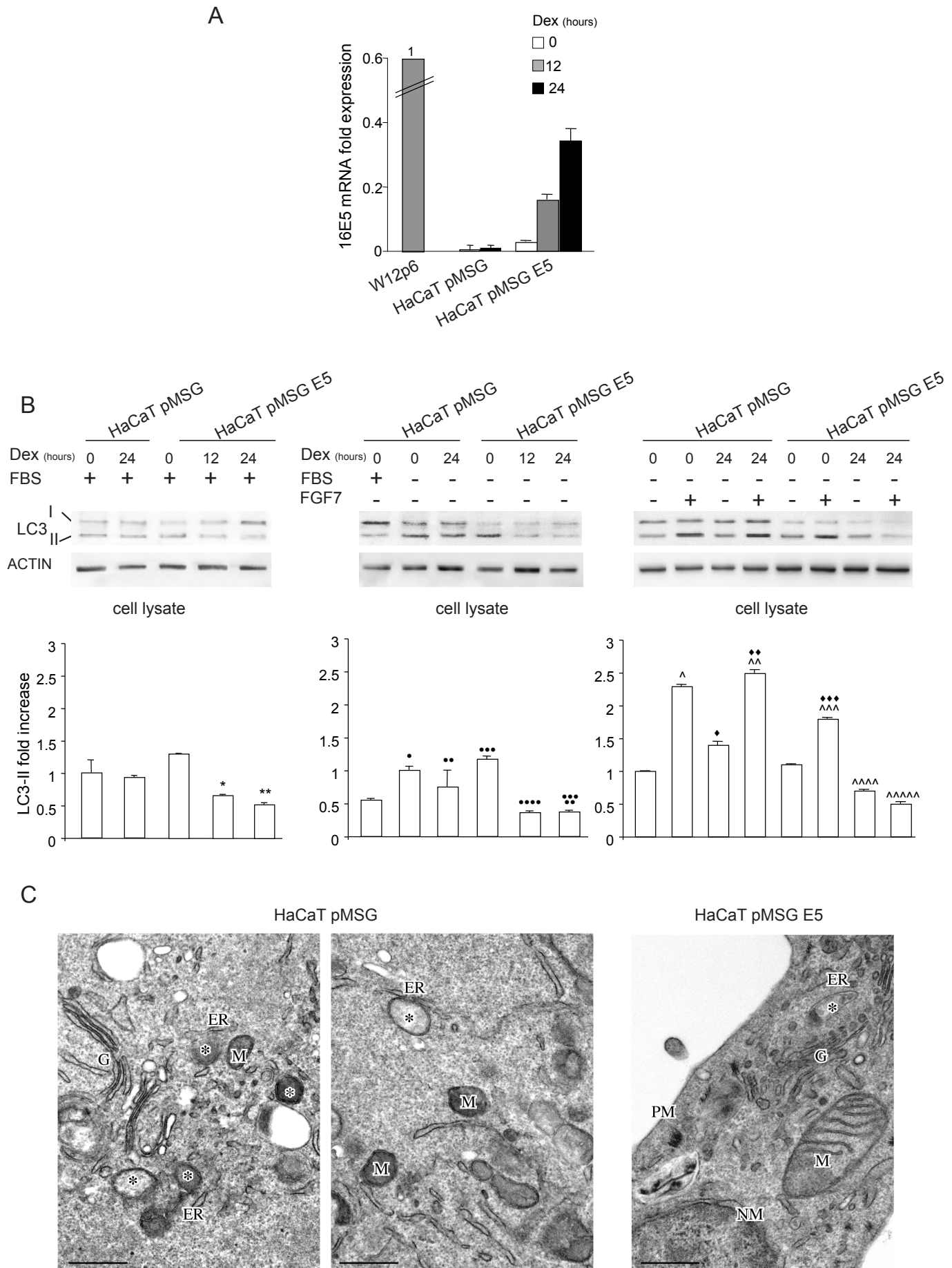


Figure 17

**Figure 17.** Impairment of autophagy in cells stably expressing 16E5. (A) HaCaT pMSG and HaCaT pMSG E5 cells were left untreated (0 h) or treated with Dex for 12 h or 24 h. The 16E5 the increasing mRNA transcript levels were quantitated by real-time relative RT-PCR and normalized with respect to those detected in W12p6 cells. (B) Cells were kept in complete medium or either serum-starved or stimulated with FGF7 for 24 h in presence or absence of Dex induction. Western blot analysis shows that in serum-kept cells (left panel) the very weak band corresponding to LC3-II is decreased at 12 h and 24 h of Dex treatment in HaCaT pMSG E5 cells, while no changes in the band intensity are observed in HaCaT pMSG cells. Upon serum starvation (middle panel) or FGF7 stimulation (right panel) the evident increase of LC3-II band is abolished by Dex treatment only in HaCaT pMSG E5 cells, but not in control cells. In absence of Dex treatment, the increase of LC3-II protein induced FGF7 is lower in HaCaT pMSG E5 than in control cells. The densitometric analysis and Student *t* test were performed as above: \*, \*\* $p < 0.05$  vs the corresponding Dex-untreated cells, •  $p < 0.05$  vs the corresponding serum-cultured cells, •• NS vs the corresponding Dex-untreated cells, ••• NS vs the corresponding HaCaT pMSG cells, ••••, •••••  $p < 0.05$  vs the corresponding Dex-untreated cells, ^, ^^ $p < 0.05$  vs the corresponding FGF7-unstimulated cells, ◆◆◆NS vs the corresponding Dex-untreated cells, ^^^ $p < 0.01$  vs the corresponding FGF7-unstimulated cells, ^^^^ $p < 0.05$  vs the corresponding Dex-untreated cells, ^^^^ $p < 0.01$  vs the corresponding Dex-untreated cells, ◆◆◆ $p < 0.05$  vs the corresponding HaCaT pMSG cells. (C) Ultrastructural analysis of HaCaT pMSG and HaCaT pMSG E5 cells stimulated with FGF7 for 24 h in presence of Dex: the number of double-membrane autophagic vacuoles (asterisks) is lower in HaCaT pMSG E5 (right panel) compared to HaCaT pMSG cells (left and middle panels). ER, endoplasmic reticulum; M, mitochondrion; NM, nuclear membrane; PM, plasma membrane; G, Golgi complex. Bars: 0.5  $\mu\text{m}$ .

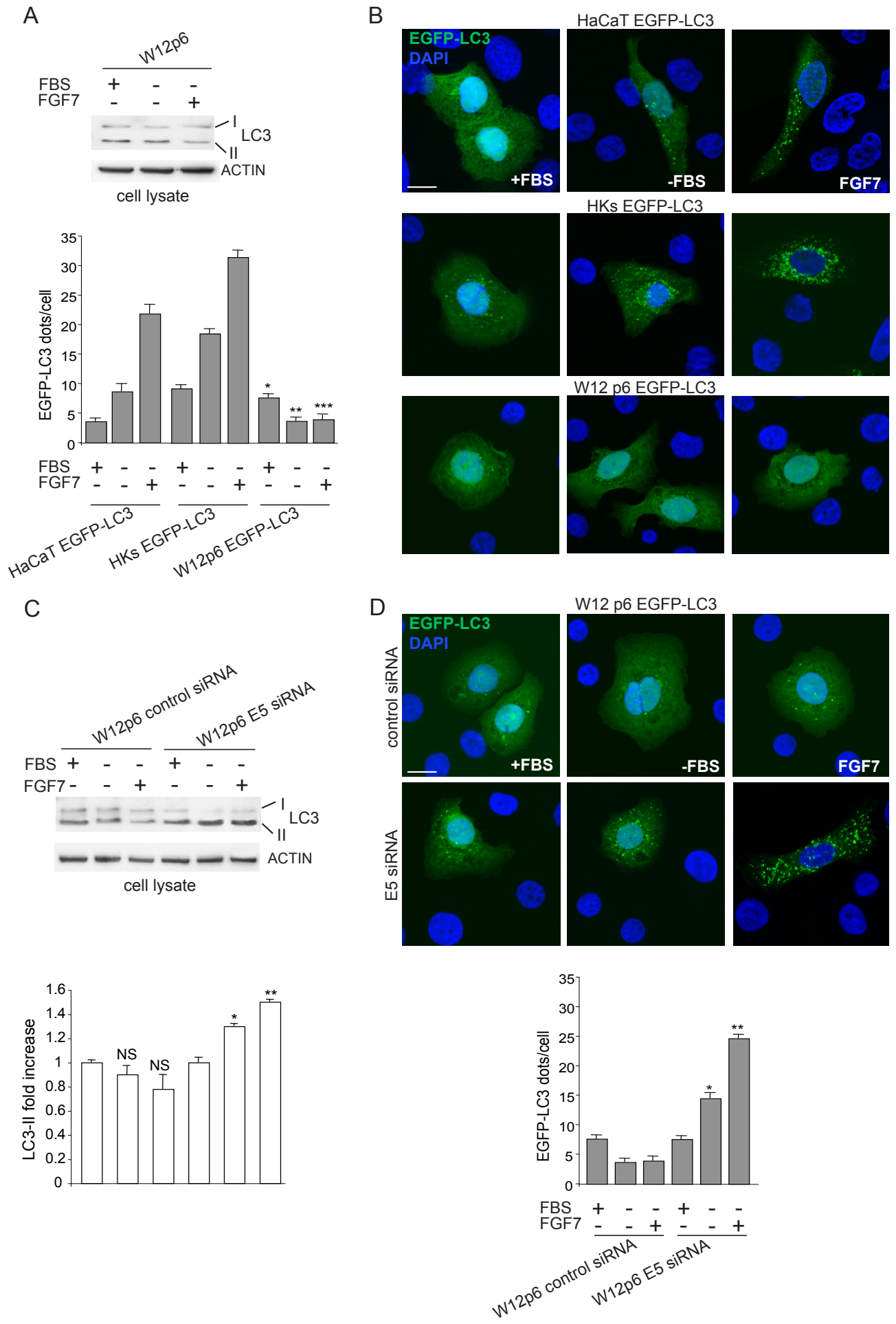


Figure 18

**Figure 18.** The unresponsiveness of W12p6 cells to autophagic stimuli depends on 16E5 expression. (A) Cells were kept in complete medium or serum-starved in the presence or absence of FGF7 for 24 h. Western blot shows no changes in the levels of LC3-II marker in W12p6 cells upon both serum deprivation or FGF7 stimulation. (B) W12p6 cells were transfected with EGFP-LC3 and treated as above. Fluorescence analysis shows an increase in the number of LC3-positive dots per cell after serum starvation and/or FGF7 stimulation in HaCaT EGFP-LC3 and HKs EGFP-LC3 control cells, but not in W12p6 EGFP-LC3 cells. The quantitative analysis and Student t test were performed as above: \* $p < 0.05$  vs the corresponding EGFP-LC3 HaCaT cells; \*\*, \*\*\* $p > 0.001$  vs the corresponding EGFP-LC3 HaCaT cells or vs the corresponding EGFP-LC3 HKs. (c) W12p6 cells were transfected with E5 siRNA or with an unrelated siRNA as control and treated as above. The LC3-II levels are progressively increased by serum deprivation and by FGF7 in W12p6 E5 siRNA, while no changes are observed in W12p6 control siRNA. The densitometric analysis and Student t test were performed as above: NS vs the corresponding serum-cultured cells; \*, \*\* $p < 0.05$  vs the corresponding W12p6 control siRNA cells. (D) W12p6 cells were cotransfected with EGFP-LC3 and with E5 siRNA or with a control siRNA and treated as above. Fluorescence approaches show a significant increase of LC3-positive dots in 16E5-depleted W12 cells upon serum deprivation and even more upon FGF7 stimulation. No increase is found in control siRNA-transfected cells. \*, \*\* $p < 0.001$  vs the corresponding control siRNA. Bars 10  $\mu\text{m}$ .

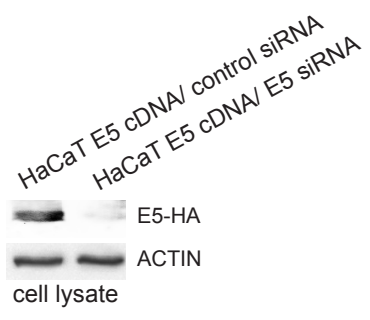


Figure 19

**Figure 19.** E5 siRNA induce an efficient depletion of 16E5 protein in transiently transfected HaCaT E5 cells. HaCaT cells were doubly transfected with pCI-neo E5-HA cDNA and E5 siRNA or control unrelated siRNA. Western blot analysis using anti-HA monoclonal antibody shows that the band at the molecular weight corresponding to 16E5 protein is decreased in HaCaT E5 cDNA/E5siRNA as expected.

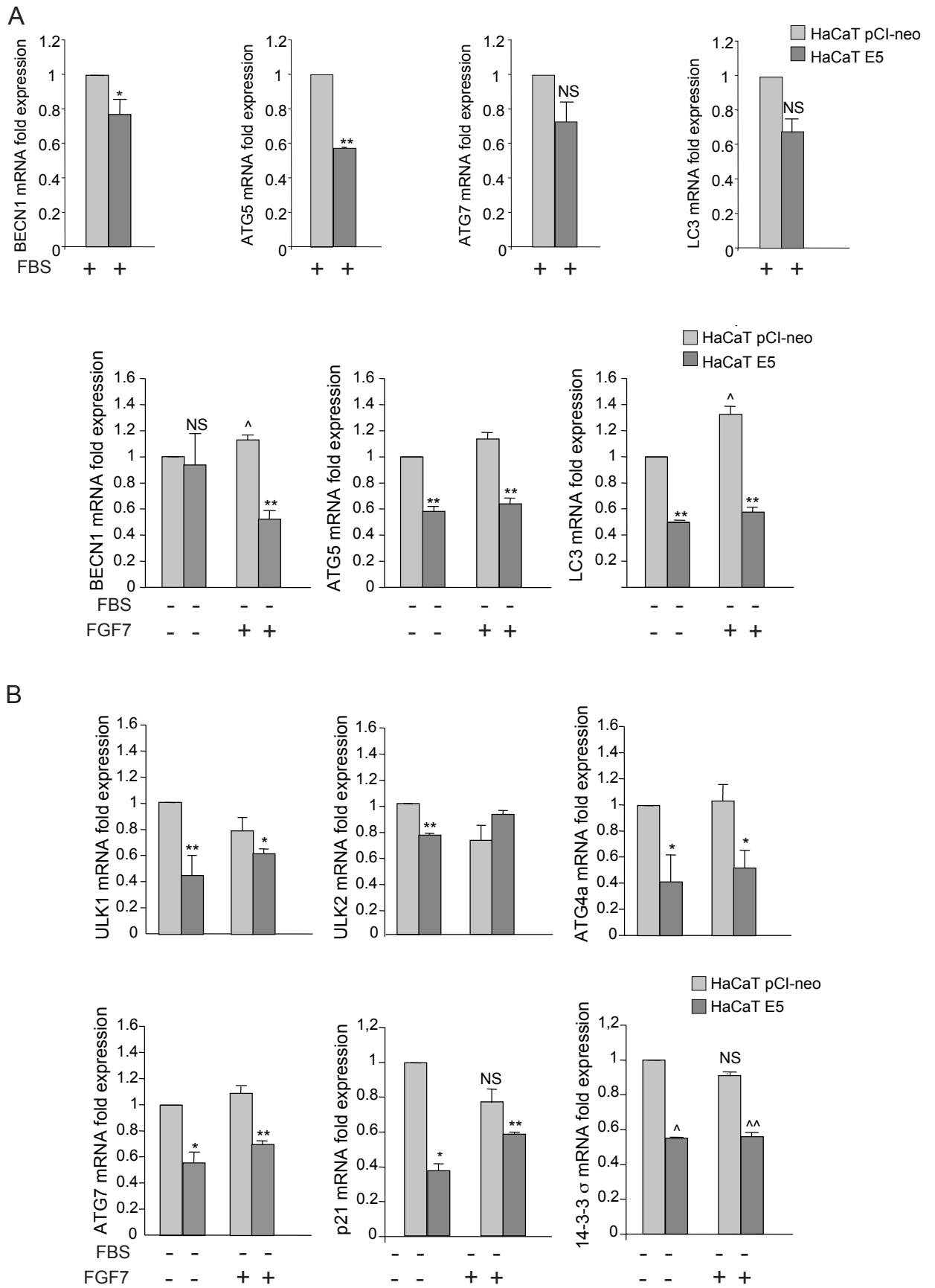
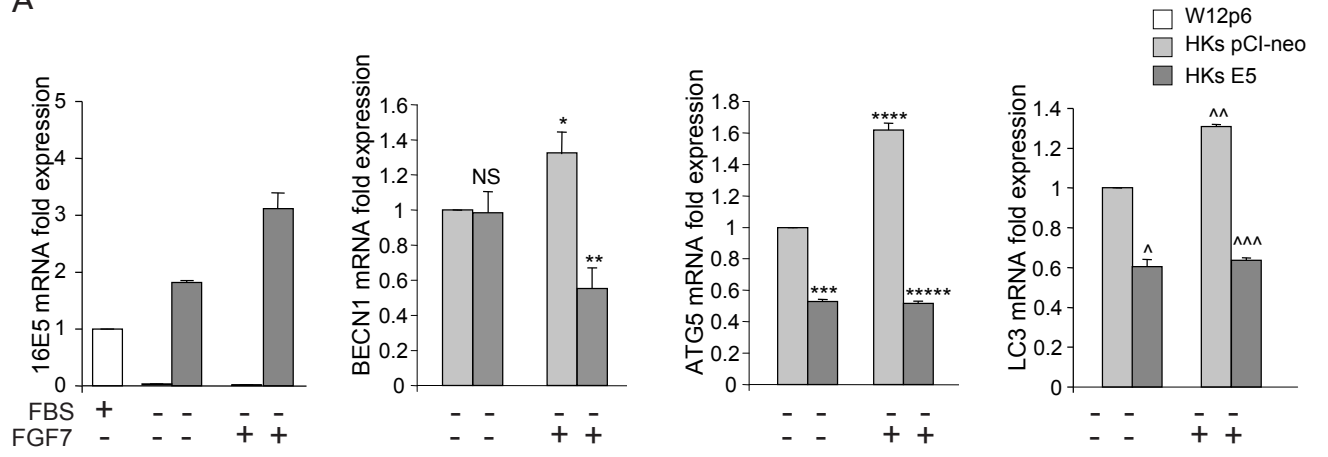


Figure 20

**Figure 20.** 16E5 expression down-modulates the autophagy gene expression in HaCaT cells. (A, B) HaCaT pCI-neo and HaCaT E5 cells were kept in complete medium or serum-starved or stimulated with FGF7 as above. Real-time relative RT-PCR of key regulatory autophagy genes (A) or p53-target autophagic (ULK1, ULK2, ATG4a, ATG7) or autophagy-independent (p21, 14-3-3- $\sigma$ ) genes (B). Results are expressed as mean  $\pm$  standard error (SE) from three different experiments in triplicate. Student t test was performed and significance levels have been defined as  $p < 0.05$ : (A) \* $p < 0.05$  and \*\* $p < 0.01$  vs the corresponding HaCaT pCI-neo cells, NS vs the corresponding HaCaT pCI-neo cells, ^ $p < 0.05$  vs the corresponding FGF7-unstimulated cells. (B) \*, \*\*, ^, ^^ $p < 0.05$  vs the corresponding HaCaT pCI-neo cells, NS vs the corresponding FGF7-unstimulated cells.

A



B

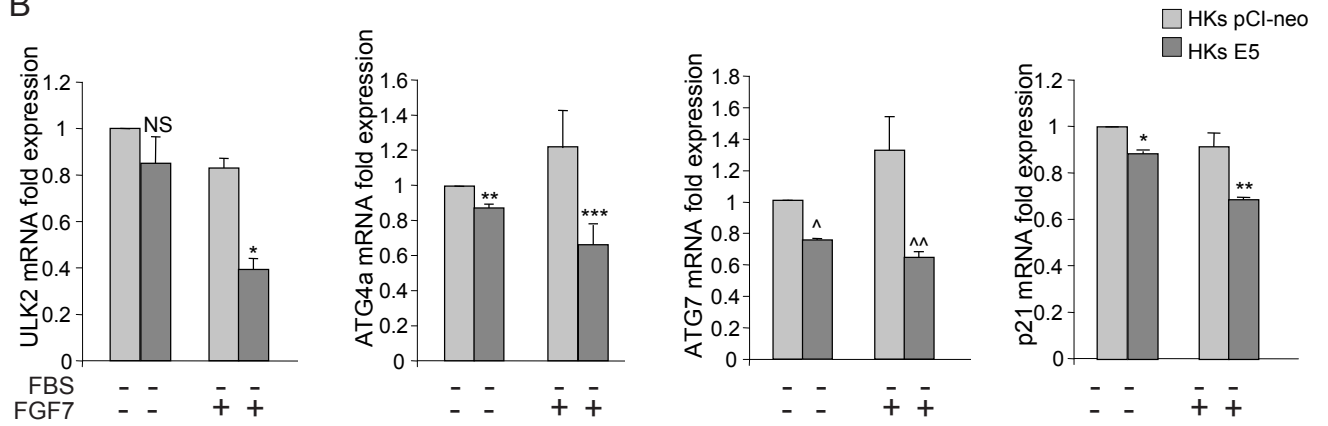


Figure 21

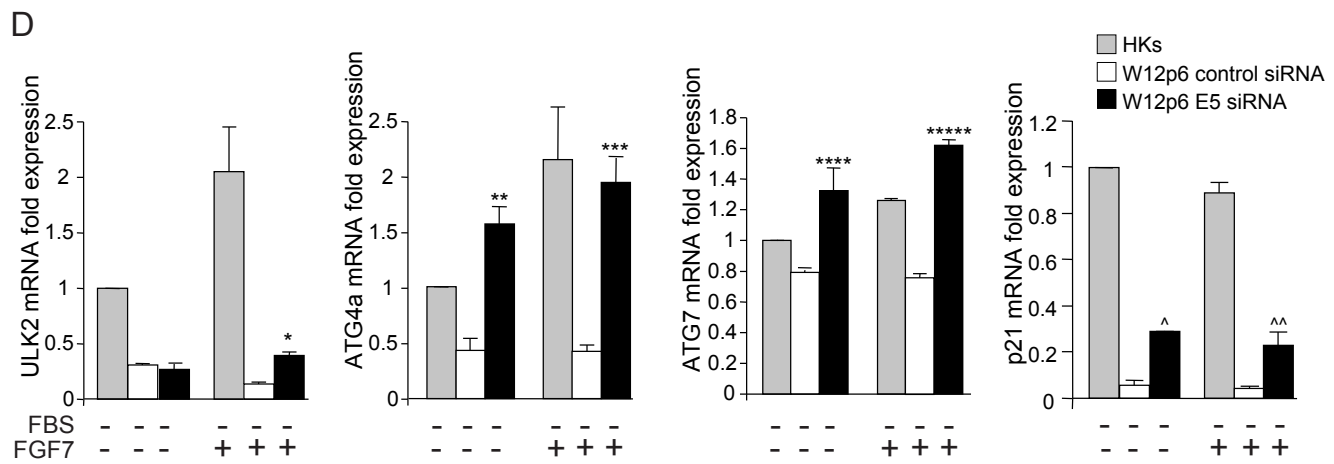
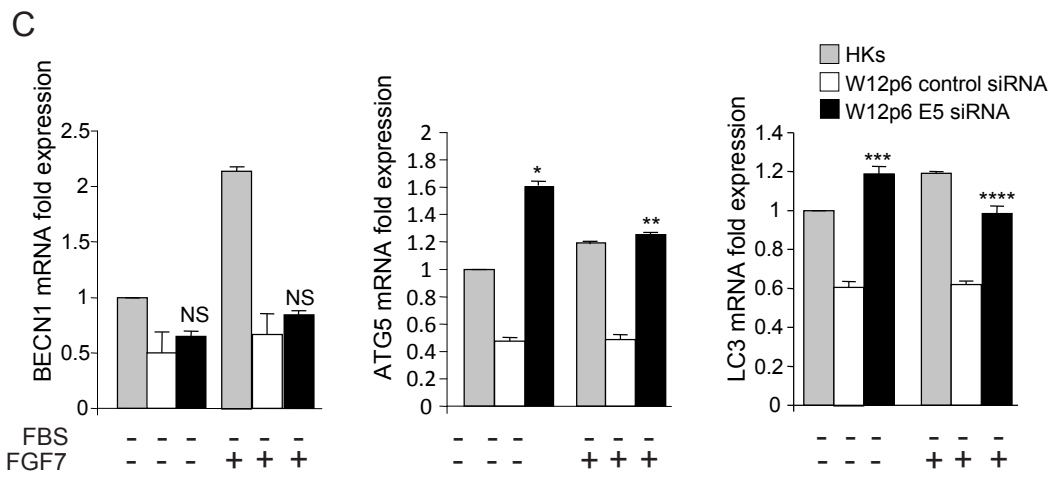


Figure 21

**Figure 21.** 16E5 depletion in the W12p6 cervical carcinogenesis model restores the autophagic gene expression. (A,B) HKs pCI-neo and HKs E5 cells were kept in complete medium or serum-starved or stimulated with FGF7 as above. Real-time relative RT-PCR of key regulatory autophagy genes (A) or p53-target genes (B). (C, D) W12p6 control siRNA and W12p6 E5 siRNA cells and HKs were treated as above. Real-time relative RT-PCR of key regulatory autophagy genes (C) or p53-target genes (D). Results are expressed as mean  $\pm$  standard error (SE). Student t test was performed and significance levels have been defined as above: (A) \* $p < 0.05$  and \*\*\*\* and  $^{^^}p < 0.005$  vs the corresponding FGF7-unstimulated cells, \*\* $p < 0.05$ ,  $^p < 0.005$  and \*\*\*, \*\*\*\*\*,  $^{^^^}p < 0.001$  vs the corresponding HKs pCI-neo cells, NS vs the corresponding HKs pCI-neo cells; (B) \*, \*\*, \*\*\*,  $^{^^}p < 0.05$  and  $^p < 0.001$  vs the corresponding HKs pCI-neo cells, NS vs the corresponding HKs pCI-neo cells; (C) \*, \*\* $p < 0.001$  and \*\*\*, \*\*\*\* $p < 0.05$  vs the corresponding W12p6 control siRNA, NS vs the corresponding W12p6 control siRNA; (D) \*, \*\*, \*\*\*,  $^{^^}p < 0.05$  and \*\*\*\*, \*\*\*\*\*,  $^p < 0.005$  vs the corresponding W12p6 control siRNA.

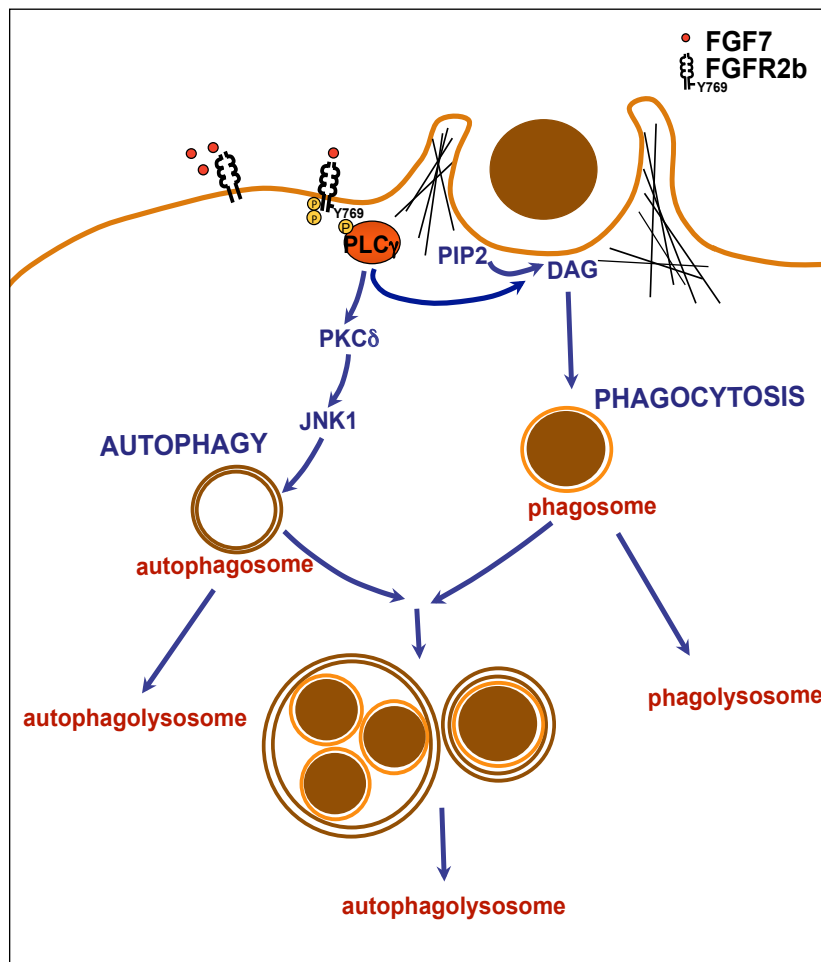


Figure 22

**Figure 22.** Schematic drawing of the proposed role of FGFR2b and its PLC $\gamma$  signaling in the regulation of autophagy and phagocytosis interplay. FGF7-mediated FGFR2b activation induces phosphorylation of the Y769 residue, which is required for activation and recruitment of PLC $\gamma$  to the receptor. PLC $\gamma$  signaling in turn induces both phagocytosis through diacylglycerol (DAG) formation and autophagy through JNK1 activation via PKC $\delta$ . The two membrane pathways partially converge toward lysosomal degradation.

## **REFERENCES**

Agoff SN, Hou J, Linzer DI, Wu B. (1993). Regulation of the human hsp70 promoter by p53. *Science* 259: 84–87.

Aguilera MO, Berón W, Colombo MI. (2012). The actin cytoskeleton participates in the early events of autophagosome formation upon starvation induced autophagy. *Autophagy* 8: 1590-1603.

Akinduro O, Sully K, Patel A, Robinson DJ, Chikh A, McPhail G, Braun KM, Philpott MP, Harwood CA, Byrne C, O'Shaughnessy RF, Bergamaschi D4. (2016). Constitutive autophagy and nucleophagy during epidermal differentiation. *J Invest Dermatol.* 136: 1460-1470.

Altomare DA, Testa JR. (2005). Perturbations of the AKT signaling pathway in human cancer. *Oncogene* 24: 7455–7464.

Ashra GH, Haghshenas MR, Marchetti B, O'Brien PM, Campo MS. (2005). E5 protein of human papillomavirus type 16 selectively downregulates surface HLA class I. *Int J Cancer* 113: 276–283.

Axe EL, Walker SA, Manifava M, Chandra P, Roderick HL, Habermann A, Griffiths G, Ktistakis NT. (2008). Autophagosome formation from membrane compartments enriched in phosphatidylinositol 3-phosphate and dynamically connected to the endoplasmic reticulum. *J. Cell Biol.* 182: 685–701.

Aymard E, Barruche V, Naves T, Bordes S, Closs B, Verdier M, Ratinaud MH. (2011). Autophagy in human keratinocytes: an early step of the differentiation? *Exp Dermatol.* 20: 263-268.

Bach M, Larance M, James DE, Ramm G. (2011). The serine/threonine kinase ULK1 is a target of multiple phosphorylation events. *Biochem J* 440: 283-291.

Barbaresi S, Cortese MS, Quinn J, Ashra GH, Graham SV, Campo MS. (2010). Effects of human papillomavirus type16E5 deletion mutants on epithelial

morphology: functional characterization of each transmembrane domain. *J Gen Virol.* 91: 521–530.

Belleudi F, Leone L, Aimati L, Stirparo MG, Cardinali G, Marchese C, Frati L, Picardo M, Torrasi MR. (2006). Endocytic pathways and biological effects induced by UVB-dependent or ligand-dependent activation of the keratinocyte growth factor receptor. *FASEB J* 20: 395-397.

Belleudi F, Leone L, Purpura V, Cannella F, Scrofani C, Torrasi MR. (2011). HPV16 E5 affects the KGFR/FGFR2b- mediated epithelial growth through alteration of the receptor expression, signaling and endocytic traffic. *Oncogene* 30: 4963–4976.

Belleudi F, Purpura V, Caputo S, Torrasi MR. (2014). FGF7/KGF regulates autophagy in keratinocytes: A novel dual role in the induction of both assembly and turnover of autophagosomes. *Autophagy* 10: 803-821.

Belleudi F, Purpura V, Scrofani C, Persechino F, Leone L, Torrasi MR. (2011). Expression and signaling of the tyrosine kinase FGFR2b/KGFR regulates phagocytosis and melanosome uptake in human keratinocytes. *FASEB J* 25: 170-181.

Belleudi F, Purpura V, Torrasi MR. (2011). The receptor tyrosine kinase FGFR2b/KGFR controls early differentiation of human keratinocytes. *PLoS One* 6: e24194.

Belleudi F, Scrofani C, Torrasi MR, Mancini P. (2011). Polarized endocytosis of the keratinocyte growth factor receptor in migrating cells: role of SRC-signaling and cortactin. *PLoS One* 6: e29159.

Bento CF, Renna M, Ghislat G, Puri C, Ashkenazi A, Vicinanza M, Menzies FM, Rubinsztein DC. (2016). Mammalian Autophagy: How Does It Work? *Annu Rev Biochem.* 85: 685-713.

Boissy RE. (2003) Melanosome transfer to and translocation in the keratinocytes. *Exp Dermatol* 12: 5-12.

Bonilla DL, Bhattacharya A, Sha Y, Xu Y, Xiang Q, Kan A, Jagannath C, Komatsu M, Eissa NT. (2013). Autophagy regulates phagocytosis by modulating the expression of scavenger receptors. *Immunity* 39: 537-547.

Boukamp P, Petrussevska RT, Breitkreutz D, Hornung J, Markham A, Fusenig NE. (1988). Normal keratinization in a spontaneously immortalized aneuploid human keratinocyte cell line. *J Cell Biol.* 106: 761-771.

Brooks AN, Kilgour E, Smith PD. (2012). Molecular pathways: fibroblast growth factor signaling: a new therapeutic opportunity in cancer. *Clin Cancer Res.* 18: 1855-1862.

Cai BH, Hsu PC, Hsin IL, Chao CF, Lu MH, Lin HC, Chiou SH, Tao PL, Chen JY. (2012). p53 acts as a co-repressor to regulate keratin 14 expression during epidermal cell differentiation. *PLoS One* 7: e41742.

Candi E, Cipollone R, Rivetti di Val Cervo P, Gonfloni S, Melino G, Knight R. (2008). p63 in epithelial development. *Cell Mol Life Sci.* 65: 3126-3133.

Capone A, Visco V, Belleudi F, Marchese C, Cardinali G, Bellocchi M, Picardo M, Frati L. and Torrisi MR. (2000). Up-modulation of the expression of functional keratinocyte growth factor receptors induced by high cell density in the human keratinocyte HaCaT cell line. *Cell Growth Differ.* 11: 607-614.

Cardinali G, Bolasco G, Aspite N, Lucania G, Lotti LV, Torrisi MR, Picardo M. (2008). Melanosome transfer promoted by keratinocyte growth factor in light and dark skin-derived keratinocytes. *J Invest Dermatol* 128: 558-567.

Cardinali G, Ceccarelli S, Kovacs D, Aspite N, Lotti LV, Torrisi MR, Picardo M. (2005). Keratinocyte growth factor promotes melanosome transfer to keratinocytes. *J Invest Dermatol* 125: 1190-1199.

Ceccarelli S, Cardinali G, Aspite N, Picardo M, Marchese C, Torrisi MR, Mancini P. (2007) Cortactin involvement in the keratinocyte growth factor and fibroblast growth factor 10 promotion of migration and cortical actin assembly in human keratinocytes. *Exp. Cell Res.* 313: 1758-1777.

Cecconi F, Levine B. (2008). The role of autophagy in mammalian development: cell makeover rather than cell death. *Dev Cell* 15: 344-357.

Ceridono M, Belleudi F, Ceccarelli S, Torrisi MR. (2005). Tyrosine 769 of the keratinocyte growth factor receptor is required for receptor signaling but not endocytosis. *Biochem Biophys Res Commun.* 327: 523-532.

Cha JY, Maddileti S, Mitin N, Harden TK, Der CJ. (2009). Aberrant receptor internalization and enhanced FRS2-dependent signaling contribute to the transforming activity of the fibroblast growth factor receptor 2 IIIb C3 isoform. *J Biol Chem.* 284: 6227-40.

Chatterjea SM, Resing KA, Old W, Nirunsuksiri W, Fleckman P. (2011). Optimization of Filaggrin Expression and Processing in Cultured Rat Keratinocytes. *J Dermatol Sci.* 61: 51-59.

Chen JL, Lin HH, Kim KJ, Lin A, Forman HJ, Ann DK. (2008). Novel roles for protein kinase Cdelta-dependent signaling pathways in acute hypoxic stress-induced autophagy. *J Biol Chem.* 283: 34432-34444.

Chen JL, Lin HH, Kim KJ, Lin A, Ou JH, Ann DK. (2009). PKC delta signaling: a dual role in regulating hypoxic stress-induced autophagy and apoptosis. *Autophagy* 5: 244-246.

Chikh A, Matin RN, Senatore V, Hufbauer M, Lavery D, Raimondi C, Ostano P, Mello-Grand M, Ghimenti C, Bahta A, Khalaf S, Akgül B, Braun KM, Chiorino G, Philpott MP, Harwood CA, Bergamaschi D. (2011). iASPP/p63 autoregulatory feedback loop is required for the homeostasis of stratified epithelia. *EMBO J.* 30: 4261-4273.

Chikh A, Sanzà P, Raimondi C, Akinduro O, Warnes G, Chiorino G, Byrne C, Harwood CA, Bergamaschi D. (2014). iASPP is a novel autophagy inhibitor in keratinocytes. *J Cell Sci.* 127: 3079-3093.

Cinque L, Forrester A, Bartolomeo R, Svelto M, Venditti R, Montefusco S, Polishchuk E, Nusco E, Rossi A, Medina DL, Polishchuk R, De Matteis MA, Settembre C. (2015). FGF signalling regulates bone growth through autophagy. *Nature* 528: 272-275.

Decraene D, Van Laethem A, Agostinis P, De Peuter L, Degreef H, Bouillon R, Garmyn M. (2004). AKT status controls susceptibility of malignant keratinocytes to the early-activated and UVB- induced apoptotic pathway. *J Invest Dermatol.* 123: 207-212.

Deffieu M, Bhatia-Kissova I, Salin B, Galinier A, Manon S, Camougrand N. (2009). Glutathione participates in the regulation of mitophagy in yeast. *J Biol Chem.* 284: 14828-14837.

Desjardins M, Griffiths G. (2003). Phagocytosis: latex leads the way. *Curr Opin Cell Biol* 15: 498-503.

Di Bartolomeo S, Corazzari M, Nazio F, Oliverio S, Lisi G, Antonioli M, Pagliarini V, Matteoni S, Fuoco C, Giunta L, D'Amelio M, Nardacci R, Romagnoli A, Piacentini M, Cecconi F, Fimia GM. (2010). The dynamic interaction of AMBRA1 with the dynein motor complex regulates mammalian autophagy. *J Cell Biol.* 191: 155-168.

Di Bartolomeo S, Nazio F, Cecconi F. (2010). The role of autophagy during development in higher eukaryotes. *Traffic* 11: 1280-1289.

DiMaio, Petti. (2012). The E5 proteins. *Virology*. 445: 99-114.

Dooley HC, Razi M, Polson HE, Girardin SE, Wilson MI, Tooze SA. (2014). WIPI2 links LC3 conjugation with PI3P, autophagosome formation, and pathogen clearance by recruiting Atg12-5-16L1. *Mol. Cell*. 55:238-252.

Dunn WA Jr, Cregg JM, Kiel JAKW, van der Klei IJ, Oku M, Sakai Y, Sibirny AA, Stasyk OV, Veenhuis M. (2005). Pexophagy: the selective autophagy of peroxisomes. *Autophagy* 1: 75- 83.

Dupont N, Jiang S, Pilli M, Ornatowski W, Bhattacharya D, Deretic V. (2011). Autophagy-based unconventional secretory pathway for extracellular delivery of IL-1 $\beta$ . *EMBO J* 30: 4701-4711.

Eom YW, Oh JE, Lee JI, Baik SK, Rhee KJ, Shin HC, Kim YM, Ahn CM, Kong JH, Kim HS, Shim KY. (2014). The role of growth factors in maintenance of stemness in bone marrow-derived mesenchymal stem cells. *Biochem Biophys Res Commun*. 445: 16-22.

Eswarakumar VP, Lax I, Schlessinger J. (2005). Cellular signaling by fibroblast growth factor receptors. *Cytokine Growth Factor Rev*. 16: 139-149.

Fehrmann F, Laimins LA. (2003). Human papillomaviruses: targeting differentiating epithelial cells for malignant transformation. *Oncogene*. 22: 5201-5207.

Feng Y, He D, Yao Z, Klionsky D. (2014). The machinery of macroautophagy. *Cell Res*. 24: 24-41.

Florey O, Gammoh N, Kim SE, Jiang X, Overholtzer M. (2015). V-ATPase and osmotic imbalances activate endolysosomal LC3 lipidation. *Autophagy* 11: 88-99.

Freeman SA, Grinstein S. (2014). Phagocytosis: receptors, signal integration, and the cytoskeleton. *Immunol Rev.* 262: 193-215.

French D, Belleudi F, Mauro MV, Mazzetta F, Raffa S, Fabiano V, Frega A, Torrisi MR. (2013). Expression of HPV16 E5 down-modulates the TGFbeta signaling pathway. *Mol Cancer* 12: 38.

Funderburk SF, Wang QJ, Yue Z. (2010). The Beclin 1-VPS34 complex—at the crossroads of autophagy and beyond. *Trends Cell Biol.* 20: 355-362.

Ganesan AK, Ho H, Bodemann B, Petersen S, Aruri J, Koshy S, Richardson Z, Le LQ, Krasieva T, Roth MG, Farmer P, White MA. (2008). Genome-wide siRNA-based functional genomics of pigmentation identifies novel genes and pathways that impact melanogenesis in human cells. *PLoS Genet* 4: e1000298.

Ganley IG, Lam du H, Wang J, Ding X, Chen S, Jiang X. (2009). ULK1.ATG13.FIP200 complex mediates mTOR signaling and is essential for autophagy. *J Biol Chem.* 284: 12297- 12305.

Garami A, Zwartkruis FJ, Nobukuni T, Joaquin M, Rocco M, Stocker H, Kozma SC, Hafen E, Bos JL, Thomas G. (2003). Insulin activation of Rheb, a mediator of mTOR/S6K/4E-BP signaling, is inhibited by TSC1 and 2. *Mol Cell* 11: 1457-1466.

Ge L, Melville D, Zhang M, Schekman R. (2013). The ER-Golgi intermediate compartment is a key membrane source for the LC3 lipidation step of autophagosome biogenesis. *eLife* 2: e00947.

Ge L, Zhang M, Schekman R. (2014). Phosphatidylinositol 3-kinase and COPII generate LC3 lipidation vesicles from the ER-Golgi intermediate compartment. *eLife* 3: e04135.

- Goetz R, Mohammadi M. (2013). Exploring mechanisms of FGF signalling through the lens of structural biology. *Nat Rev Mol Cell Biol.* 14: 166-180.
- Gotoh N. (2008). Regulation of growth factor signaling by FRS2 family docking/scaffold adaptor proteins. *Cancer Sci.* 99: 1319-1325.
- Gray E, Pett MR, Ward D, Winder DM, Stanley MA, Roberts I, Scarpini CG, Coleman N. (2010). In vitro progression of human papillomavirus 16 episome-associated cervical neoplasia displays fundamental similarities to integrant-associated carcinogenesis. *Cancer Res.* 70: 4081-4091.
- Greco D, Kivi N, Qian K, Leivonen SK, Auvinen P, Auvinen E. (2011). Human Papillomavirus 16 E5 Modulates the Expression of Host MicroRNAs. *PLoS One* 6: e21646.
- Griffin LM, Cicchini L, Pyeon D. (2013). Human papillomavirus infection is inhibited by host autophagy in primary human keratinocytes. *Virology* 437: 12-19.
- Gutierrez MG, Master SS, Singh SB, Taylor GA, Colombo MI, Deretic V. (2004). Autophagy is a defense mechanism inhibiting BCG and Mycobacterium tuberculosis survival in infected macrophages. *Cell* 119: 753-766.
- Gwinn DM, Shackelford DB, Egan DF, Mihaylova MM, Mery A, Vasquez DS, Turk BE, Shaw RJ. (2008). AMPK phosphorylation of raptor mediates a metabolic checkpoint. *Mol Cell* 30: 214-226.
- Hadari YR, Gotoh N, Kouhara H, Lax I, Schlessinger J. (2001) Critical role for the docking-protein FRS2 alpha in FGF receptor-mediated signal trasduction pathways. *Proc natl Acad Sci USA* 98: 8578-8583.
- Hadari YR, Kouhara H, Lax I, Schlessinger J. (1998). Binding of Shp2 tyrosine phosphatase to FRS2 is essential for fibroblast growth factor-induced PC12 cell differentiation. *Mol Cell Biol.* 18: 3966-3973.

Hailey DW, Rambold AS, Satpute-Krishnan P, Mitra K, Sougrat R, Kim PK, Lippincott-Schwartz J. (2010). Mitochondria supply membranes for autophagosome biogenesis during starvation. *Cell* 141: 656–667.

Hamasaki M, Furuta N, Matsuda A, Nezu A, Yamamoto A, Fujita N, Oomori H, Noda T, Haraguchi T, Hiraoka Y, Amano A, Yoshimori T. (2013). Autophagosomes form at ER- mitochondria contact sites. *Nature* 495: 389–393.

Hanning JE, Saini HK, Murray MJ, Caffarel MM, van Dongen S, Ward D, Barker EM, Scarpini CG, Groves IJ, Stanley MA, Enright AJ, Pett MR, Coleman N. (2013). Depletion of HPV16 early genes induces autophagy and senescence in a cervical carcinogenesis model, regardless of viral physical state. *J Pathol.* 231: 354–366.

Haruna K, Suga Y, Muramatsu S, Taneda K, Mizuno Y, Ikeda S, Ueno T, Kominami E, Tanida I, Hanada K. (2008). Differentiation-specific expression and localization of an autophagosomal marker protein (LC3) in human epidermal keratinocytes. *J Dermatol Sci.* 52: 213-215.

Hayashi-Nishino M, Fujita N, Noda T, Yamaguchi A, Yoshimori T, Yamamoto A. (2009). A subdomain of the endoplasmic reticulum forms a cradle for autophagosome formation. *Nat. Cell Biol.* 11: 1433–1437.

Honda S, Arakawa S, Nishida Y, Yamaguchi H, Ishii E, Shimizu S. (2014). Ulk1-mediated Atg5-independent macroautophagy mediates elimination of mitochondria from embryonic reticulocytes. *Nat. Commun.* 5: 4004.

Hosokawa N, Hara T, Kaizuka T, Kishi C, Takamura A, Miura Y, Iemura S, Natsume T, Takehana K, Yamada N, Guan JL, Oshiro N, Mizushima N. (2009). Nutrient-dependent mTORC1 association with the ULK1-Atg13-FIP200 complex required for autophagy. *Mol Biol Cell* 20: 1981- 1991.

Hosokawa N, Hara T, Kaizuka T, Kishi C, Takamura A, Miura Y, Iemura S, Natsume T, Takehana K, Yamada N, Guan JL, Oshiro N, Mizushima N. (2009).

Nutrient-dependent mTORC1 association with the ULK1-Atg13-FIP200 complex required for autophagy. *Mol Biol Cell* 20: 1981-1991.

Igarashi M, Finch PW, Aaronson SA. (1998). Characterization of recombinant human fibroblast growth factor (FGF)-10 reveals functional similarities with keratinocyte growth factor (FGF)-7. *J. Biol. Chem.* 273: 13230-13235.

Inok K, Li Y, Zhu T, Wu J, Guan KL. (2002). TSC2 is phosphorylated and inhibited by AKT and suppresses mTOR signalling. *Nat Cell Biol.* 4: 648-657.

Inoki K, Li Y, Xu T, Guan KL. (2003). Rheb GTPase is a direct target of TSC2 GAP activity and regulates mTOR signaling. *Genes Dev.* 17: 1829-1834.

Ishibashi K, Uemura T, Waguri S, Fukuda M. (2012). Atg16L1, an essential factor for canonical autophagy, participates in hormone secretion from PC12 cells independently of autophagic activity. *Mol Biol Cell* 23: 3193-3202.

Jewell JL, Russell RC, Guan KL. (2013). Amino acid signalling up-stream of mTOR. *Nat Rev Mol Cell Biol.* 14: 133-139.

Juenemann K, Reits EA. (2012). Alternative Macroautophagic Pathways. *Int J Cell Biol.* 2012: 189794.

Juhász G. (2012). Interpretation of bafilomycin, pH neutralizing or protease inhibitor treatments in autophagic flux experiments. *Autophagy* 8: 1875-1876.

Jung CH, Jun CB, Ro SH, Kim YM, Otto NM, Cao J, Kundu M, Kim DH. (2009). ULK-Atg13-FIP200 complexes mediate mTOR signaling to the autophagy machinery. *Mol Biol Cell* 20: 1992-2003.

Jung CH, Jun CB, Ro SH, Kim YM, Otto NM, Cao J, Kundu M, Kim DH. (2009). ULK-Atg13-FIP200 complexes mediate mTOR signaling to the autophagy machinery. *Mol Biol Cell* 20: 1992-2003.

Kabeya Y, Mizushima N, Ueno T, Yamamoto A, Kirisako T, Noda T, Kominami E, Ohsumi Y, Yoshimori T. (2000). LC3, a mammalian homologue of yeast Apg8p, is localized in autophagosome membranes after processing. *EMBO J* 19: 5720-5728.

Kabeya Y, Mizushima N, Yamamoto A, Oshitani-Okamoto S, Ohsumi Y, Yoshimori T. (2004). LC3, GABARAP and GATE16 localize to autophagosomal membrane depending on form-II formation. *J Cell Sci.* 117: 2805- 2812.

Katz M, Amit I, Yarden Y. (2007). Regulation of MAPKs by growth factors and receptor tyrosine kinases. *Biochim Biophys Acta* 1773: 1161-1176.

Kenzelmann Broz D, Spano Mello S, Biegging KT, Jiang D, Dusek RL, Brady CA, Sidow A, Attardi LD. (2013). Global genomic profiling reveals an extensive p53-regulated autophagy program contributing to key p53 responses. *Genes Dev.* 27: 1016-1031.

Kim E, Goraksha-Hicks P, Li L, Neufeld TP, Guan KL. (2008). Regulation of TORC1 by Rag GTPases in nutrient response. *Nat Cell Biol.* 10: 935-945.

Kim HJ, Kim JH, Bae SC, Choi JY, Kim HJ, Ryoo HM. (2003). The protein kinase C pathway plays a central role in the fibroblast growth factor-stimulated expression and transactivation activity of Runx2. *J Biol Chem.* 278: 319-326.

Kim J, Kim YC, Fang C, Russell RC, Kim JH, Fan W, Liu R, Zhong Q, Guan KL. (2013). Differential regulation of distinct Vps34 complexes by AMPK in nutrient stress and autophagy. *Cell* 152: 290-303.

Kim J, Kundu M, Viollet B, Guan KL. (2011). AMPK and mTOR regulate autophagy through direct phosphorylation of Ulk1. *Nat Cell Biol.* 13: 132-141.

Kivi N, Greco D, Auvinen P, Auvinen E. (2008). Genes involved in cell adhesion, cell motility and mitogenic signaling are altered due to HPV 16 E5 protein expression. *Oncogene* 27: 2532-2541.

Knaevelsrud H, Carlsson SR, Simonsen A. (2013). SNX18 tubulates recycling endosomes for autophagosome biogenesis. *Autophagy* 9: 1639-1641.

Ktistakis NT, Tooze SA. (2016). Digesting the Expanding Mechanisms of Autophagy. *Trends Cell Biol.* 26: 624-635.

Kusama Y, Sato K, Kimura N, Mitamura J, Ohdaira H, Yoshida K. (2009). Comprehensive analysis of expression pattern and promoter regulation of human autophagy-related genes. *Apoptosis* 14: 1165-1175.

La Rochelle WJ, Dirsch OR, Finch PW, Cheon HG, May M, Marchese C, Pierce JH, Aaronson SA. (1995). Specific receptor detection by a functional keratinocyte growth factor-immunoglobulin chimera. *J. Cell. Biol.* 129: 357-366.

Lamb CA, Yoshimori T, Tooze SA. (2013). The autophagosome: origins unknown, biogenesis complex. *Nat Rev Mol Cell Biol.* 14: 759-774.

Laplante M, Sabatini DM. (2012). mTOR signaling in growth control and disease. *Cell* 149: 274-293.

Levine B, Mizushima N, Virgin HW. (2011). Autophagy in immunity and inflammation. *Nature* 469: 323-335.

Lew ED, Furdai CM, Anderson KS, Schlessinger J. (2009) The precise sequence of FGF receptor autophosphorylation is kinetically driven and is disrupted by oncogenic mutations. *Sci Signal.* 2(58).

Li L, Chen X, Gu H. (2016). The signaling involving in autophagy machinery in keratinocytes and therapeutic approaches for skin diseases. *Oncotarget* [Epub ahead of print].

Lima JG, de Freitas Vinhas C, Gomes IN, Azevedo CM, dos Santos RR, Vannier-Santos MA, Veras PS. (2011). Phagocytosis is inhibited by autophagic induction in murine macrophages. *Biochem Biophys Res Commun.* 405: 604-609.

Lin X, Zhang Y, Liu L, McKeethan WL, Shen Y, Song S, Wang F. (2011). FRS2 $\alpha$  is essential for the fibroblast growth factor to regulate the mTOR pathway and autophagy in mouse embryonic fibroblasts. *Int J Biol Sci.* 7: 1114-1121.

Liu J, Yang D, Minemoto Y, Leitges M, Rosner MR, Lin A. (2006). NF-kappaB is required for UV-induced JNK activation via induction of PKCdelta. *Mol Cell* 21: 467-480.

Lotti LV, Rotolo S, Francescangeli F, Frati L, Torrisi MR, Marchese C. (2007). AKT and MAPK signaling in KGF- treated and UVB-exposed human epidermal cells. *J Cell Physiol.* 212: 633-642.

Mack H.I.D., Munger K. (2012). Modulation of autophagy-like processes by tumor viruses. *Cells* 1: 204-247.

Marchese C, Chedid M, Dirsch OR, Csaky KG, Santanelli F, Latini C, LaRochelle WJ, Torrisi MR, Aaronson SA. (1995) Modulation of keratinocyte growth factor and its receptor in reepithelializing human skin. *J Exp. Med.* 82: 1369-1376.

Marchese C, Sorice M, De Stefano C, Frati L, and Torrisi MR. (1997). Modulation of keratinocyte growth factor receptor expression in human cultured keratinocytes. *Cell Growth Differ.* 8: 989-997.

Marshall CJ. (1995). Specificity of receptor tyrosine kinase signaling: transient versus sustained extracellular signal-regulated kinase activation. *Cell* 80: 179-185.

Martinez J, Malireddi RK, Lu Q, Cunha LD, Pelletier S, Gingras S, Orchard R, Guan JL, Tan H, Peng J, Kanneganti TD, Virgin HW, Green DR. (2015). Molecular

characterization of LC3-associated phagocytosis reveals distinct roles for Rubicon, NOX2 and autophagy proteins. *Nat Cell Biol.* 17: 893-906.

Martynova E, Pozzi S, Basile V, Dolni D, Zambelli F, Imbriano C, Pavesi G, Mantovani R. (2012). Gain-of-function p53 mutants have widespread genomic locations partially overlapping with p63. *Oncotarget* 3: 132-143.

Mi N, Chen Y, Wang S, Chen M, Zhao M, Yang G, Ma M, Su Q, Luo S, Shi J, Xu J, Guo Q, Gao N, Sun Y, Chen Z, Yu L. (2015). CapZ regulates autophagosomal membrane shaping by promoting actin assembly inside the isolation membrane. *Nat Cell Biol.* 17: 1112-1123.

Miki T, Bottaro DP, Fleming TP, Smith CL, Burgess WH, Chan AML, Aaronson SA. (1992). Determination of ligand binding specificity by alternative splicing: two distinct growth factor receptors encoded by single gene. *Proc. Natl. Acad. Sci. USA* 89: 246-250.

Mizushima N, Noda T, Yoshimori T, Tanaka Y, Ishii T, George MD, Klionsky DJ, Ohsumi M, Ohsumi Y. (1998). A protein conjugation system essential for autophagy. *Nature* 395: 395-398.

Mizushima N, Yamamoto A, Hatano M, Kobayashi Y, Kabeya Y, Suzuki K, Tokuhiisa T, Ohsumi Y, Yoshimori T. (2001). Dissection of autophagosome formation using Apg5-deficient mouse embryonic stem cells. *J Cell Biol.* 152: 657-668.

Mizushima N, Yoshimori T, Ohsumi Y. (2011). The Role of Atg Proteins in Autophagosome Formation. *Annu Rev Cell Dev Biol.* 27: 107-132.

Mohammadi M, Honegger AM, Rotin D, Fisher R, Bellot F, Li W, Dionne CA, Jaye M, Rubinstein M, Schlessinger J. (1991). A tyrosine-phosphorylated carboxy-terminal peptide of the fibroblast growth factor receptor (Flg) is a binding site for the SH2 domain of phospholipase C-c. *Mol. Cell. Biol.* 11: 5068-5078.

Mohammadi M, Olsen S.K, Ibrahimi OA. (2005). Structural basis for fibroblast growth factor receptor activation. *Cytokine Growth Factor Rev.* 16: 107–137.

Molejon MI., Ropolo A, Re AL, Boggio V, Vaccaro MI. (2013). The VMP1–Beclin 1 interaction regulates autophagy induction. *Sci. Rep.* 3: 1055.

Moody CA, Laimnins LA. (2010). Human papillomavirus oncoproteins: pathways to transformation. *Nat Rev Cancer* 10: 550–560.

Moreau K, Ravikumar B, Renna M, Puri C, Rubinsztein DC. (2011). Autophagosome precursor maturation requires homotypic fusion. *Cell* 146: 303–317.

Moriyama M, Moriyama H, Uda J, Matsuyama A, Osawa M, Hayakawa T. (2014). BNIP3 Plays Crucial Roles in the Differentiation and Maintenance of Epidermal Keratinocytes. *J Invest Dermatol.* 134: 1627-1635.

Murase D, Hachiya A, Takano K, Hicks R, Visscher MO, Kitahara T, Hase T, Takema Y, Yoshimori T. (2013). Autophagy has a significant role in determining skin color by regulating melanosome degradation in keratinocytes. *J Invest Dermatol.* 133: 2416-2424.

Muto V, Stellacci E, Lamberti AG, Perrotti E, Carrabba A, Matera G, Sgarbanti M, Battistini A, Liberto MC, Focà A. (2011). Human papillomavirus type 16 E5 protein induces expression of beta interferon through interferon regulatory factor 1 in human keratinocytes. *J Virol.* 85: 5070–5080.

Nakanishi Y, Mizuno H, Sase H, Fujii T, Sakata K, Akiyama N, Aoki Y, Aoki M, Ishii N. (2015). ERK signal suppression and sensitivity to CH5183284/Debio 1347, a selective FGFR inhibitor. *Mol Cancer Ther.* 14: 2831-2839.

Nguyen BC, Lefort K, Mandinova A, Antonini D, Devgan V, Della Gatta G, Koster MI, Zhang Z, Wang J, Tommasi di Vignano A, Kitajewski J, Chiorino G, Roop DR,

Missero C, Dotto GP. (2006). Cross-regulation between Notch and p63 in keratinocyte commitment to differentiation. *Genes Dev.* 20: 1028–1042.

Nishida Y, Arakawa S, Fujitani K, Yamaguchi H, Mizuta T, Kanaseki T, Komatsu M, Otsu K, Tsujimoto Y, Shimizu S. (2009). Discovery of Atg5/Atg7-independent alternative macroautophagy. *Nature* 461: 654–658.

Oelze I, Kartenbeck J, Crusius K, Alonso A. (1995). Human papillomavirus type 16 E5 protein affects cell-cell communication in an epithelial cell line. *J Virol.* 69: 4489–4494.

Ogier-Denis E, Pattingre S, El Benna J, Codogno P. (2000). Erk1/2-dependent phosphorylation of Galpha-interacting protein stimulates its GTPase accelerating activity and autophagy in human colon cancer cells. *J Biol Chem.* 275: 39090–39095.

Oh JM, Kim SH, Lee YI, Seo M, Kim SY, Song YS, Kim WH, Juhn YS. (2009) Human papillomavirus E5 protein induces expression of the EP4 subtype of prostaglandin E2 receptor in cyclic AMP response element-dependent pathways in cervical cancer cells. *Carcinogenesis* 30: 141–149.

Olsen SK, Ibrahimi OA, Raucci A, Zhang F, Eliseenkova AV, Yayon A, Basilico C, Linhardt RJ, Schlessinger J, Mohammadi M. (2004). Insights into the molecular basis for fibroblast growth factor receptor autoinhibition and ligand-binding promiscuity. *Proc. Natl. Acad. Sci. U.S.A.* 101: 935–940.

Orr-Urtreger A, Bedford MT, Burakova T, Arman E, Zimmer Y, Yayon A, Givol D, Lonai P. (1993) Developmental localization of the splicing alternatives of fibroblast growth factor receptor-2 (FGFR2). *Dev. Biol.* 158: 475–486.

Orsi A, Razi M, Dooley HC, Robinson D, Weston AE, Collinson LM, Tooze SA. (2012). Dynamic and transient interactions of Atg9 with autophagosomes, but not membrane integration, is required for autophagy. *Mol. Biol. Cell* 23: 1860–1873.

Pankiv S, Clausen TH, Lamark T, Brech A, Bruun JA, Outzen H, Overvatn A, Bjorkoy G, Johansen T. (2007). p62/ SQSTM1 binds directly to Atg8/LC3 to facilitate degradation of ubiquitinated protein aggregates by autophagy. *J Biol Chem.* 282: 24131–24145.

Panos RJ, Bak PM, Simonet WS, Rubin JS, Smith LJ. (1995). Intratracheal instillation of keratinocyte growth factor decreases hyperoxia-induced mortality in rats. *J Clin Invest.* 96: 2026-2033.

Paramio JM, Segrelles C, Lain S, Gomez-Casero E, Lane DP, Lane EB, Jorcano JL. (2000). p53 is phosphorylated at the carboxyl terminus and promotes the differentiation of human HaCaT keratinocytes. *Mol Carcinog.* 29: 251–262.

Pett MR, Alazawi WOF, Roberts I, Downen S, Smith DI, Stanley MA, Coleman N. (2004). Acquisition of high-level chromosomal instability is associated with integration of human papillomavirus type 16 in cervical keratinocytes. *Cancer Res.* 64: 1359–1368.

Pimentel-Muiños FX, Boada-Romero E. (2014) Selective autophagy against membranous compartments: Canonical and unconventional purposes and mechanisms. *Autophagy* 10: 397-407.

Potter CJ, Pedraza LG, Xu T. (2002). AKT regulates growth by directly phosphorylating Tsc2. *Nat Cell Biol.* 4: 658-665.

Puri C, Renna M, Bento CF, Moreau K, Rubinsztein DC. (2014). ATG16L1 meets ATG9 in recycling endosomes: additional roles for the plasma membrane and endocytosis in autophagosome biogenesis. *Autophagy* 10: 182–184.

Purpura V, Belleudi F, Caputo S, Torrisi MR. (2013). HPV16 E5 and KGFR/FGFR2b interplay in differentiating epithelial cells. *Oncotarget* 4: 192-205.

Ravikumar B, Moreau K, Jahreiss L, Puri C, Rubinsztein DC. (2010). Plasma membrane contributes to the formation of pre-autophagosomal structures. *Nat. Cell Biol.* 12: 747-757.

Ravikumar B, Sarkar S, Davies JE, Futter M, Garcia-Arencibia M, Green-Thompson ZW, Jimenez-Sanchez M, Korolchuk VI, Lichtenberg M, Luo S, Massey DC, Menzies FM, Moreau K, Narayanan U, Renna M, Siddiqi FH, Underwood BR, Winslow AR, Rubinsztein DC. (2010). Regulation of Mammalian Autophagy in Physiology and Pathophysiology. *Physiol Rev.* 90: 1383-1435.

Rouschop KM, van den Beucken T, Dubois L, Niessen H, Bussink J, Savelkoul K, Keulers T, Mujcic H, Landuyt W, Voncken JW, Lambin P, van der Kogel AJ, Koritzinsky M, Wouters BG. (2010). The unfolded protein response protects human tumor cells during hypoxia through regulation of the autophagy genes MAP1LC3B and ATG5. *J Clin Invest.* 120: 127-141.

Rubin JS, Osada H, Finch PW, Taylor WG, Rudikoff S, Aaronson SA. (1989). Purification and characterization of newly identified growth factor specific for epithelial cells. *Proc. Natl. Acad. Sci. USA* 86: 802-806.

Russell RC, Tian Y, Yuan H, Park HW, Chang YY, Kim J, Kim H, Neufeld TP, Dillin A, Guan KL. (2013). ULK1 induces autophagy by phosphorylating Beclin-1 and activating VPS34 lipid kinase. *Nat Cell Biol.* 15: 741-750.

Russell RC, Yuan HX, Guan KL. (2014). Autophagy regulation by nutrient signaling. *Cell Res.* 24: 42-57.

Sakoh-Nakatogawa M, Matoba K, Asai E, Kirisako H, Ishii J, Noda NN, Inagaki F, Nakatogawa H, Ohsumi Y. (2013). Atg12-Atg5 conjugate enhances E2 activity of Atg3 by rearranging its catalytic site. *Nat. Struct. Mol. Biol.* 20: 433-439.

Salabei JK, Cummins TD, Singh M, Jones SP, Bhatnagar A, Hill BG. (2013). PDGF-mediated autophagy regulates vascular smooth muscle cell phenotype and resistance to oxidative stress. *Biochem J.* 451: 375-388.

Sancak Y, Bar-Peled L, Zoncu R, Markhard AL, Nada S, Sabatini DM. (2010). Ragulator-Rag complex targets mTORC1 to the lysosomal surface and is necessary for its activation by amino acids. *Cell* 141: 290-303.

Sancak Y, Peterson TR, Shaul YD, Lindquist RA, Thoreen CC, Bar-Peled L, Sabatini DM. (2008). The Rag GTPases bind raptor and mediate amino acid signaling to mTORC1. *Science* 320: 1496-1501.

Sanjuan MA, Dillon CP, Tait SW, Moshiah S, Dorsey F, Connell S, Komatsu M, Tanaka K, Cleveland JL, Withoff S, Green DR. (2007). Toll-like receptor signalling in macrophages links the autophagy pathway to phagocytosis. *Nature* 450: 1253-7.

Scheffner M, Werness BA, Huibregtse JM, Levine AJ, Howley PM. (1990). The E6 oncoprotein encoded by human papillomavirus types 16 and 18 promotes the degradation of p53. *Cell* 63: 1129-1136.

Schlessinger J, Plotnikov AN, Ibrahimi OA, Eliseenkova AV, Yeh BK, Yayon A, Linhardt RJ, Mohammadi M. (2000) Crystal structure of a ternary FGF-FGFR-heparin complex reveals a dual role for heparin in FGFR binding and dimerization. *Mol.Cell.* 6: 743-750.

Silva LM, Jung JU. (2013). Modulation of the autophagy pathway by human tumor viruses. *Semin Cancer Biol.* 23: 323-328.

Sobolewska A, Gajewska M, Zarzy ska J, Gajkowska B, Motyl T. (2009). IGF-I, EGF, and sex steroids regulate autophagy in bovine mammary epithelial cells via the mTOR pathway. *Eur J Cell Biol.* 88: 117-130.

- Stanley MA, Browne HM, Appleby M, Minson AC. (1989). Properties of a non-tumorigenic human cervical keratinocyte cell line. *Int J Cancer* 43: 672-676.
- Steinberg SF. (2008). Structural basis of protein kinase C isoform function. *Physiol Rev.* 88: 1341-1378.
- Takeuchi H, Kanzawa T, Kondo Y, Kondo S. (2004). Inhibition of platelet-derived growth factor signalling induces autophagy in malignant glioma cells. *Br J Cancer* 90: 1069-1075.
- Tan X, Thapa N, Sun Y, Anderson RA. (2015). A kinase-independent role for EGF receptor in autophagy initiation. *Cell* 160: 145-160.
- Tee AR, Manning BD, Roux PP, Cantley LC, Blenis J. (2003). Tuberous sclerosis complex gene products, Tuberin and Hamartin, control mTOR signaling by acting as a GTPase-activating protein complex toward Rheb. *Curr Biol.* 13: 1259-1268.
- Thastrup O, Cullen PJ, Drøbak BK, Hanley MR, Dawson AP. (1990). Thapsigargin, a tumor promoter, discharges intracellular Ca<sup>2+</sup> stores by specific inhibition of the endoplasmic reticulum Ca<sup>2+</sup>(+)-ATPase. *Proc Natl Acad Sci U S A* 87: 2466- 2470.
- Truong AB, Kretz M, Ridky TW, Kimmel R, Khavari PA. (2006). p63 regulates proliferation and differentiation of developmentally mature keratinocytes. *Genes Dev.* 20: 3185-3197.
- Turner N, Grose R. (2010). Fibroblast growth factor signalling: from development to cancer. *Nat. Rev. Cancer* 10: 116-129.
- Van Den Bossche K, Naeyaert JM, Lambert J. (2006) The Quest for the mechanism of melanin transfer. *Traffic* 7: 1-10.

Venuti A, Paolini F, Nasir L, Corteggio A, Roperto S, Campo MS, Borzacchiello G. (2011). Papillomavirus E5: the smallest oncoprotein with many functions. *Mol Cancer* 10: 140.

Virador VM, Muller J, Wu X, Abdel-Malek ZA, Yu ZX, Ferrans VJ, Kobayashi N, Wakamatsu K, Ito S, Hammer JA, Hearing VJ. (2002). Influence of alpha-melanocyte-stimulating hormone and of ultraviolet radiation on the transfer of melanosomes to keratinocytes. *FASEB J* 16: 105-107.

Wang J, Whiteman MW, Lian H, Wang G, Singh A, Huang D, Denmark T. (2009). A non-canonical MEK/ERK signaling pathway regulates autophagy via regulating Beclin 1. *J Biol Chem.* 284: 21412- 21424.

Wang X, Qi H, Wang Q, Zhu Y, Wang X, Jin M, Tan Q, Huang Q, Xu W, Li X, Kuang L, Tang Y, Du X, Chen D, Chen L. (2015). FGFR3/fibroblast growth factor receptor 3 inhibits autophagy through decreasing the ATG12-ATG5 conjugate, leading to the delay of cartilage development in achondroplasia. *Autophagy* 11: 1998-2013.

Wang ZG, Wang Y, Huang Y, Lu Q, Zheng L, Hu D, Feng WK, Liu YL, Ji KT, Zhang HY, Fu XB, Li XK, Chu MP, Xiao J. (2015). bFGF regulates autophagy and ubiquitinated protein accumulation induced by myocardial ischemia/ reperfusion via the activation of the PI3K/ AKT/mTOR pathway. *Sci Rep.* 5: 9287.

Wasmeier C, Hume AN, Bolasco G, Seabra MC. (2008) Melanosomes at a glance. *J. Cell Sci.* 121: 3995-3999.

Wei Y, Pattingre S, Sinha S, Bassik M, Levine B. (2008). JNK1-mediated phosphorylation of Bcl-2 regulates starvation-induced autophagy. *Mol Cell* 30: 678-688.

Wei Y, Zou Z, Becker N, Anderson M, Sumpter R, Xiao G, Kinch L, Koduru P, Christudass CS, Veltri RW, Grishin NV, Peyton M, Minna J, Bhagat G, Levine B.

(2013). EGFR-Mediated Beclin 1 phosphorylation in autophagy suppression, tumor progression, and tumor chemoresistance. *Cell* 154: 1269-1284.

Westfall MD, Mays DJ, Sniezek JC, Pietenpol JA. (2003). The DeltaNp63 alpha phosphoprotein binds the p21 and 14-3-3 sigma promoters in vivo and has transcriptional repressor activity that is reduced by Hay-Wells syndrome-derived mutations. *Mol Cell Biol.* 23: 2264-2276.

Wolff K, Konrad K. (1972). Phagocytosis of latex beads by epidermal keratinocytes in vivo. *J Ultrastruct Res* 39: 262-280.

Wu G, Osada M, Guo Z, Fomenkov A, Begum S, Zhao M, Upadhyay S, Xing M, Wu F, Moon C, Westra WH, Koch WM, Mantovani R, Califano JA, Ratovitski E, Sidransky D, Trink B. (2005). DeltaNp63alpha up-regulates the Hsp70 gene in human cancer. *Cancer Res.* 65: 758-766.

Wu J, Dang Y, Su W, Liu C, Ma H, Shan Y, Pei Y, Wan B, Guo J, Yu L. (2006). Molecular cloning and characterization of rat LC3A and LC3B--two novel markers of autophagosome. *Biochem Biophys Res Commun* 339: 437-442.

Xu Y, Jagannath C, Liu XD, Sharafkhaneh A, Kolodziejska KE, Eissa NT. (2007). Toll-like receptor 4 is a sensor for autophagy associated with innate immunity. *Immunity* 27: 135-144.

Yang Z and Klionsky DJ. (2010). Mammalian autophagy: core molecular machinery and signaling regulation. *Curr Opin Cell Biol.* 22: 124-131.

Yayon A, Zimmer Y, Shen GH, Avivi A, Yarden Y, Givol D. (1992). A confined variable region confers ligand specificity on fibroblast growth factor receptors: implications for the origin of the immunoglobulin fold. *EMBO J.* 11: 1885-1890.

Yuan HX, Russell RC, Guan KL. (2013). Regulation of PIK3C3/ VPS34 complexes by MTOR in nutrient stress-induced autophagy. *Autophagy* 9: 1983-1995.

Yugawa T, Handa K, Narisawa-Saito M, Ohno S, Fujita M, Kiyono T. (2007). Regulation of Notch1 gene expression by p53 in epithelial cells. *Mol Cell Biol.* 27: 3732-3742.

Zhang J, Liu J, Huang Y, Chang JY, Liu L, McKeehan WL, Martin JF, Wang F. (2012). FRS2 $\alpha$ -mediated FGF signals suppress premature differentiation of cardiac stem cells through regulating autophagy activity. *Circ Res.* 110: e29-39.

Zhu JH, Horbinski C, Guo F, Watkins S, Uchiyama Y, Chu CT. (2007). Regulation of autophagy by extracellular signal-regulated protein kinases during 1-methyl-4-phenylpyridinium-induced cell death. *Am. J. Pathol.* 170: 75-86.

zur Hausen H. (2002). Papillomaviruses and cancer: from basic studies to clinical application. *Nat Rev Cancer.* 2: 342-350.